Chronic Cortical Pathology in Multiple Sclerosis

Molecular Studies on Normal-Appearing and Demyelinated Cortex and a Novel Animal Model for Chronic Inflammatory Demyelination

Inauguraldissertation
zur
Erlangung der Würde eines Doktors der Philosophie
vorgelegt der
Philosophisch-Naturwissenschaftlichen Fakultät
der Universität Basel
von

Lukas Simon Enz

Basel, 2020

Genehmigt von der Philosophisch-Naturwissenschaftlichen Fakultät
auf Antrag von

Prof. Dr. Nicole Schaeren-Wiemers
Prof. Dr. Christoph Hess
Prof. Dr. Doron Merkler

Basel, den 18.2.2020

_____

Prof. Dr. Martin Spiess
Dekan

"Normal science, the activity in which most scientists inevitably spend almost all their time, is predicated on the assumption that the scientific community knows what the world is like. Normal science often suppresses fundamental novelties because they are necessarily subversive of its basic commitments."

Thomas. S. Kuhn
The Structure of Scientific Revolutions

"Here is some puzzle-solving normal science. But how do we know if the puzzle is solved?"

Lukas S. Enz
Chronic Cortical Pathology in Multiple Sclerosis

Table of Contents

Figure Index

Table Index

1 Acknowledgments

I would like to sincerely thank Nicole Schaeren-Wiemers, not just for her supervision of my thesis, but also for introducing me to a science focused on precision and driven by content – I thank her for her guidance, assistance and unconditional support throughout my time in her lab.

Further, I would like to thank Christoph Hess and Roland Martin for all their initiative, effort and support invested into me and my thesis from before it even began. I would also like to thank Doron Merkler for all his support and input.

Special thanks goes to Thomas Zeis for being a good mentor, an intellectual sparring partner and a dear friend.

This thesis would not have been possible without the work and support from all the people involved. I especially thank Christine Stadelmann, Stefan Nessler, Anne Winkler, Franziska van der Meer and Claudia Wrzos for their cordial welcome in Göttingen and for all of their help throughout my time with them.

A further special thanks goes to Boris Dasen for introducing me to the molecular world of DNA, to the fine art of viral design and to the virtue of focusing on the important things.

In order of appearance greatest thanks to all of the members of the lab for all the good and fun times with each and every one of you: Daniela Schmid, Melanie Gentner, Anne-Murielle Hollinger, Annalisa Hauck, Sigrid Müller, Sandro Ernst, Stephanie Jaggi, Gordana Jakimoski and Paula Huemer.

From the heart my utmost thanks to the people around me with whom I have shared with thought and folly, adventures and high tide, trial and tribulation: my parents, my brothers and my cherished new found sisters, my friends and all the people who have accompanied me.

2 List of publications

This thesis is based on the following articles published in scientific journals or currently in preparation for publication:

1. **Enz, L. S.***, Zeis, T.*, Schmid, D., Geier, F., van der Meer, F., Steiner, G., Certa, U., Binder, T.M.C., Stadelmann, C., Martin, R., Schaeren-Wiemers, N. (2020). Increased HLA-DR expression and cortical demyelination in multiple sclerosis patients are linked with the HLA-DR15 haplotype. *Neurol Neuroimmunol Neuroinflamm* 2020; 7:e656. doi:10.1212/NXI.0000000000000656

2. **Enz, L. S.**, Jakimoski, G., Zeis, T., Schmid, D., Geier, F., Steiner, G., Certa, U., Schaeren-Wiemers, N. (2020). Altered gene expression levels of olfactory receptors in neurons and blood vessels of multiple sclerosis cortical grey matter lesions. *Manuscript in preparation.*

3. **Enz, L. S.**, Winkler, A., Wrzos, C., Nessler, S., Stadelmann, C., Schaeren-Wiemers, N. (2020). A novel animal model for meningeal inflammation and chronic inflammatory demyelination of the cerebral cortex. *Manuscript in preparation.*

* These authors contributed equally to the work.

3 Abbreviations

AbsLog2FC	Absolute of the logarithm base 2 of the fold change
CD68	Cluster of differentiation 68
ColIV	Collagen IV
FC	Fold change
GO	Gene ontology
HLA	Human leukocyte antigen
Ifng	Interferon gamma
MHC	Major histocompatibility complex
MOG	Myelin oligodendrocyte glycoprotein
MRI	Magnetic resonance imaging
MS	Multiple sclerosis
NCBI	National Center for Biotechnology Information
NeuN	Neuronal nucleus antigen
OLIG2	Oligodendrocyte transcription factor 2
OR	Olfactory receptor
p.m. time	Post-mortem time
PPMS	Primary progressive multiple sclerosis
PRMS	Progressive-relapsing multiple sclerosis
RRMS	Relapsing-remitting multiple sclerosis
SPMS	Secondary progressive multiple sclerosis
Tnf	Tumor necrosis factor

4 Abstract

The chronic cortical pathology of multiple sclerosis (MS) composes of demyelination and neurodegeneration and has been studied since the early pathoanatomical descriptions of MS. Due to the technical difficulties in detecting the extent of cortical damage accumulating during the disease process it has only been recognized as a major aspect of MS pathology 20 years ago. The presented thesis comprises of three studies investigating the chronic cortical pathology of MS.

The first study describes gene expression changes between cortex from control cases and MS normal-appearing cortical grey matter without apparent signs of cortical pathology, *id est* no demyelination, inflammation or cell loss. HLA-DRB1 was detected as differentially upregulated within the MS cerebral cortex. This upregulation appeared in a bimodal distribution pattern, with its expression being either high or low within each case. Genotyping revealed that all carriers of the major MS risk allele *HLA-DRB1*15:01* belonged to the high expressing group, irrespective of whether they had MS or were control cases. Immunofluorescent-colocalization revealed the expression of HLA-DRB1 by microglia within MS and control cases. The higher gene expression of HLA-DRB1 further associated with higher protein expression of HLA-DRB1 and with the extent of cortical demyelination, effectively demonstrating a link between the strongest genetic risk factor, ribonucleic acid and protein expression of HLA-DRB1 and cortical demyelination.

The second study describes gene expression changes between MS demyelinated cortical grey matter lesions and normal-appearing grey matter. Gene set enrichment analysis revealed a cluster of olfactory receptors to be differentially higher expressed within the lesions. Immunofluorescent-colocalization of three selected olfactory receptors revealed one to be expressed on neurons (OR5P2), another to be expressed on neurons and blood vessels (OR52I1/OR52I2) and a third one to be expressed on blood vessels (OR9K2). Closer investigation of the expression pattern revealed a higher number of neurons to be positive for the respective receptor in the area of the demyelinated lesion, whereas the blood vessels showed a higher number of positive vessels for the respective receptor throughout the cortex. Olfactory receptors have previously been shown to be differentially regulated in other neurodegenerative diseases, such as Parkinson's disease, Alzheimer's disease, Creutzfeldt-Jakob disease and chronic schizophrenia, possibly linking MS chronic cortical pathology to more general mechanisms of neurodegenerative diseases.

The third study aimed to establish and investigate a novel animal model to study the effects of chronic cortical demyelination and meningeal inflammation. For this, rats were immunized-against myelin-oligodendrocyte glycoprotein and injected with lentiviruses overexpressing tumor necrosis factor alpha and interferon gamma, simulating the release of these cytokines in follicles located in the meninges and associated with cortical grey matter lesions in MS. The animals developed demyelination and meningeal inflammation stable for at least ten weeks and showed neuronal and oligodendrocyte loss, blood-brain barrier leakage and signs of remyelination, efficiently reproducing MS grey matter lesion phenotypes. This model will be of interest to study chronic adaptations of cortical grey matter to meningeal inflammation and demyelination as seen in MS.

In summary, this thesis gives novel insights into molecular changes within normal-appearing cortex and cortical grey matter lesions in MS, and describes a novel animal model to study chronic cortical changes caused by demyelination and meningeal inflammation.

5 Introduction

5.1 Multiple Sclerosis

Multiple Sclerosis (MS) is the most common chronic inflammatory demyelinating disease of the central nervous system showing both neurodegenerative and immunological aspects. The main pathological hallmarks of MS are foci with complete loss of myelin in the grey and white matter termed lesions. The cause of MS remains elusive, but the development of MS includes a complex genetic trait and several environmental risk factors, which act in concert and contribute to the main pathomechanisms including inflammation, de- and remyelination, axonal and neuronal loss, astroglia activation and metabolic changes (for review see: Olsson, Barcellos et al. 2017).

Whereas changes within the white matter have been the primary focus of MS research since the first neuropathological description, in the past two decades changes within the grey matter and especially the cerebral cortical grey matter have become more and more recognized.

5.1.1 History of Multiple Sclerosis Research

Though historical cases suggestive of MS predate, the first clear clinical reports of MS can be attributed to physicians such as Robert Carswell (Carswell 1838) and Jean Cruveilhier (Cruveilhier 1829) and others during the first half of the nineteenth century. In 1863 major aspects of microscopic MS pathology were described, such as the loss of myelin around the nerve fibers and the presence of central veins within the lesions (Rindfleisch 1863). The first study clearly distinguishing MS from other diseases and giving it the name “la sclérose en plaque” was published by Jean-Martin Charcot (Charcot 1868). During his clinical lectures he characterized the disease as follows (Bourneville and Guérard 1869):

> *Le nom de sclérose (σκληρός) indique communément un endurcissement, une induration morbides des tissus, caractérisés par l'atrophie ou la disparation des éléments constitutif d'un organe et par la substitution en leur lieu et place du tissu conjonctif. [...] Quant à la sclérose en plaques disséminées (Charcot), elle consiste, son nom l'indique, en un nombre variable d'îlots scléreux répandus sans ordre sur les différents cordons de la moelle et sur les diverses parties de l'encéphale.*

With this brief macroscopic description, the major hallmark of MS is already denominated and characterized: the sclerotic lesions, appearing in a disseminated pattern within both the brain and the spinal cord.

Joseph Babinski, a student of Charcot, first described the presence of thinner myelin sheaths with shorter internodes compared to the surrounding tissue (Babinski 1885). This was later interpreted by Otto Marburg as signs of remyelination (Marburg 1906). Babinski also noted the association of demyelination and inflammation and described macrophages loaded with myelin fragments (Babinski 1885). Many basic questions posed during these early decades of MS research are still unanswered today, such as the central question, whether the immune infiltrates are a primary or secondary event and what exactly causes the primary tissue injury (Lassmann 2005).

During the decades following the description of MS by Charcot several variants of MS were described. The first was Devic's disease, also termed neuromyelitis optica or today neuromyelitis optica spectrum disease (Devic 1894), further Marburg's acute sclerosis (Marburg 1906), Schilder's diffuse sclerosis (Schilder 1912) and Balo's concentric sclerosis (Balo 1928). Neuromyelitis optica spectrum disorder is no longer regarded to be a variant of MS, but rather a distinct autoimmune disease directed against aquaporin 4 channels on astrocytes (Lennon, Wingerchuk et al. 2004, Hinson, Pittock et al. 2007, Takahashi, Fujihara et al. 2007, for review see: Akaishi, Nakashima et al. 2017). The other variants are still considered to be extreme forms of MS (for review see: Kutzelnigg and Lassmann 2014).

Advancements in the fields of immunology and the development of the main animal model for MS, the experimental autoimmune encephalomyelitis model, furthered the understanding of the immunological aspects of MS, up to a dogmatic interpretation of MS as an autoimmune disease (Lassmann 2005). The dominant immune cells within active MS lesions were identified as major histocompatibility complex (MHC) class II restricted CD4 positive T-cells (Traugott, Reinherz et al. 1983), and many studies mapped the pathways of immune cell migration into the central nervous system, gaining knowledge which serves as the basis for modern pharmacological MS therapy (for review see: Diebold and Derfuss 2016).

During the past decades, the scope of MS research has broadened and many old concepts are reemerging. Oligodendrocytes are no longer seen as sole victims of an immune attack (for review see: Zeis, Enz et al. 2016) and the neurodegenerative aspects such as loss of neurons and axons are receiving increasing attention. Consequently, there are attempts of pharmacological therapy targeted towards remyelination and neuroprotection and furthermore,

tissue areas showing only little or no inflammation are being investigated, describing changes throughout the central nervous system, which are independent of the peripheral immune system.

5.2 Epidemiology of Multiple Sclerosis

5.2.1 Global distribution pattern

The global prevalence of MS is estimated to 83 per 100'00, adding to around 2.3 million people with MS worldwide (Browne, Chandraratna et al. 2014). The distribution strongly varies between different regions with a prevalence as low as 2 per 100'000 in Japan to over 100 per 100'000 in northern Europe, southern Australia and North America (for reviews see: Noseworthy, Lucchinetti et al. 2000, Howard, Trevick et al. 2016). In Switzerland around 10'000-15'000 people are affected by MS, adding to about 160 per 100'000 people (Blozik, Rapold et al. 2017). While the geographical distribution may in part be explained by genetic factors, a large meta-analysis has found a gradient along increasing latitude, which persists even after correcting for the strongest genetic risk factor, HLA-DRB1 allelic variants, suggesting environmental factors such as exposure to UV light and vitamin D availability to play a role within the global distribution pattern (Simpson, Blizzard et al. 2011).

5.2.2 Gender and age distribution

In Europe the prevalence rates range from 11 to 282 per 100'000 in women and from 10 to 123 per 100'000 in men, with a female to male ratio between 1.1 to 3.4, while the incidence rate in Europe is 4 cases per 100'000 people per year (for review see: Pugliatti, Rosati et al. 2006). The incidence ratio between female and male also seems to fit into the range of the prevalence (Kingwell, Marriott et al. 2013). This higher prevalence and incidence in women was found in the majority of epidemiological studies (Kingwell, Marriott et al. 2013). Apart from the higher incidence in women, some differences in the disease course have also been observed: whereas women have a higher rate of relapses, men show a worse recovery after the initial disease relapse and accumulate disability with an increased rate over time (Ribbons, McElduff et al. 2015).

Concerning the age distribution, MS is commonly diagnosed after the onset of the first symptoms in people around 30 years of age. Up to 10% of people however show a late onset after 50 years of age (Martinelli, Rodegher et al. 2004). In Europe the highest prevalence rate has been detected in the age group from 35-49 (Pugliatti, Rosati et al. 2006).

5.2.3 Genetic risk factors

The observation that monozygotic twins have a recurrence rate of around 30%, whereas dizygotic twins have a recurrence rate of only 5% already implies a genetic component of MS (for review see: Dyment, Sadnovich et al. 1997). The genetic risk factors of MS are however complex and involve multiple genetic loci, each alone only modestly increasing MS susceptibility. The main genetic risk factor for MS has been linked to the *HLA-DR15* serotype group, comprising of the *HLA-DRB1*15:01*, *HLA-DRB5*01:01*, *HLA-DQA*01:02* and *HLA-DQB*06:02* alleles, with carriers showing an about threefold increase in the risk of developing MS (Patsopoulos, Barcellos et al. 2013). Further HLA alleles with an independent association include *HLA-DRB1*03:01*, **13:03*, **04:04*, **04:01* and **14:01* and *HLA-DPB1*03:01* and MHC class I alleles such as *HLA-A*02:01*, *HLA-B*37:01* and **38:01* (Patsopoulos, Barcellos et al. 2013). Protective effects have been demonstrated for other alleles, such as *HLA-DRB1*14:01*, *DRB1*11*, *DRB1*13~DQB1*06:03* and *HLA-A*02:01* (for review see: Hollenbach and Oksenberg 2015).

Notably, it was recently demonstrated that genetic variants associated with other progressive neurological disorders, such as hereditary spastic paraplegia, are relatively overrepresented in primary progressive MS, with some patients showing a clinical overlap of these diseases (Jia, Madireddy et al. 2018).

Today genome-wide association studies have identified more than 200 genetic loci associated with MS, explaining about half of the observed heritability and many, but not all, reside within the HLA region on chromosome 6 (for reviews see: Sawcer, Franklin et al. 2014, Patsopoulos 2018).

5.2.4 Environmental factors

The main environmental risk factors associated with MS include Vitamin D levels, UV-light, Epstein-Barr virus, diet, sex hormones, cigarette smoking and trauma (for reviews see: Ascherio and Munger 2007, Ascherio and Munger 2007).

Being negative for the Epstein-Barr virus seems to offer a complete protection from MS (Pakpoor, Disanto et al. 2013), whereas a symptomatic Epstein-Barr virus infection doubles the risk of developing MS at a later time point (Handel, Williamson et al. 2010). The mechanistic role of Epstein-Barr virus remains unclear, but molecular mimicry and B-cell immortalization have been discussed to play a role (for review see: Dobson and Giovannoni 2019). It was pointed out that people not infected with Epstein-Barr virus and not developing MS seem to contradict the notion of the hygiene-hypothesis that exposure to different infectious agents

during the early childhood protects from developing MS later. This has been termed the Epstein-Barr virus paradox (Ascherio and Munger 2007).

The gradient of MS prevalence along the geographical latitude strongly correlates with the exposure to ultraviolet B light, which stimulates the production of vitamin D in the skin. Novel studies analyzing single nucleotide polymorphisms associated with low vitamin D levels have revealed that a decrease of one standard deviation in vitamin D levels leads to a twofold increase in the risk for MS (Mokry, Ross et al. 2015).

Smoking increases the risk for MS by about 50% and it was pointed out that the decline of smoking especially in men may partially account for the increasing gender gap (Palacios, Alonso et al. 2011).

5.3 Clinical features and diagnosis of Multiple sclerosis

The symptoms of MS are very heterogeneous, but nonetheless some are more common than others. Typical initial presentations include acute unilateral optic neuritis causing pain and vision loss, spinal cord symptoms such as hemiparesis, mono- or paraparesis, hypoesthesia, dysesthesia, paraesthesia and urinary or faecal sphincter dysfunction, brainstem and cerebellar symptoms such as diplopia, oscillopsy, vertigo, gait ataxia, dysmetria, intentional tremor, facial paresis and hypoesthesia or cerebral symptoms such as faciobrachial-crural hemiparesis or hemihypoesthesia (for review see: Oh, Vidal-Jordana et al. 2018).

Upon presentation with symptoms suggestive of MS, magnetic resonance imaging (MRI) is performed to search for brain and spinal cord abnormalities in accordance with MS and to rule out other diseases. Suggestive of MS are T2-hyperintense lesions located periventricular, juxtacortical or infratentorial which may be hypointense in T1-weighted images, so called black holes. At the time point of the clinically isolated syndrome, up to 50% of the patients also show lesions within the spinal cord, which may extend over two vertebral segments (for reviews see: Wattjes, Rovira et al. 2015, Thompson, Baranzini et al. 2018). The widespread use of MRI has led to the detection of MS-typical lesions in patients with no symptoms of MS, called radiologically isolated syndrome. Of these patients, a third will develop MS within the next five years (Wattjes, Rovira et al. 2015).

In addition, an examination of the cerebro-spinal fluid can be performed, where a mild raise of lymphocytes and protein and raised IgG levels with oligoclonal bands not present in the serum are found in 90% of all MS patients (Thompson, Baranzini et al. 2018). If required for differential diagnosis, testing of sensory evoked potentials may also be performed, where increased latency with preserved shape of the signal may be interpreted as a demyelinating

lesion, demonstrating dissemination in space, supporting the diagnosis of MS. Further laboratory tests performed routinely usually are of little value in MS diagnostics, but targeted laboratory tests based on the patient's history or abnormal examination or MRI findings may be used to exclude differential diagnoses.

Differential diagnoses of MS with a relapsing-remitting disease course are very broad and need to be considered carefully. This includes acute disseminated encephalomyelitis (ADEM), neuromyelitis optica spectrum disorder (NMOSD), neurosarcoidosis, vasculitis of the central nervous system, Susac's syndrome, cerebral autosomal dominant arteriopathy with subcortical infarcts and leukoencephalopathy (CADASIL), connective tissue disorders such as systemic lupus erythematosus, Sjögren's syndrome, antiphospholipid syndrome, Behçet's disease, chronic lymphocytic inflammation with pontine perivascular enhancement responsive to steroids syndrome (CLIPPERS) and Leber's hereditary optic neuropathy (Thompson, Baranzini et al. 2018). Differential diagnoses of MS presenting with a progressive disease course include dural arteriovenous fistula, nutritional myelinopathy (vitamin B12 deficiency), primary lateral sclerosis, leukodystrophies such as adrenomyeloneuropathy, Krabbe's disease, Alexander's disease, hereditary diffuse leukoencephalopathy with axonal spheroids, or diseases such as hereditary spastic paraplegia or spinocerebellar ataxias (Thompson, Baranzini et al. 2018).

Apart from the clinically apparent symptoms, subtler ones also develop, especially during the progressive disease phase. Up to 70% of MS patients may suffer from measurable cognitive impairments. Visual and verbal memory and processing speed are the most frequent disturbed domains (Brass, Benedict et al. 2006, for review see: Chiaravalloti and DeLuca 2008). Epilepsies were also linked to grey matter damage, however mostly indirect, as in vivo lesion detection in cortical grey matter remains difficult (for review see: van Munster, Jonkman et al. 2015).

The heterogeneity of symptoms and clinical signs apparent in MS, all of which may also be caused by other diseases, renders a definite diagnosis technically impossible (Thompson, Baranzini et al. 2018). With the emergence of the first clinical trials and therapies however arose the need for a specific and a sensitive diagnosis of MS to in- and exclude patients as uniformly as possible. This led to the first diagnostic criteria suggested by Schumacher et al. in 1965 (Schumacher, Beebe et al. 1965). These criteria were based on: (1) objective abnormalities during neurological examination clearly attributable to the central nervous system, (2) evidence from examination or patient history that two or more parts of the central nervous system are involved, (3) the central nervous system damage must mainly reflect white matter involvement,

(4) the damage must have occurred either in two distinct episodes at least one month apart or in a slow progression over six months, (5) the patients must be 10-50 years old and (6) there is no better explanation. It stands out that these criteria do not involve any laboratory parameters, though the quantification of the gamma-globulin content was mentioned to support the diagnosis of MS.

The 1983 publication of the Poser criteria introduced a more complex system, taking advantage of the advancements in laboratory measurement of oligoclonal bands and increased immunoglobulin G (Poser, Paty et al. 1983). These criteria defined clinically definite, laboratory-supported definite, clinically probable and laboratory-supported probable MS diagnosis. Interestingly, the authors stated that "gray matter lesions occur rarely enough in MS that they should not be considered in establishing the diagnosis". In 2001 for the first time the McDonald criteria for the diagnosis were published, which have since then been revised in 2005 and 2010 (McDonald, Compston et al. 2001, Polman, Reingold et al. 2005, Polman, Reingold et al. 2011). These new criteria introduced magnetic resonance imaging (MRI) of the brain and later included also the spinal cord as the most important investigation for the diagnosis of MS, greatly supporting the main diagnostic criteria, which remain dissemination of the symptoms and lesions in time and space. The evolution of the criteria has greatly improved the sensitivity and specificity of the diagnosis and has further reduced the critical delay time between onset of symptoms to diagnosis and treatment from two years with the Poser criteria to less than six months with the newest version of the McDonald criteria. Even though cortical lesions are to date not part of the diagnostic criteria of MS, they might be of interest for differential diagnosis, as cortical lesions are very rare in migraine and neuromyelitis optica spectrum disorder (Filippi, Rocca et al. 2016).

To better monitor the effects of particular treatments, further clinical parameter needed to be established and evaluated. This led to the development of a clinical score, composed of the assessment of:

(1) mental functions, (2) visual functions, (3) brainstem functions, (4) cerebellar system functions (5) pyramidal tract functions, (6) sensory functions, (7) excretory functions and (8) other functions. These systems are then combined to a final neurological status score ranging from 0 (normal neurological function) to 10 (death due to MS). The major milestones include a score of 5 (no longer able to work a full day without special provisions) and a score of 7 (restricted to the wheel chair) (Kurtzke 1955, for review see: Kurtzke 2008).

5.4 Disease course and prognosis

The most common disease course of MS is a pattern of symptomatic relapses followed by a partial or complete remission, termed relapsing-remitting MS (RRMS, Figure 1A, B). This disease course is observed in around 85% of MS patients during the first years of the disease (Confavreux and Vukusic 2006). Over time, this may develop into a form of progressive disability with incomplete recovery, termed secondary progressive MS (SPMS, Figure 1B). The conversion rate from RRMS to SPMS is linear with a probability of 2-3% per year and an average time to conversion of 19 years (Confavreux and Vukusic 2006). Around 40% of the patients still have phases of relapses during this progressive stage. In about 15% of the patients the disease develops with a steady decline without an initial phase of relapses, this course is termed primary progressive MS (PPMS, Figure 1A). In a few cases, the disease starts with progressive disability acquisition, superimposed by relapses. This disease course is termed progressive-relapsing MS (PRMS, Figure 1, A). The difference in the disease courses has led to the speculation that what we term MS may in fact be more than one single disease – but instead a minimum of two, one inflammatory, manifesting in relapses, and the other neurodegenerative, manifesting in chronic progression. These two diseases may occur separately from each other, but are strongly associated. Contradicting this hypothesis however on an epidemiological level, it has been pointed out that age is the major determinant for the clinical phenotype – RRMS is the disease of younger whereas the progressive courses SPMS, PPMS and PRMS are the disease phenotype of the older (Confavreux and Vukusic 2006). The time to reach certain stages of disability is linked to age and is not evidently influenced by relapses or by the initial course of the disease (Confavreux, Vukusic et al. 2000). Therefore, the emergence of progression might not be defined by a change in the pathogenesis of MS, thereby hypothetically unifying all variants of MS as one disease with progression as its main pathology, often but not always preceded or accompanied by relapses.

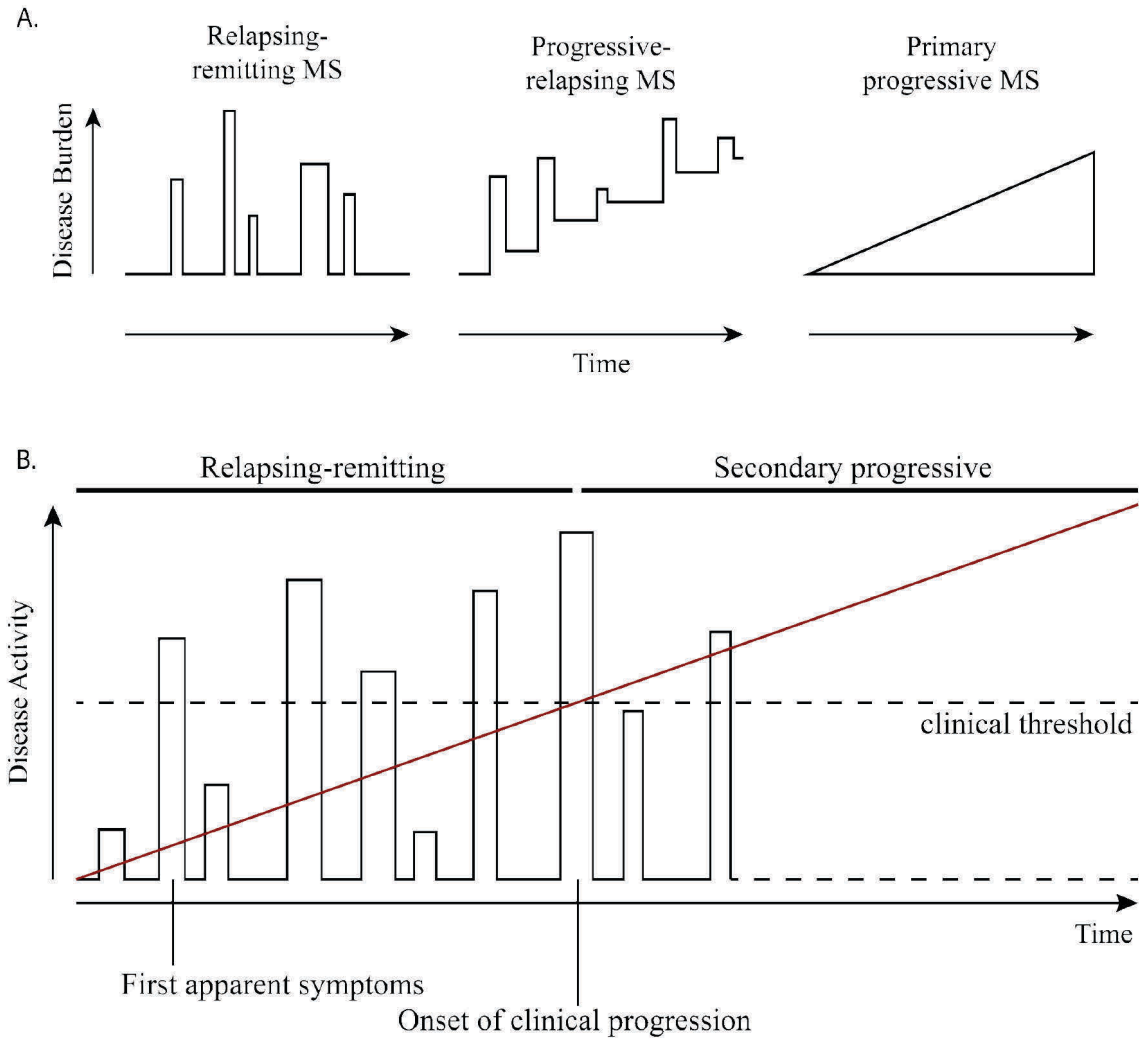

Figure 1. Disease courses of MS
(A) Figure depicting the evolution of symptoms over time for the different disease courses relapsing remitting MS, progressive-relapsing and primary progressive MS. (B) Figure depicting the relation of relapsing-remitting MS to secondary progressive MS. The black columns depict the inflammation-related relapses, while the red line depicts the evolution of disease progression. The phase of secondary progressive disease commences where the progression reaches the clinical threshold. Scales are arbitrary.

5.5 Treatment approaches

MS is to date an incurable disease and the pharmacological treatment mainly aims to reduce the relapse and progression rate, ameliorate symptoms, and thereby improve the quality of life of people with MS.

It is common practice to treat acute exacerbations with corticosteroids, using their anti-inflammatory and immunosuppressive properties to ameliorate symptoms and shorten the recovery phase (for review see: Frohman, Shah et al. 2007). They have however been shown to have no effect on the degree of recovery from an exacerbation and on the long-term disease course (Frohman, Shah et al. 2007, Goodin 2014). For long-term benefit, numerous disease-modifying therapies have been approved over the past three decades, aiming to prevent damage

from early disease stages on (for review see: Diebold and Derfuss 2016). Whereas the aim of today's therapy in RRMS patients is to achieve no evidence of disease activity (NEDA), defined as absence of relapses, absence of progression and absence of T2-hyperintense and/or T1-gadolinium-enhancing lesions in brain MRI (NEDA-3) (Stangel, Penner et al. 2014), the main challenge is to decide, which patient benefits the most from which particular treatment.
Interferon beta was the first disease-modifying therapy on the market for the treatment of MS, followed by glatirameracetate, reducing the relapse rate in RRMS patients by 30% (Diebold and Derfuss 2016). The next major breakthrough in RRMS therapy was achieved by blocking the entry of T-cells into the central nervous system, by administering Natalizumab, an antibody blocking α4 integrin. This treatment led to a marked reduction in the number of relapses and in MRI measurements of central nervous system inflammation. A major adverse effect was however the emergence of progressive multifocal leukoencelopathy, caused by the JC virus and the immunosuppression through Natalizumab. Further treatment approaches include targeting the sphingosine receptor S1P to trap the lymphocytes, especially naïve and central memory T-cells, within the lymph nodes (Fingolimod), inhibiting key enzymes in activated lymphocytes (Teriflunomide) and changing the immune balance towards a more tolerogenic and anti-inflammatory profile (Dimethylfumarate) (Diebold and Derfuss 2016, Montes Diaz, Hupperts et al. 2018).

Though disease-modifying therapies markedly reduced the relapse rate in MS, they have also demonstrated that MS is more than inflammation, with progressive disability being acquired irrespective of anti-inflammatory treatment. Some explanations for the failure of anti-inflammatory treatment to completely halt or cure MS include the inability to achieve therapeutic drug concentrations within the no longer inflamed central nervous system with a tighter blood-brain barrier or that previous inflammation may have triggered self-sustaining neurodegenerative cascades no longer dependent on the peripheral immune system. Alternatively it has also been suggested that neurodegeneration may be the prime pathology in MS, only modulated by an inflammatory response, but not dependent on it, thereby explaining both effect and limitations of the disease modifying therapies (for review see: Kawachi and Lassmann 2017).
Despite the recently demonstrated effectiveness of one disease modifying therapy for progressive MS (Montalban, Hauser et al. 2017), an effective disease modifying treatment of the progressive disease courses remains an unmet need (for review see: Feinstein, Freeman et al. 2015). The most important symptoms of these patients include balance and mobility

impairment, weakness, reduced cardiovascular fitness, ataxia, fatigue, bladder dysfunction, spasticity, pain, cognitive deficits, depression, and pseudobulbar affect. For these symptoms various symptomatic therapies are available; basing them on experimental evidence, however, is challenging and larger studies based on multiple interdisciplinary interventions of a narrowly selected study population with precisely defined outcome measures are required to further study the effectiveness of the symptomatic therapies (for reviews see: Feinstein, Freeman et al. 2015, Zhang, Salter et al. 2019).

5.6 Pathology of Multiple Sclerosis

5.6.1 Demyelination and inflammation

MS has been traditionally viewed as an autoimmune disease mediated primarily by an aberrant T-cell and B-cell reaction directed against the central nervous system myelin and oligodendrocytes (for review see: Kawachi and Lassmann 2017). However, the identity of a speculated target antigen remains elusive and the hypothesis of a truly immunological etiology is increasingly challenged.

The central feature of MS pathology is the focal loss of myelin and oligodendrocytes anywhere in the central nervous system, whereas the axons themselves are relatively preserved (for review see: Lassmann 2018). Within the white matter, the lesions develop in the presence of inflammatory infiltrates of T-cells, B-cells and macrophages, originating from a central vein. In three dimensional space the lesions forming around the veins appear as tubes termed Dawson fingers (Dawson 1916). This pattern of perivenous selective demyelination is unique for MS, and is one of few clear distinctions from other focal demyelinating diseases, such as white matter lesions in stroke, where tissue damage is unspecific or NMOSD and the JC virus-induced progressive multifocal leukoencephalopathy, where oligodendrocytes are selectively lost, but in a pattern following the territories of the oligodendrocytes and not a perivenous pattern (Lassmann 2018).

In early MS cases active plaques dominate, making up around 75% of all lesions and showing dense infiltrates of macrophages containing myelin debris. As the disease develops and lesions accumulate, the relative number of active plaques decreases to nearly zero (Frischer, Weigand et al. 2015). In chronic MS, after over 30 years of disease duration, chronic inactive lesions are the most abundant lesion type found in autopsies and make out about 50% of the lesions present. In contrast to acute lesions, they are sharply demarcated, and show a paucity of immune cells in the center, a variable degree of periplaque microglia activation, and a prominent reactive gliosis. A quarter of the lesions in late MS still show a rim of activated microglia and ongoing

demyelination and are termed smoldering lesions. Shadow plaques are lesions with remyelination, where the axons have been myelinated with relatively thin sheaths and shortened internodes (Prineas, Barnard et al. 1993). In late-stage MS completely reymelinated lesions make up 20% of all lesions (Frischer, Weigand et al. 2015). The lesions may fully remyelinate or show a mixture of remyelinated and demyelinated areas. Remyelination varies significantly from patient to patient and it was shown to be highly efficient in cortical grey matter and more efficient in subcortical white matter compared to periventricular white matter (Patrikios, Stadelmann et al. 2006).

The most abundant immune cells over all lesions in MS brain are CD3 positive T-cells, with a predominance of CD8 positive T-cells compared to CD4 positive T-cells (Lassmann 2018). The perivascular, meningeal and diffuse parenchymal infiltrates, however, differ in their composition. Perivascular and meningeal infiltrates show a large number of CD4 T-cells and CD20 B-cells and plasma cells (Babbe et al. 2000; Frischer et al. 2009). The meningeal infiltrates may show features of tertiary lymphatic tissue (Serafini et al. 2004; Franciotta et al. 2008; Pikor et al. 2016).

Inflammation is seen in MS in all stages of the disease, including the progressive phases with lack of relapses, and is seen in not only in active lesions, but also in chronic inactive, in reymelinated and in normal-appearing white matter (Frischer, Bramow et al. 2009, Frischer, Weigand et al. 2015). During the ongoing tissue injury astrocytes are activated. After the acute demyelinating phase, the lesions can develop into gliotic scar tissue (sclerosis), and become chronic active or inactive lesions or they may remyelinate to form shadow plaques.

Apart from the demyelinated lesions, changes have also been described within the so-called normal-appearing white and normal-appearing grey matter. These changes are more pronounced during the progressive phases of the disease and include perivascular inflammatory infiltrates, edema, diffuse microglia activation and diffuse axonal injury and astrocytic gliosis (Kutzelnigg, Lucchinetti et al. 2005). These changes are in part attributed to focal lesions, leading to Wallerian (anterograde) and retrograde degeneration of the neurons. Further, changes within the normal-appearing white and grey matter develop independent of focal lesions and partially associate with meningeal inflammation of the spinal cord and the cortex (Androdias et al. 2010; Haider et al. 2016).

Whether the initial event triggering MS is an aberrant immune-system damaging the central nervous system (outside-in hypothesis) or a primary degenerative mechanism, secondarily triggering an immune-response (inside-out hypothesis) remains unclear as of today, and while

there is evidence for both concepts, the data provided so far are not yet conclusive (for reviews see: Stys, Zamponi et al. 2012, Hemmer, Kerschensteiner et al. 2015, Zeis, Enz et al. 2016).

5.6.2 Neurodegeneration and cortical atrophy

Neurodegeneration is a central feature of MS pathology and includes neuronal, axonal and synaptic degeneration and loss. It has been suggested to be the main driver of disease progression and takes place independent of inflammatory relapses (Kutzelnigg and Lassmann 2014). This is reflected by the notion that the various approaches on anti-inflammatory treatment show little or no effect during the progressive disease courses (Stys, Zamponi et al. 2012).

The central drivers of neurodegeneration revolve around different aspects of oxidative injury and stress caused by involve oxidative burst damage by microglia and macrophages, mitochondrial damage leading to energy failure and axonal damage, local hypoxia, Wallerian degeneration, iron-accumulation, meningeal inflammation and astrocyte activation (Kawachi and Lassmann 2017). Some of these mechanisms target the energy household of the neurons, which is also directly hampered by the ongoing demyelination: Myelin enables saltatory nerve signal conduction along the axons by providing an effective electrical insulation and by concentrating the ion channels required for signal transmission at the nodes of Ranvier. This enables the axon to efficiently transmit the signals with relatively low energy costs. Upon demyelination however, the ion channels need to be distributed over the demyelinated area of the axonal plasma membrane, leading to a recovery of the signal transmission, but less efficient, and consequently to a higher energy cost per signal conducted, putting a strain on the energy support. While the end-points of axonal and neuronal loss are also found in other neurodegenerative diseases, the severity of oxidative damage reported in MS lesions seems to specifically occur in MS (Lassmann 2018). Why this is the case is and what process drives the mechanisms of neurodegeneration described to date remains to be determined.

The widespread use of MRI in MS diagnosis and surveillance led to the detection of brain atrophy as a central feature in MS pathology. This aspect had previously been overlooked by the pathological studies, but has received increasing interest over the past decades (Kutzelnigg and Lassmann 2014). MRI studies have demonstrated that the cortex of MS patients is in average thinned by 10% of the volume and occurs already in early disease stages (Wegner, Esiri et al. 2006, Bergsland, Horakova et al. 2012). The atrophy is not restricted to sites of inflammation and demyelination, but occurs globally throughout the brain, suggesting non-inflammatory and non-demyelinating disease mechanisms to be involved (Kutzelnigg and

Lassmann 2014). It has further been shown that grey matter atrophy correlates better with clinical and functional scores, linking atrophy to long-term disability in MS patients (Fisniku, Chard et al. 2008, Roosendaal, Bendfeldt et al. 2011).

6 Cortical grey matter pathology of Multiple Sclerosis

6.1 History of cortical grey matter pathology research

Research on grey matter pathology of MS can be traced back to the time of the first description of MS as a unique disease. Already Charcot stated, during the autopsy of a MS patient (Bourneville and Guérard 1869):

> *Le plus souvent, on n'en rencontre pas dans la substance grise corticale: quelquefois cependendant, sur les limites des deux substancs, il semble que la plaque s'étende de l'une à l'autre.*

Though he states that lesions within the grey matter are not common ("Le plus souvent, on n'en rencontra pas dans la substance grise cortical"), Charcot clearly states that some lesions cross the cortico-subcortical border ("il semble que la plaque s'étende de l'une à l'autre"), probably referring to what we term leukocortical lesions today.
Similar statements may be found by other contemporary researchers, such as Friedrich Wilhelm Frommann, describing autopsies of MS cases (Frommann 1878):

> *Im ganzen Marklager der Hemisphären mohnkorn- bis erbsengrosse graue, nur zum kleineren Theil röthliche Heerde in ziemlicher Häufigkeit, sparsamer in den centralen Hirnganglien sowie innerhalb der grauen Hirnrinde. Einzelne derselben lagen theilweise in der letzteren, theilweise in der angrenzenden Substanz. […]*
>
> *Es fanden sich hier innerhalb der weissen Substanz, in der Nähe der grauen und zum Theil in die letztere hineinragend, dicht neben einander zwei kleine runde Heerde von 1|2 Mm. Durchmesser an Stellen, wo die vorausgegangenen Schnitte nur gesundes Gewebe erkennen liessen.*

Even though historic descriptions must be interpreted with caution as the epistemological content of both words and context may have severely changed, these are clearly descriptions of cortical grey matter lesions in MS cases. Further historical observations of lesions at the grey-white matter border and of cortical atrophy include descriptions by Sander, Dinkler and Schob (Sander, 1898; Dinkler, 1904; Schob, 1907), but during the subsequent decades, cortical grey matter lesions did not seem to play a major part within the research conducted on MS. The first publication focusing on the cortical pathology was published by Brownell and Hughes in 1962, almost a century after the seminal publication by Charcot (Brownell and Hughes 1962). After

this publication the cortical grey matter pathology slowly gained interest, until the publication by Kidd et al. in 1999, characterizing and cataloging the various types of cortical grey matter lesions, initiated a fast increasing number of studies (Figure 2A, B).

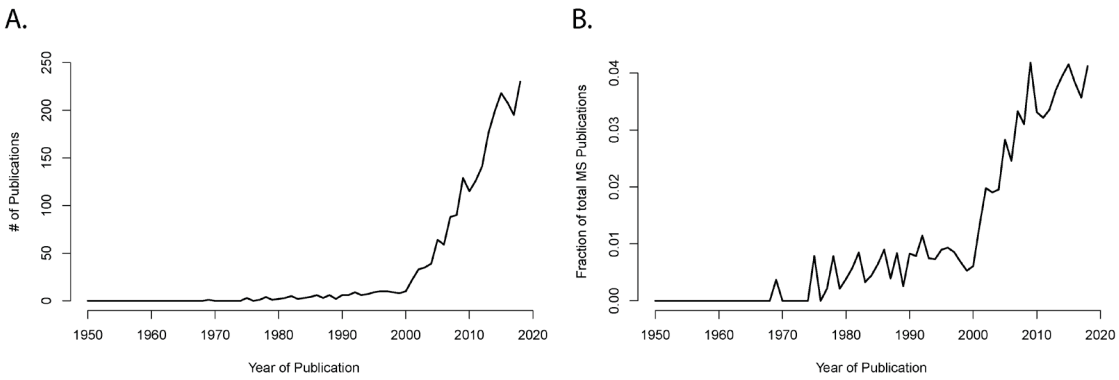

Figure 2. Development of publication numbers on cortical grey matter in MS
Figure depicting (A) the number of publications found on PubMed (www.ncbi.nlm.nih.gov/pubmed/, last called 30.11.2019, United States National Library of Medicine, Bethesda, Maryland, USA) using the search term "Multiple+Sclerosis+(Gray+OR+Grey)+Matter" from January 1950 until December 2018 and (B) the number of publications as in A divided by the number of publications retrieved on PubMed using the search term "Multiple+Sclerosis" to show the relative increase on grey matter publications among MS publications.

6.2 Cortical grey matter lesions

Cortical demyelination may be present from the earliest clinical disease stages (Lucchinetti, Popescu et al. 2011) and increases strongly, when patients reach the progressive stage (Kutzelnigg, Lucchinetti et al. 2005). Modern research on cortical grey matter lesions commenced in 1999 with the mapping and classification of seven different types of grey matter lesions (Kidd, Barkhof et al. 1999). Kidd et al. proposed a system of seven different lesion types according to the anatomical structure of the involved blood vessels. Type 1 lesions are located in the deeper cortical laminae and extend to the subcortical white matter. Type 2 lesions extend over all layers of the cortex but do not involve the subcortical white matter. Type 3 lesions are only located in the superficial cortical layers. Type 4 lesions only extended along the subcortical U-fibers. Type 5 lesions are large lesions affecting all layers of the cortex and the subcortical white matter. Type 6 lesions are small lesions occurring anywhere within the cortex. Type 7 lesions are the largest lesions, extending over both banks of a gyrus and may or may not extend into the subcortical white matter.

This classification system was however rather difficult to comprehend and use, and strongly suggested an etiological role of the vein system, as seen in white matter lesions and not taking into account other possibly involved structures, such as the meninges. A more neutral, second

classification system was introduced in 2001 by Peterson et al. and updated in 2003 and has since been widely accepted and used for grey matter lesions (Peterson, Bo et al. 2001, Bø, Vedeler et al. 2003). This classification system distinguishes four lesion types: Type I lesions (Figure 3A), also termed leukocortical lesions, are in direct contact with the white matter border but do not reach the meninges. They are often confluent with white matter lesions. Type II or intracortical lesions contact neither the white matter border nor the meninges and are often perivascular (Figure 3B). Type III or subpial lesions are in direct contact with the meninges, often extend unto cortical layer 3 or 4, but do not reach the border to the subcortical white matter (Figure 3C). Subpial cortical lesions are the most common type of cortical lesions in MS and are the only lesion type not detected in any other disease with demyelination of the cortex such as tuberculous or luetic meningoencephalitis, progressive multifocal leukoencephalopathy, Rasmussen's encephalitis or paraneoplastic encephalitis (Moll, Rietsch et al. 2008, Junker, Wozniak et al. 2020). This specificity of subpial lesions demonstrates that demyelination in MS is not simply a bystander effect of inflammation, but part of a mechanism unique to this disease. Subpial lesions have a band or ribbon like appearance and may stretch over several adjacent gyri, in one specific case 69% of the forebrain cortical area was demyelinated (Kutzelnigg, Lucchinetti et al. 2005). Subpial cortical lesions have further been shown to associate with meningeal inflammation while T- and B-cell infiltrates are rare (Kutzelnigg, Lucchinetti et al. 2005). Last, type IV or pancortical lesions extend from the meninges through all cortical layers and contact the white matter border (Figure 3D). These lesions might be a specific pattern or they may simply be a fusion of type I, II or III lesion, having grown to span all cortical layers.

Cortical grey matter lesions may be staged into active, chronic active or chronic inactive lesions. To differentiate between these stages a histological marker for the major histocompatibility complex (MHC) class II is used: active lesions are characterized by a distinct MHC class II-positive cell border and lesion core and hypercellularity. Chronic active lesions are also characterized by a MHC class II cell border, but their core shows levels of MHC class II positive cells at the lesion core comparable to normal-appearing cortex. Chronic inactive lesions do not show any distinct MHC class II positive lesion border have a core comparable to normal-appearing grey matter (Peterson, Bo et al. 2001). For staging the leukocortical lesions, the white matter part of the lesion has been used as a surrogate (Peterson, Bo et al. 2001).

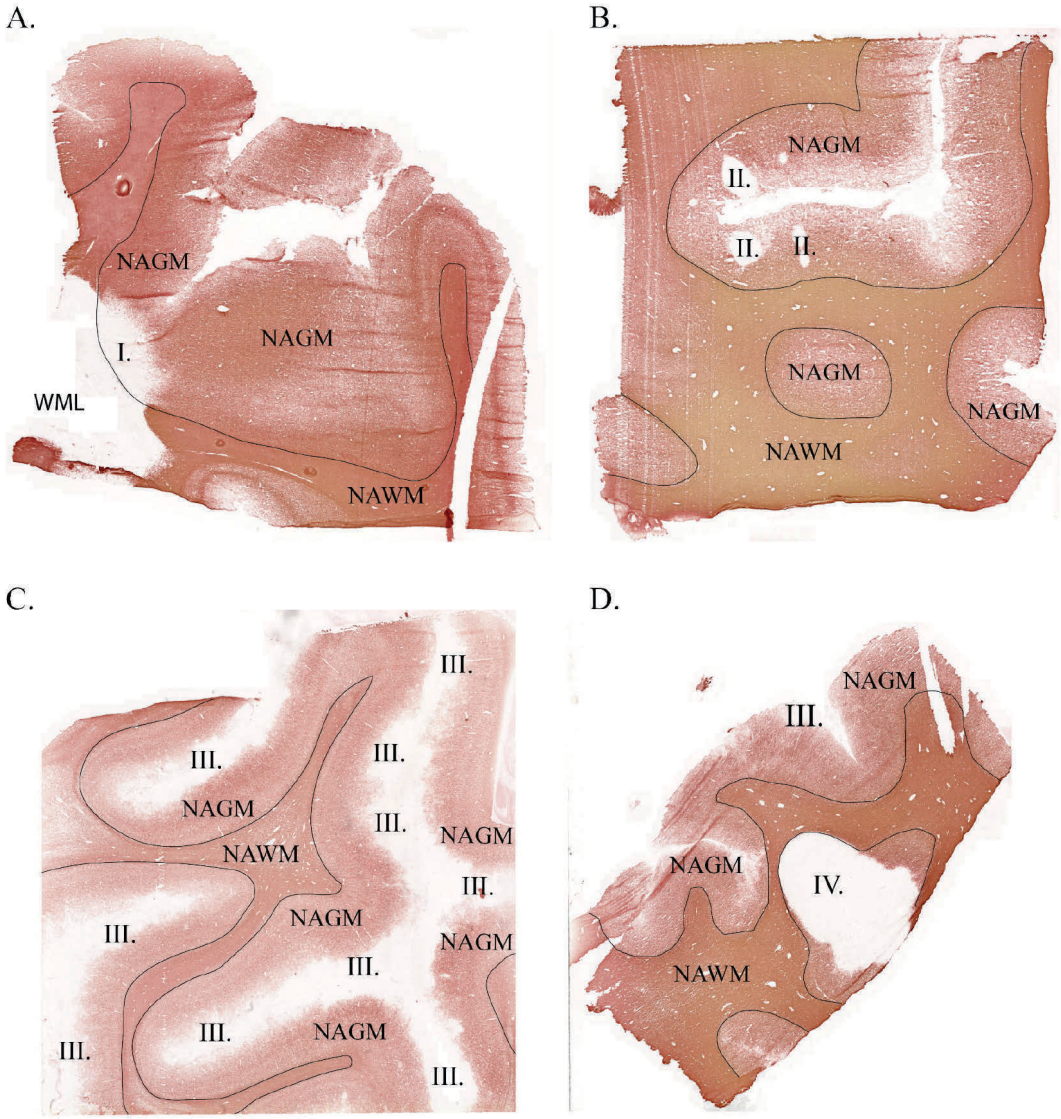

Figure 3. Types of cortical grey matter lesions
Representative images of anti-myelin oligodendrocyte glycoprotein stainings of human cortical grey matter tissue and subcortical white matter. (A.) Type I leukocortical lesion (I.) with adjacent subcortical white matter lesion (WML). (B.) Type II intracortical lesions (II.). (C.) Type III subpial lesion (III.) spanning multiple gyri. (D.) Type IV pancortical lesion (IV.). Abbreviations: NAGM: normal-appearing grey matter; NAWM: normal-appearing white matter. The black line delineates the border between grey and white matter.

6.2.1 Comparison to white matter lesions

Compared to white matter demyelination, cortical demyelination may be much more extensive, with an extreme case published, where more than 60% of the cortex was demyelinated (Haider, Simeonidou et al. 2014). Cortical grey matter lesions were shown to contain fewer CD68+ cells and fewer CD3+ cells if compared to active white matter lesions or chronic active white matter lesions (Peterson et al. 2001).

Cortical grey matter lesions are more difficult to detect in MRI compared to lesions within the white matter. While leukocortical (Type I) and pancortical (Type IV) lesions can be detected

by MRI with a prospective detection rate of 100% respectively 68%, the intracortical lesions (Type II) and the subpial lesions (Type III) are not well detected (11% respectively 32%) (Kilsdonk, Jonkman et al. 2016). Even retrospectively, after histological analysis, still 40% of the cortical grey matter lesions may be missed by MRI (Kilsdonk, Jonkman et al. 2016). This is partially explained by the longer relaxation times of normal-appearing grey matter compared to white matter. The weak inflammatory component of the grey matter lesions does not lead to a sufficient increase in the relaxation time to allow a clear separation of normal-appearing grey matter and grey matter lesions as is the case in white matter lesions (Kidd, Barkhof et al. 1999). Partial volume effects with the CSF may also play a role.

6.3 Lessons learned from gene expression studies

To date only few gene expression studies have been performed with material from cortical grey matter and cortical grey matter lesions. The first such study was performed by Dutta et al. (Dutta, McDonough et al. 2006, Dutta, McDonough et al. 2007) and compared the normal-appearing motor cortex of six MS cases to motor cortex of six controls without neurological disease. They found a downregulation of mitochondrial genes involved in the respiratory chain, specific for neurons, and a lower expression of genes involved in the pre- and postsynaptic components of GABAergic signaling. These results suggest a disturbance in the energy household of neurons, possibly contributing to neurodegeneration (Dutta, McDonough et al. 2006). They further described an upregulation of the ciliary neurotrophic factor CNTF and functionally related genes, promoting neuroprotection and anti-apoptotic pathways, suggestive of adaption mechanisms of the neurons (Dutta, McDonough et al. 2007).

In another study, brain samples from six MS cases and eight control cases without neurological disease were compared (Torkildsen, Stansberg et al. 2010). In contrast to the earlier study, both cortical grey matter and cortical grey matter lesions were included. They observed a higher expression of immunoglobulin related genes in MS grey matter, deriving from plasma cells located in the meninges.

A third study was designed and performed to distinguish MS specific gene expression changes (Fischer, Wimmer et al. 2013). This was achieved by comparing the gene expression profiles of three cases with tuberculous meningitis, three cases with Alzheimer's disease and three control cases without neurological diseases to three MS cases. By this multi-comparison, they detected changes in genes related to T-cell mediated inflammation, microglia activation, oxidative injury, DNA damage and repair, and remyelination. This study however has a major limitation, which is also reported by the authors: the brain tissue samples utilized for the gene

expression analysis were formaldehyde-fixed and paraffin-embedded, irreversibly and irreproducible worsening the integrity of the RNA, which may lead to false-positive and false-negative results.

A fourth study, from our own lab, compared the gene expression profiles of 17 control cases and normal-appearing grey matter of 18 MS cases (Zeis, Allaman et al. 2015). They identified a lower expression of astrocyte specific genes involved in the astrocyte-neuron lactate shuttle, which is important for neuronal homeostasis, and genes involved in the glutamate-glutamine cycle, which is also a support mechanism of astrocytes for the neurons. They further identified a higher expression of interleukin 1 beta within the normal-appearing grey matter, suggestive of inflammasome activation.

In summary, gene expression studies performed on cortical grey matter of MS cases have so far revealed gene expression profiles suggestive of a stressed energy household of the neurons, aggravated by a failing support of the astrocytes and the myelin sheaths.

6.4 Animal models of cortical grey matter lesion pathology

Since MS has so far only been described in the human species, animal models are necessary to gain mechanistic insights on the disease but on the other hand a single model will always fail to reproduce all aspects of the disease. Due to this, each experimental approach with an animal model has to be critically reflected and compared to the human disease to determine the scope of any meaningful interpretation.

To date several animal models inducing demyelinated cortical grey matter lesions have been generated. To mention are two comparable rat models, differing only in their implementation, but not in their theoretical mechanistic approach. Both models work by first immunizing the rats against the myelin oligodendrocyte glycoprotein (Mog), before stereotactically injecting tumor necrosis factor alpha (Tnf) and interferon gamma (Ifng) either intracortical (Merkler, Ernsting et al. 2006, Rodriguez, Wegner et al. 2014) or subarachnoidal (Gardner, Magliozzi et al. 2013). Both approaches give rise to subpial demyelination meningeal and parenchymal inflammation composed of infiltrating macrophages and activated microglia and T-cells and B-cells. The animals did not develop a clinically apparent phenotype despite the widespread cortical demyelination and inflammation. The pathology was followed by a fast and full recovery within about two weeks after the stereotactic injections.

In an attempt to chronify the model, a similar approach was conducted, but instead of a single stereotactic injection, a catheter for long-term injection at the grey and white matter border was

installed (Ucal, Haindl et al. 2017). This model also gave rise to widespread subpial cortical demyelination with the option of repeated cytokine injection through the catheter.

Another animal model leading to cortical demyelination is induced by administering the copper-chelator cuprizone to mice, leading to toxic oligodendrocyte death and white and grey matter demyelination. These models do not involve any manipulation of the animals, as cuprizone was fed to the animals with the regular chow. The protocols for feeding cuprizone and the mouse strains used, are very heterogeneous, leading to a very heterogeneous pathology (Bai et al. 2016). This model is mainly used to study remyelination, but does not recapitulate inflammation or neurodegeneration.

7 Aim of the work

The major goal of the work presented in this thesis was to increase our understanding of molecular cortical grey matter pathology both within the normally myelinated and demyelinated human brain tissue and within an animal model.

The cortical pathology of MS remains enigmatic in many aspects despite two decades of intense research. The aim of this work was to investigate the following questions:

1. Which molecular mechanisms contribute to changes in normal-appearing grey matter?
2. Which molecular mechanisms contribute to chronic grey matter lesion changes?
3. May we replicate aspects of the chronic cortical changes of MS in an animal model?

To investigate the first and second aim, we performed two gene expression studies: one comparing normal-appearing grey matter to control cortical grey matter and one comparing grey matter lesions to normal-appearing grey matter. We then investigated the most relevant findings with immunohistochemical and immunofluorescent approaches on human brain tissue. To investigate the third aim, we adapted a previously published acute animal model mimicking cortical grey matter lesions to produce chronically stable demyelination and inflammation and investigated the histopathology of this model in-depth.

8 Results

8.1 Study 1: Increased HLA-DR expression and cortical demyelination in multiple sclerosis links with the HLA-DR15 haplotype

By Lukas S. Enz, Thomas Zeis*, Daniela Schmid, Florian Geier, Franziska van der Meer, Guido Steiner, Ulrich Certa, Thomas Martin Christian Binder, Christine Stadelmann, Roland Martin, Nicole Schaeren-Wiemers*

** These Authors contributed equally to the manuscript*

Published 27. Dec. 2019

Neurol Neuroimmunol Neuroinflamm, 7 (2) e656

doi: 10.1212/NXI.0000000000000656

Contributions of Lukas S. Enz:

Sample selection and characterization, immunohistochemical characterization and analysis, immunofluorescence colocalization analysis, data analysis and interpretation, initial manuscript preparation and revisions.

Author contributions:

T.Z.: Study design, sample selection and characterization, microarray analysis, data analysis and interpretation, manuscript preparation. D.S.: Sample selection and characterization. F.G.: Data analysis and interpretation, statistics. F.v.d.M.: Immunofluorescence colocalization. G.S.: Microarray experiment design. U.C.: Study design. T.B.: Manuscript preparation. C.S.: Immunofluorescence colocalization. R.M.: Data analysis and interpretation, and manuscript preparation. N.S.W.: Study design, data analysis and interpretation, and manuscript preparation.

8.1.1 Abstract

Multiple sclerosis (MS) is a chronic inflammatory demyelinating disease of the central nervous system. Among characteristics of MS pathology are cortical grey matter abnormalities, which have been linked to clinical signs such as cognitive impairment.

Objective: To investigate molecular changes in MS cortical grey matter.

Method: We performed a whole genome gene expression microarray analysis of human brain autopsy tissues from 64 MS normal-appearing cortical grey matter samples and 42 control grey matter samples. We further examined our cases by HLA genotyping, and performed immunohistochemical and immunofluorescent analysis of all human brain tissues.

Results: HLA-DRB1 is the transcript with highest expression in MS normal-appearing grey matter with a bimodal distribution among the examined cases. Genotyping revealed that every case with the MS-associated *HLA-DR15* haplotype also shows high HLA-DRB1 expression and also of the tightly linked *HLA-DRB5* allele. Quantitative immunohistochemical analysis confirmed the higher expression of HLA-DRB1 in *HLA-DRB1*15:01* cases at the protein level. Analysis of grey matter lesion size revealed a significant increase of cortical lesion size in cases with high HLA-DRB1 expression.

Conclusions: Our data indicate that increased HLA-DRB1 and -DRB5 expression in the brain of MS patients may be an important factor in how the *HLA-DR15* haplotype contributes to MS pathomechanisms in the target organ.

8.1.2 Introduction

Multiple sclerosis (MS), the most common inflammatory neurologic disease affecting young adults, is a chronic autoimmune demyelinating disease of the central nervous system. If untreated, MS leads to disability in a substantial proportion of patients. The etiology of MS includes a complex genetic trait and several environmental risk factors, which act in concert and contribute to the main pathomechanisms including autoimmune inflammation, de- and remyelination, axonal and neuronal loss, astroglia activation and metabolic changes (for review see: Olsson, Barcellos et al. 2017). The relative severity of these factors leads to the enormous heterogeneity of MS with respect to clinical signs, course, and response to treatment, but also pathological composition of demyelinated lesions. The pathologic hallmark of MS is the formation of focal areas of myelin loss in the central nervous system. Besides the most commonly described white matter lesions, extensive grey matter lesions can be found in MS cerebral cortex (for review see: Calabrese, Magliozzi et al. 2015). In addition to the well described demyelinated grey matter lesions also diffuse grey matter abnormalities in non-

lesional normally myelinated areas have been described (Dutta, McDonough et al. 2006, Kutzelnigg, Faber-Rod et al. 2007, for review see: Stadelmann, Albert et al. 2008). At the molecular level, little is known about changes in normal-appearing grey matter and grey matter lesions in MS. In the last years, several transcriptome studies of MS brain tissues have been performed, and a number of possible pathomechanisms could be identified such as mitochondrial dysfunction, metabolic changes in astrocytes, inflammation and oxidative stress (Dutta, McDonough et al. 2006, Torkildsen, Stansberg et al. 2010, Fischer, Wimmer et al. 2013, Zeis, Allaman et al. 2015). A limitation of all these studies is the low number of tissue samples and cases and consequently the limited statistical power. The problem is further accentuated by the heterogeneity of MS, reflected by the variable clinical course, different clinical symptoms and imaging findings as well as variability in pathology. As part of our published studies (Zeis, Graumann et al. 2008, Zeis, Allaman et al. 2015, Zeis, Howell et al. 2018) we collected a large number of well-characterized human brain tissue samples from control and MS cases.

Here we compared the expression pattern of MS normal-appearing cortical grey matter with control GM in order to understand if there are alterations that may underlie or contribute to the formation of the wide-spread cortical lesions as an important aspect of MS pathology.

8.1.3 Material and Methods

Tissue selection and characterization

MS- and control tissue samples were provided by the UK MS Tissue Bank (UK Multicentre Research Ethics Committee, MREC/02/2/39), funded by the MS Society of Great Britain and Northern Ireland registered charity 207495. Further MS brain tissues were obtained from the archives of the Institute of Neuropathology at the University Medical Centre Göttingen. Additional control samples were provided by the Pathology Department of the University Hospital Basel. All cases were routinely screened by a neuropathologist to confirm diagnosis of MS and to exclude other confounding pathologies (Reynolds, Roncaroli et al. 2011). In total, 104 grey matter tissue blocks from 34 control cases and 101 normal-appearing grey matter tissue blocks from 51 MS cases were used for this study (Table 1). Criteria of in- and exclusion are described in Figure 4A. Tissues were characterized further by staining for NeuN (neurons), OLIG2 (oligodendrocytes), MOG (myelin), CD68 (microglia) (Figure 4B). Cryostat sections (12 µm) from fresh frozen tissue blocks were stained as described before (Zeis, Graumann et al. 2008, Zeis, Allaman et al. 2015). Antibodies and detailed protocols are described in Table 2A, B.

Table 1. Patient Data

A.

Cases	Sex	Cause of Death	p.m. time [h]	Age [a]	Disease Duration [a]	MS Type	*HLA-DRB1 *15:01*	# Brain Tissue Blocks	# Samples Microarray NAGM-CoGM	HLA-DRB1 expression
Control cases:										
C01	M	Myocardial infarction	8	70			Others	1		
C02	M	Cardiac failure, Pneumonia	14	65			Others	5		
C04	F	Acute pancreatitis	20	58			**15:01**	6		
C07	M	Rectal cancer, Pneumonia	9	89			Others	1	1	low
C09	F	Pneumonia	10	95			**15:01**	2	1	high
C10	F	Oesophagus cancer	9	85			Others	3		
C11	F	Bronchopneumonia, Cerebrovascular accident	9	93			Others	1	1	low
C13	M	Cardiogenic shock	21	73			Others	4	2	high
C14	M	Lung cancer, metastasised	26	77			Others	3	3	high
C15	M	Myocardial infarction	18	64			Others	4	4	low
C17	F	Congestive cardiac failure	24	84			Others	4	3	low
C18	M	Carcinoma of the tongue	22	35			**15:01**	6	4	high
C20	F	Ovarian cancer	13	60			Others	5	5	low
C21	M	Cerebrovascular accident, pneumonia	17	75			Others	4	9	low
C22	M	Prostate cancer, metastasised	22	88			Others	1		
C25	M	Bladder cancer, pneumonia	5	84			Others	3	4	low
C26	F	Breast cancer, metastasised	12	87			Others	1	2	low
C27	M	Renal failure, multiple myeloma	24	75			Others	1	2	high
C28	F	Cardiac failure	21	60			**15:01**	4		
C29	M	Pneumonia	20	60			Others	4		
C30	M	Pericardial tamponade	7	68			Others	4		
C31	M	Anaphylaxis	14	72			**15:01**	4		
C32	F	Pneumonia	16	71			**15:01**	4		
C33	F	Cardiac failure	12	83			Others	4		
C37	F	Pneumonia	14	72			Others	4		
C38	F	Pneumonia	3	88			Others	2		
C39	M	Acute cardiac death	10	69			**15:01**	6		
C44	F	Multi-organ failure	9	72			**15:01**	4		
C45	M	Cardio pulmonary degeneration, prostate cancer	22	77			Others	1	1	low
C47	M	Cardiac failure, acute erosive enteritis	15	53			Others	2		
C48	M	Asphyxia	11	61			**15:01**	2		
C49	F	Cardiac failure	16	77			Others	2		
C50	M	Cardiac failure	21	75			**15:01**	2		
	14 F 19 M		**Ø=15.0**	**Ø=73.2**			**10 15:01 23 Others**	**104**	**42**	
MS cases:										
M01	F	Breast cancer, pneumothorax	8	56	31	SPMS	Others	7	5	low
M02	F	Peritonitis	16	58	22	PPMS	Others	5	2	low
M03	F	NA	18	78	14	SPMS	Others	3	1	low
M04	F	Respiratory failure	21	42	18	SPMS	**15:01**	1		
M05	F	Sepsis	19	74	26	SPMS	**15:01**	1		high (*)
M06	F	Pneumonia	6	58	21	PPMS	**15:01**	6	10	high
M07	F	Pulmonary embolus, pneumonia	17	45	20	PPMS	Others	2		low (*)
M09	M	Aspiration pneumonia	8	75	38	SPMS	Others	1	1	high
M10	F	Pneumonia	8	72	41	SPMS	Others	1	2	high
M11	M	Pneumonia	26	66	31	SPMS	Others	1		
M12	F	NA	11	69	31	NA	**15:01**	3		high (*)
M13	M	Pneumonia	11	63	39	SPMS	Others	2		low (*)
M14	F	Pneumonia	9	77	31	PPMS	Others	4	3	low
M15	F	Multiple Sclerosis	15	51	21	SPMS	Others	2	2	high
M16	F	Adenocarcinoma of unknown primary	6	56	17	PRMS	**15:01**	1	1	high
M17	F	Respiratory infection	10	49	19	SPMS	Others	1		
M18	F	Pneumonia	13	66	30+	NA	**15:01**	3		
M20	F	Pneumonia	21	86	56	NA	Others	2		
M21	F	Pneumonia	11	86	36	SPMS	Others	1		
M22	F	Multiple sclerosis	21	77	22	PPMS	**15:01**	1	1	high
M23	F	Lung cancer, metastasised	5	78	42	SPMS	**15:01**	4	5	high
M24	F	Renal failure	31	49	18	SPMS	Others	2	1	low
M26	F	Bowel blockage, heart failure	24	71	35	SPMS	**15:01**	1		high (*)
M27	F	Pneumonia	9	49	25	SPMS	Others	1		
M28	F	Pneumonia	22	54	20	SPMS	**15:01**	3		high (*)
M30	F	Pneumonia	7	77	21	SPMS	Others	2	1	low
M31	M	Urinary tract infection, multiple sclerosis	12	53	11	SPMS	Others	1		low (*)
M32	F	Pneumonia	18	39	21	PRMS	**15:01**	1	4	high
M33	M	Pneumonia	19	38	17	PRMS	Others	2	1	low
M34	M	NA	9	92	54	PPMS	**15:01**	1	2	high
M36	M	Pneumonia	16	44	16	SPMS	**15:01**	2		high (*)
M40	M	Respiratory failure	10	40	9	SPMS	**15:01**	3		
M42	F	Multiple sclerosis	12	50	31	SPMS	Others	2		low (*)
M43	F	Pneumonia	12	34	NA	SPMS	**15:01**	1		high (*)
M44	F	Small bowel obstruction	13	80	36	SPMS	Others	2	1	low
M46	F	Multi-organ failure, sepsis	28	45	6	SPMS	**15:01**	2	3	high
M47	M	Intestinal obstruction	12	37	27	PPMS	Others	2		low (*)
M48	F	Pneumonia	24	78	47	SPMS	Others	1	2	low
M51	F	Pneumonia	12	59	27	PPMS	Others	3	2	high
M52	M	Pneumonia	24	45	25	SPMS	**15:01**	1		high (*)
M53	F	Sepsis, pneumonia	16	47	17	SPMS	**15:01**	4	4	high
M54	M	Multiple Sclerosis	9	45	18	SPMS	**15:01**	1		high (*)
M55	F	Multiple Sclerosis	26	37	17	SPMS	Others	2		
M56	F	Pneumonia	22	88	32	PPMS	**15:01**	1	2	high
M57	F	COPD	17	58	16	PPMS	Others	2	3	low
M58	F	Multiple Sclerosis	7	80	37	SPMS	**15:01**	1		
M59	F	Multiple Sclerosis	13	42	11	SPMS	**15:01**	2		high (*)
M60	F	Respiratory Failure	9	59	4	PPMS	**15:01**	2	3	high
M61	M	Pancreatic Cancer	10	61	26	SPMS	**15:01**	1	2	high
	37 F 12 M		**Ø=14.8**	**Ø=59.9**	**Ø=25.5**	**32 SPMS 11 PPMS 3 PRMS 3 NA**	**24 15:01 25 Others**	**101**	**64**	

B. Additional Cases for Immunofluorescence Colocalization

Patient	Sex	Cause of Death	Age [a]	Disease duration [a]	MS Type
Control cases:					
C1	M	Sepsis, multi-organ failure	60		
C2	F	Breast cancer	38		
C3	F	Pulmonary embolism	38		
C4	M	Head trauma, laceration	65		
	2 F **2 M**		**Ø=50.3**		
MS cases:					
MS1	F	NA	61	18	CPMS
MS2	F	NA	45	n/a	CPMS
MS3	M	NA	71	n/a	CPMS
MS4	M	NA	63	18	SPMS
MS5	M	NA	28	2.5	PPMS
MS6	F	NA	63	n/a	CPMS
MS7	M	NA	63	>15	CPMS
MS8	M	NA	59	22	SPMS
MS9	M	NA	58	26	SPMS
	3 F **6 M**		**Ø=56.8**	**Ø=16.9**	**3 SPMS** **5 CPMS** **1 PPMS**

Table shows the patient data. (A) Carriers of the *HLA-DRB1*15:01* allele are highlighted in bold. High, respective low, expressers which were characterized using the gene expression data from the grey matter lesion microarray are marked with an asterisk. (B) Additional cases from Göttingen, Germany, used for the immunofluorescence colocalization. Abbreviations: CoGM: Control case cortical grey matter; CPMS: Chronic progressive MS; NA: Data not available; NAGM: Normal-appearing cortical grey matter; p.m. time: Post-mortem time; PPMS: Primary progressive MS; PRMS: Progressive-relapsing MS; SPMS: Secondary progressive MS.

Table 2. Antibodies and staining protocols

A.

Antibody	Company	Cat.Nr.	Dilution	Tissue
Primary Antibodies				
Peroxidase				
mouseaMOG (Clone Z12)	kindly provided by Prof. R.Reynolds, Cambridge, UK	-	1:200	FF
mouseaNEUN	Millipore, Billerica, Massachusetts, USA	MAB377	1:500	FF
rabbitaOLIG2	Millipore, Billerica, Massachusetts, USA	ab9610	1:500	FF
mouseaCD68	Abcam, Cambridge, UK	ab845	1:500	FF
rabbitaHLA-DRB1	GeneTex, Irvine, California, USA	GTX104919	1:200	FF
Fluorescence colocalization				
rabbitaHLA-DRB1	GeneTex, Irvine, California, USA	GTX104919	1:200	FF / PE
HLA-DR (L243)	kindly provided by Prof. R.Martin	-	1:200	FF
mouseaCD68	kindly provided by Prof. H.-J. Radzun, Göttingen, DE	-	1:50	PE
chickenaGFAP	Aves Labs, Davis, California, USA	AB_10672299	1:200	FF
mouseaGFAP	Synaptic Systems, Göttingen, Germany	134B1	1:300	PE
mouseaNEUN	Millipore, Billerica, Massachusetts, USA	MAB377	1:200	FF
rabbitaNEUN	Abcam, Cambridge, UK	ab177487	1:3000	PE
mouseaOLIG2	Sigma-Aldrich, St. Louis, Missouri, USA	SAB1404798	1:200	FF
rabbitaOLIG2	IBL International, Hamburg, Germany	JP18953	1:300	PE
mouseaColIV	Sigma-Aldrich, St. Louis, Missouri, USA	C1926	1:200	FF
mouseaCD34 Class II	Dako, Santa Clara, California, USA	GA63261-2	1:50	PE
Secondary Antibodies				
donkeyarabbit-Biotin	Jackson ImmunoResearch, Cambridgeshire, UK	711-065-152	1:500	FF
donkeyamouse-Biotin	Jackson ImmunoResearch, Cambridgeshire, UK	715-065-151	1:500	FF
donkeyagoat-Biotin	Jackson ImmunoResearch, Cambridgeshire, UK	705-065-147	1:500	FF
donkeyarabbit-Cy2	Jackson ImmunoResearch, Cambridgeshire, UK	715-225-151	1:500	FF
donkeyamouse-Cy3	Jackson ImmunoResearch, Cambridgeshire, UK	715-165-151	1:500	FF
goatarabbit-AlexaFluor488	Life Technologies, Carlsbad, California, USA	A-11034	1:100	PE
goatamouse-AlexaFluor555	Life Technologies, Carlsbad, California, USA	A-21424	1:100	PE
Alexa Fluor 555 Tyramide Super Boost Kit	Thermo Fisher Scientific, Waltham, Massachusetts, USA	B40933	-	PE

B.

Staining	Fixation		Permeabilization		Antigen Retrieval		Background Removal		Permeabilization		Blocking		1st Antibody		2nd Antibody		Signal Amplification		Color Reaction	
	Method	Time (min)	Solution	Time (min)	Method	Time (min)	Solution	Time (min)	Solution	Time (min)	Solution	Time (min)	Temp.	Time	Temp.	Time (min)	Method	Time (min)	Method	Time (min)
MOG	4% PFA in PBS, RT	10	-		-		80% Methanol, 0.6% H202 in PBS, RT	30	100% Methanol, -20°C	8	1% NDS, 0.1% Triton-X100, 0.05% Tween-20 in PBS	60	4°C	overnight	RT	60	ABC Kit	30	AEC	8
NeuN	4% PFA in PBS, RT	10	-		-		0.6% H2O2 in PBS, RT	30	-		1% NDS, 0.1% Triton-X100, 0.05% Tween-20 in PBS	60	4°C	overnight	RT	60	ABC Kit	30	AEC	6
OLIG2	4% PFA in PBS, RT	3	-		-		0.6% H2O2 in PBS, RT	30	-		1% NDS, 0.3% Triton-X100, 0.15% Tween-20 in PBS	60	4°C	overnight	RT	60	ABC Kit	30	AEC	6
CD68	4% PFA in PBS, RT	10	-		-		0.6% H2O2 in PBS, RT	30	-		1% NDS, 0.1% Triton-X100, 0.05% Tween-20 in PBS	60	4°C	overnight	RT	60	ABC Kit	30	AEC	6
HLA-DRB1	4% PFA in PBS, 4°C	overnight	100% Acetone, 4°C	5	10mM Citrat Buffer pH 6.0 (90°C)	30	0.1% H2O2 in PBS, RT	30	-		10% NDS in PBS	60	4°C	overnight	4°C	overnight	ABC Kit	30	AEC	8

Table shows antibodies (A) used for the immunohistochemical and immunofluoresecence stainings and protocols (B) used for the immunohistochemical stainings. Abbreviations: FF: fresh frozen; NDS: normal donkey serum; PE: Paraffin-embedded; RT: Room temperature.

Ethical approvals

Ethical approvals for all human tissues used were given by the UK Multicentre Research Ethics Committee, MREC/02/2/39 for the cases from London, by the Ethics Committee of the University Hospital Basel for all cases from Basel and by the ethical review committee of the University Medical Center Göttingen (#19/09/10) for all cases from Göttingen.

RNA isolation and quality assessment

Total RNA from grey matter tissue was isolated using the Zymo ZR RNA Microprep Kit (Zymo Research, Irvine, CA, USA) as described before(Zeis, Allaman et al. 2015). Degraded (RIN < 6) and/or contaminated (260/280 nm ratio < 1.8; 230/280 nm ratio < 1.8) samples were excluded from the study.

Microarray analysis and statistical analysis

In total, 42 tissue samples from 14 control as well as 64 tissue samples from 25 MS cases were used for the gene expression analysis between normal-appearing grey matter and control GM (Table 1). To minimize experimental bias microarray experiments were performed together. All samples used for the gene expression study originated from the UK MS Tissue Bank. Gene expression profiling was done using the Illumina cDNA-mediated annealing, selection, extension, and ligation (DASL) assay according to the manufacturer's protocol (Fan, Yeakley et al. 2004) (Part No. 15018210, Revision history D, April 2012, Illumina, San Diego, CA, USA). Beadchips were scanned by the iScan Array scanner (Illumina). All subsequent data analyses were performed using the statistical software R (R core development Team 2008; R version 3.5.0). Specifically, the Bioconductor packages beadarray (version 2.30.0) and illuminaHumanWGDASLv4.db (version 1.26.0) were used for reading-in data files and for probe annotation (probes n=48107). Between-array normalization was performed by variance stabilizing transformation followed by a quantile normalization using functions from the Bioconductor package lumi (version 2.32.0). Only probes mapping to an ENTREZ gene ID were retained. Probes with quality status 'bad' were removed. Bad quality probes are probe matches repeat sequences, intergenic or intronic regions, or is unlikely to provide specific signal for any transcript (according to illuminaHumanWGDASLv4 annotation). Since the resulting probes (n=25081) were still not unique, we selected the probe with the highest variance across all samples, neglecting sample values, which fall into the expression range of negative control probes. This way, each gene is represented by the probe, which contains most information on potential expression differences, but ignores probes, which appear artificially regulated due to false-negative regulation introduced by SNPs. This strategy gave rise to 17908 unique gene-level probes.

HLA genotyping

HLA genotyping was performed by Histogenetics (NY, USA). Allelic variants were typed by sequencing at high-resolution (3-field). Alleles bearing suffix 'G' in the A locus have identical sequences in exon 2 and exon 3 antigen recognition sites. Alleles bearing suffix 'G' in the DRB locus have identical sequences in exon 2 antigen recognition sites. Genotypes are shown in Table 3.

Immunofluorescence colocalization

Immunofluorescent colocalization was performed as described before (Zeis, Graumann et al. 2008, Zeis, Allaman et al. 2015). As tissue preservation is not optimal in fresh frozen tissues, further paraffin-embedded tissue blocks were stained for colocalization. Paraffin-embedded tissue sections (2-3 µm) were deparaffinized in xylene, rehydrated and transferred to 3% H_2O_2 in PBS for 20 min at 4°C to block the endogenous peroxidase. After three washing steps with PBS the sections were incubated with blocking buffer (10% fetal calf serum in PBS) for at least 20 minutes to reduce unspecific antibody binding. Primary antibodies (Table 2A) were diluted in blocking buffer and incubated overnight at 4°C and then washed three times with PBS. Secondary antibodies were incubated for 1-2 hours (Table 2A).

Histological quantification

HLA-DRB1 protein expression was measured with Fiji (image processing package including ImageJ) (Schindelin, Arganda-Carreras et al. 2012) using the count objects algorithm with the following parameters: lower threshold 0, upper threshold 120 in green channel of RGB colour space, size of objects 10µm^2-100µm^2 and circularity 0.25-1.00. Cortical lesions were defined as areas with complete loss of anti-MOG staining or areas with reduced myelin density clearly demarcated from surrounding normal-appearing tissue. Only cortical grey matter ranging from the white matter to the meninges and with all six neuronal layers visible in the adjacent NeuN staining was used. Cortical normal-appearing grey matter and grey matter lesion areas were outlined in Adobe Photoshop CS6 (Version 13.0 x64, Adobe Systems, CA, USA), exported and evaluated for area (in mm^2) in ImageJ software ((Schindelin, Arganda-Carreras et al. 2012, Rueden, Schindelin et al. 2017), Version 1.51s, Fiji distribution, NIH, Maryland, USA). A schematic drawing is shown in Figure 8C.

Statistical analysis

All statistical analyses were performed using R (R Development Core Team 2010). A p-value respectively FDR-adjusted p-value smaller 0.05 was considered statistically significant. Expression data were analyzed using R and the Bioconductor package limma (version 3.36.5). Statistical analysis was performed using a linear model with disease group and sex as factors. Since some patients contributed multiple tissue samples (tissue blocks), we additionally distinguished these "technical" replicates from true biological replicates (patients) in the model to avoid a potential inflation of significance by pseudo-replication. Specifically, the duplicateCorrelation function of the limma package was used to estimate a consensus

correlation between technical replicates and this value together with patient ID as a block factor entered into the model fit function. To test the correlation between HLA-DRB1 and HLA-DRA gene expression, a linear model was used (Figure 5J). To test the influence of the HLA-DRB1*15:01 genotype and the HLA-DRB1 gene expression on the demyelinated grey matter lesion area per total grey matter area, p-values were derived from a linear model weighted by number of tissue blocks per patient (Figure 8D). For all other statistical tests, a two-sided welch t-test was used.

Data availability

The gene expression data discussed in this publication was deposited in NCBI's Gene Expression Omnibus (Edgar, Domrachev et al. 2002), accession number GSE131282 (https://www.ncbi.nlm.nih.gov/geo/query/acc.cgi?acc=GSE131282).

Table 3. Human leukocyte antigen genotyping

Patient	HLA-A1	HLA-A2	HLA-DRB11	HLA-DRB12	HLA-DRB31	HLA-DRB32	HLA-DRB41	HLA-DRB42	HLA-DRB51	HLA-DRB52
C01	02:01:01G	24:02:01G	**04:01:01**	16:01:01	-	-	01:01:01G	-	02:02:01G	-
C02	24:02:01G	26:01:01G	11:04:01	12:01:01G	02:02:01G	02:02:01G	-	-	-	-
C04	02:01:01G	02:01:01G	**15:01:01G**	16:01:01	-	-	-	-	01:01:01	02:02:01G
C07	02:01:01G	03:01:01G	**03:01:01G**	**03:01:01G**	01:01:02G	02:02:01G	-	-	-	-
C09	02:01:01G	29:02:01G	01:01:01G	**15:01:01G**	-	-	-	-	01:01:01	-
C10	02:01:01G	31:01:02G	**04:01:01**	**04:04:01**	-	-	01:01:01G	01:01:01G	-	-
C11	01:01:01G	03:01:01G	**03:01:01G**	**04:01:01**	01:01:02G	-	01:01:01G	-	-	-
C13	01:01:01G	33:01:01	01:02:01	**03:01:01G**	01:01:02G	-	-	-	-	-
C14	02:01:01G	32:01:01G	**03:01:01G**	16:01:01	01:01:02G	-	-	-	02:02:01G	-
C15	02:01:01G	23:01:01G	01:01:01G	11:04:01	02:02:01G	-	-	-	-	-
C17	02:01:01G	68:01:02G	**04:01:01**	09:01:02G	-	-	01:01:01G	01:01:01G	-	-
C18	01:01:01G	01:01:01G	14:54:01	**15:01:01G**	02:02:01G	-	-	-	01:01:01	-
C20	01:01:01G	02:05:01	04:02:01	13:05:01	02:02:01G	-	01:01:01G	-	-	-
C21	01:01:01G	11:01:01	**04:04:01**	11:01:01	02:02:01G	-	01:01:01G	-	-	-
C22	02:01:01G	23:01:01G	01:01:01	11:04:01	02:02:01G	-	-	-	-	-
C25	01:01:01G	01:01:01G	**03:01:01G**	07:01:01G	01:01:02G	-	01:01:01G	-	-	-
C26	01:01:01G	02:01:01G	04:08:01	07:01:01G	-	-	01:01:01G	01:01:01G	-	-
C27	01:01:01G	01:01:01G	**03:01:01G**	10:01:01	01:01:02G	-	-	-	-	-
C28	24:02:01G	26:01:01G	07:01:01G	**15:01:01G**	-	-	01:01:01G	-	01:01:01	-
C29	02:01:01G	31:01:02G	04:08:01	14:54:01	02:02:01G	-	01:01:01G	-	-	-
C30	11:01:01	30:01:01	07:01:01G	16:02:01	-	-	01:01:01G	-	02:02:01G	
C31	03:01:01G	03:01:01G	**15:01:01G**	**15:01:01G**	-	-	-	-	01:01:01	01:01:01
C32	11:01:01	32:01:01	11:01:01	**15:01:01G**	02:02:01G	-	-	-	01:01:01	-
C33	03:01:01G	32:01:01	**04:04:01**	13:02:01	03:01:01G	-	01:01:01G	-	-	-
C37	02:01:01G	30:01:01	07:01:01G	11:01:01	02:02:01G	-	01:01:01G	-	-	-
C38	32:01:01G	68:01:02G	10:01:01	11:01:01	02:02:01G	-	-	-	-	-
C39	03:01:01G	68:01:01G	01:02:01	**15:01:01G**	-	-	-	-	01:01:01	-
C44	02:01:01G	68:01:02G	**15:01:01G**	**15:01:01G**	-	-	-	-	01:01:01	01:01:01
C45	01:01:01G	68:02:01G	13:02:01	13:02:01	03:01:01G	03:01:01G	-	-	-	-
C47	02:01:01G	24:02:01G	**03:01:01G**	14:54:01	01:01:02G	02:02:01G	-	-	-	-
C48	02:01:01G	32:01:01G	13:02:01	**15:01:01G**	03:01:01G	-	-	-	01:01:01	-
C49	02:01:01G	03:01:01G	03:37	13:02:01	02:02:01G	03:01:01G	-	-	-	-
C50	03:01:01G	03:01:01G	**03:01:01G**	**15:01:01G**	01:01:02G	-	-	-	01:01:01	-
M01	01:01:01G	03:01:01G	**03:01:01G**	**04:01:01**	01:01:02G	-	01:01:01G	-	-	-
M02	02:01:01G	03:01:01G	01:01:01	**04:04:01**	-	-	01:01:01G	-	-	-
M03	01:01:01G	11:01:01G	**03:01:01G**	13:02:01	01:01:02G	03:01:01G	-	-	-	-
M04	03:01:01G	68:01:02G	**04:01:01**	**15:01:01G**	-	-	01:01:01G	-	01:01:01	-
M05	02:01:01G	24:02:01G	**04:01:01**	**15:01:01G**	-	-	01:01:01G	-	01:01:01	-
M06	24:02:01G	31:01:02G	**15:01:01G**	**15:01:01G**	-	-	-	-	01:01:01	01:01:01
M07	24:02:01G	68:02:01G	13:02:01	**13:03:01**	01:01:02G	03:01:01G	-	-	-	-
M09	11:01:01G	11:01:01G	01:01:01G	07:01:01G	-	-	01:01:01G	-	-	-
M10	02:01:01G	03:01:01G	01:01:01	**08:01:01G**	-	-	-	-	-	-
M11	11:01:01	29:02:01G	07:01:01G	07:01:01G	-	-	01:01:01G	01:01:01G	-	-
M12	02:01:01G	02:01:01G	07:01:01G	**15:01:01G**	-	-	01:01:01G	-	01:01:01	-
M13	02:06:01	03:01:01G	**08:01:01G**	09:01:02G	-	-	01:01:01G	-	-	-
M14	02:01:01G	11:01:01	**04:04:01**	14:54:01	02:02:01G	-	01:01:01G	-	-	-
M15	26:01:01	32:01:01	01:01:01	**04:01:01**	-	-	01:01:01G	-	-	-
M16	01:01:01G	23:01:01G	**15:01:01G**	11:01:01G	02:02:01G	-	-	-	01:01:01	-
M17	02:01:01G	24:02:01G	**04:04:01**	13:01:01	01:01:02G	-	01:01:01G	-	-	-
M18	01:01:01G	03:01:01G	**03:01:01G**	**15:01:01G**	01:01:02G	-	-	-	01:01:01	-
M20	02:01:01G	03:01:01G	01:01:01	01:01:01	-	-	-	-	-	-
M21	02:01:01G	02:01:01G	01:01:01	04:07:01G	-	-	01:01:01G	-	-	-
M22	01:01:01G	68:01:01G	**04:04:01**	**15:01:01G**	-	-	01:01:01G	-	01:01:01	-
M23	01:01:01G	03:01:01G	**03:01:01G**	**15:01:01G**	01:01:02G	-	-	-	01:01:01	-
M24	29:02:01G	32:01:01	**07:01:01G**	11:01:01	02:02:01G	-	01:01:01G	-	-	-
M26	01:01:01G	03:01:01G	**03:01:01G**	**15:01:01G**	01:01:02G	-	-	-	01:01:01	-
M27	01:01:01G	11:01:01	01:01:01	14:54:01	02:02:01G	-	-	-	-	-
M28	03:01:01G	68:01:02G	**04:01:01**	**15:01:01G**	-	-	01:01:01G	-	01:01:01	-
M30	02:01:01G	11:01:01G	**03:01:01G**	**03:01:01G**	01:01:02G	01:01:02G	-	-	-	-
M31	24:02:01G	24:02:01G	07:01:01G	11:04:01	02:02:01G	-	01:01:01G	-	-	-
M32	01:01:01G	24:02:01G	**03:01:01G**	**15:01:01G**	01:01:02G	-	-	-	01:01:01	-
M33	31:01:02G	31:01:02G	**04:04:01**	**13:03:01**	01:01:02G	-	01:01:01G	-	-	-
M34	01:01:01G	03:01:01G	01:01:01	**15:01:01G**	-	-	-	-	01:01:01	-
M36	01:01:01G	26:01:01	07:01:01G	**15:01:01G**	-	-	01:01:01G	-	01:01:01	-
M40	11:01:01	24:02:01G	**04:01:01**	**15:01:01G**	-	-	01:01:01G	-	01:01:01	-
M42	01:01:01G	11:01:01	**03:01:01G**	**08:01:01G**	01:01:02G	-	-	-	-	-
M43	01:01:01G	30:02:01G	**03:01:01G**	**15:01:01G**	01:01:02G	-	-	-	01:01:01	-
M44	01:01:01G	01:01:01G	**03:01:01G**	07:01:01G	01:01:02G	-	01:01:01G	-	-	-
M46	01:01:01G	03:01:01G	**03:01:01G**	**15:01:01G**	02:02:01G	-	-	-	01:01:01	-
M47	24:02:01G	32:01:01G	04:08:01	13:01:01	02:02:01G	-	01:01:01G	-	-	-
M48	02:01:01G	29:02:01G	**04:01:01**	07:01:01G	-	-	01:01:01G	01:01:01G	-	-
M51	03:01:01G	11:01:01	01:01:01	01:03	-	-	-	-	-	-
M52	24:02:01G	66:01:01	**13:03:01**	**15:01:01G**	01:01:02G	-	-	-	01:01:01	-
M53	02:01:01G	11:01:01	**15:01:01G**	**15:01:01G**	-	-	-	-	01:01:01	01:01:01
M54	02:01:01G	11:01:01	**15:01:01G**	**15:01:01G**	-	-	-	-	01:01:01	01:01:01
M55	01:01:01G	03:01:01G	**03:01:01G**	**15:01:01G**	01:01:02G	-	-	-	01:01:01	-
M56	02:01:01G	29:02:01G	07:01:01G	**15:01:01G**	-	-	01:01:01G	-	01:01:01	-
M57	02:01:01G	02:01:01G	13:01:01	13:02:01	02:02:01G	03:01:01G	-	-	-	-
M58	32:01:01	68:02:01G	**13:03:01**	**15:01:01G**	01:01:02G	-	-	-	01:01:01	-
M59	02:01:01G	32:01:01	07:01:01G	**15:01:01G**	-	-	01:01:01G	-	01:01:01	-
M60	24:02:01G	26:01:01	07:01:01G	**15:01:01G**	-	-	01:01:01G	-	01:01:01	-
M61	02:01:01G	03:01:01G	**15:01:01G**	**15:01:01G**	-	-	-	-	01:01:01	01:01:01

Table shows the HLA genotypes of all cases used in this study. Marked in red and bold is the *HLA-DRB1*15:01* allele, marked in bold are other MS associated alleles described previously, namely *HLA-DRB1*03:01*, **04:01*, **04:04* and **13:03* (Patsopoulos, Barcellos et al. 2013) and **08:01* (Moutsianas, Jostins et al. 2015). Alleles bearing suffix 'G' in A locus has identical sequences in exon 2 and exon 3 antigen recognition sites. Alleles bearing suffix 'G' in DRB locus has identical sequences in exon 2 antigen recognition sites. Allele Database Version used in the report is 3.17.0, July 2014 (Robinson, Malik et al. 2000, Robinson, Halliwell et al. 2015). Abbreviations: NA: not available, id est genotyping failed.

8.1.4 Results

HLA-DRB1 is significantly upregulated in MS normal-appearing grey matter compared to control grey matter

We investigated the gene expression in MS normal-appearing grey matter and control cases. All tissues were characterized histopathologically and tissues with signs of possible confounding pathologies were excluded (Figure 4A). As a result, only tissues without signs of demyelination, neuronal degeneration, oligodendrocyte loss and without signs of inflammation such as microglia activation and macrophage infiltration were included in the microarray study (Figure 4B). Differential gene expression analysis between MS normal-appearing grey matter and control grey matter revealed HLA-DRB1 as the most significant differentially regulated gene (Figure 5A) (FC=4.62, adj.p-value=0.013). Besides HLA-DRB1, we detected a trend towards upregulation for the integrin subunit beta 1 binding protein 1 (ITGB1BP1), protein kinase cAMP-dependent type 1 regulatory subunit alpha (PRKAR1A), long intergenic non-protein coding RNA 115 (LINC00115), mitogen-activated protein kinase 7, also known as TGF1 (MAP3K7), and SLIT-ROBO Rho GTPase activating protein 2 (SRGAP2) (Figure 5A). Further analysis of HLA-DRB1 expression showed that the distribution of HLA-DRB1 expression was bimodal within both the MS and the control group (Figure 5B). Of special interest is that the majority of individuals with high HLA-DRB1 expression were in the MS group. As HLA genes often show tight linkage disequilibrium patterns (Kennedy, Ozbek et al. 2017), we further investigated the expression of DRB5, DQA1 and DQB1 as certain alleles of these genes were reported to form a tight linkage group within the DR15 haplotype (Yaouanq, Semana et al. 1997). The MS-associated *DR15* haplotype consists of five alleles, namely *DRA*01*, *DRB1*15:01*, *DRB5*01:01*, *DQA1*01:02* and *DQB1*06:02*. Although not significantly differentially expressed between MS- and control cases (FC=4.45, adj.p-value=0.529), we also identified a bimodal distribution for HLA-DRB5 (Figure 5C). HLA-DQA1 and HLA-DQB1 expression levels were normally distributed (Figure 5D, E), with HLA-DQB1 expression at the lower detection limit.

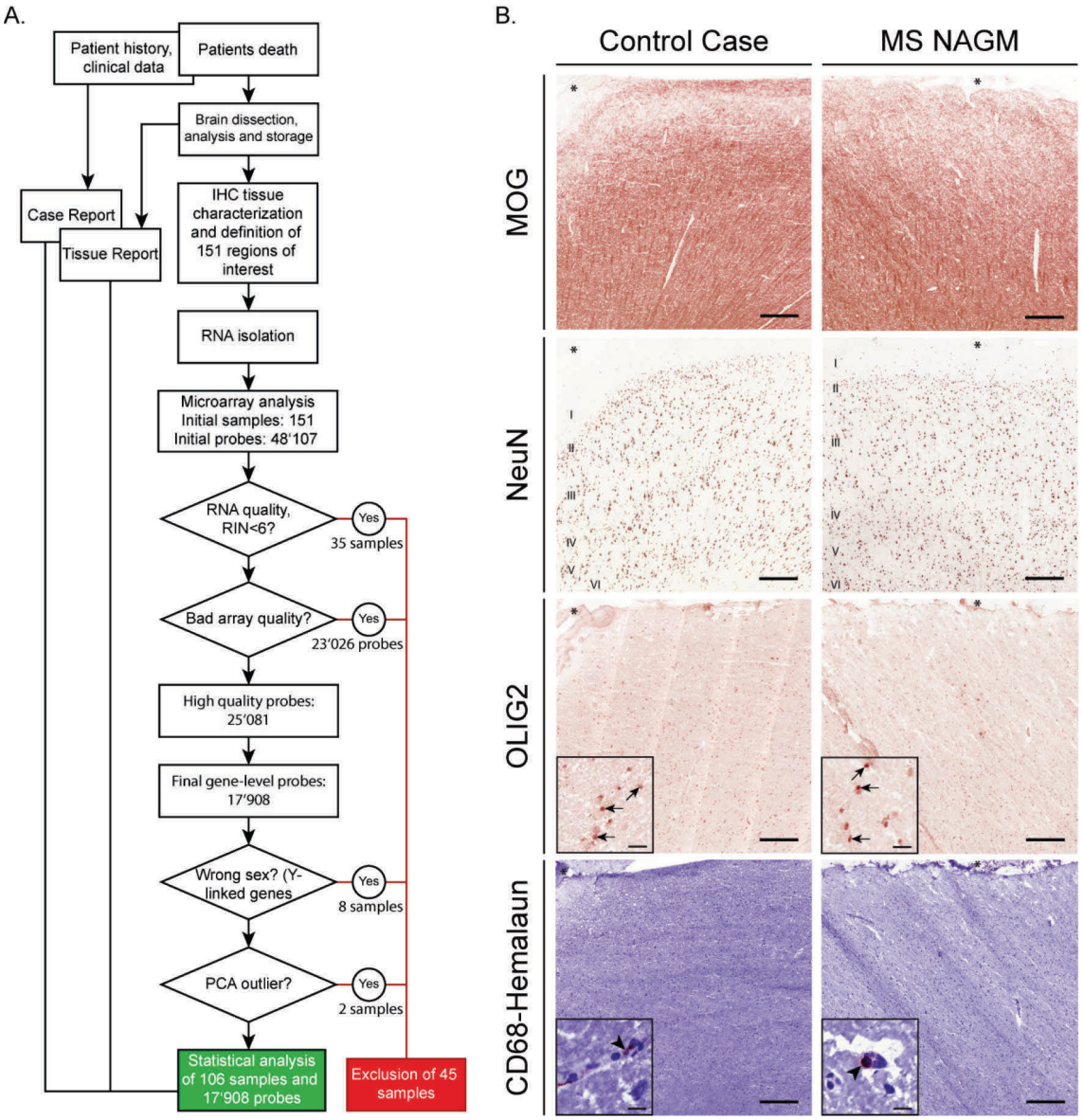

Figure 4. Tissue processing for microarray and tissue characterization

(A) Flow chart to illustrate the process from patient's death to statistical analysis of the gene expression microarray. After dissection of the brain and exclusion of confounding pathologies, the tissue blocks were sent to Basel, Switzerland. There, an immunohistochemical characterization was performed, any tissue with bad preservation was excluded and regions of interest were selected. After RNA isolation the RNA integrity index (RIN) was measured and samples with RIN smaller than 6 were excluded. Sample mix up was checked by wrong sex and by principal component analysis. (B) Representative images of control cortical grey matter (case C30) and MS normal-appearing grey matter (case MS08, asterisk delineates the meninges, I-VI indicate the six neuronal layers). Normal-appearing grey matter was defined as no loss of MOG, NeuN or OLIG2 (inset, arrows) staining compared to control cases, and no increase in CD68 compared to controls; i.e. occasional CD68+ staining intra- or perivascular (inset, arrowheads) and nearly no CD68+ staining in the tissue. Scale bars: 250µm; inset Olig2: 20µm, inset CD68: 10 µm.

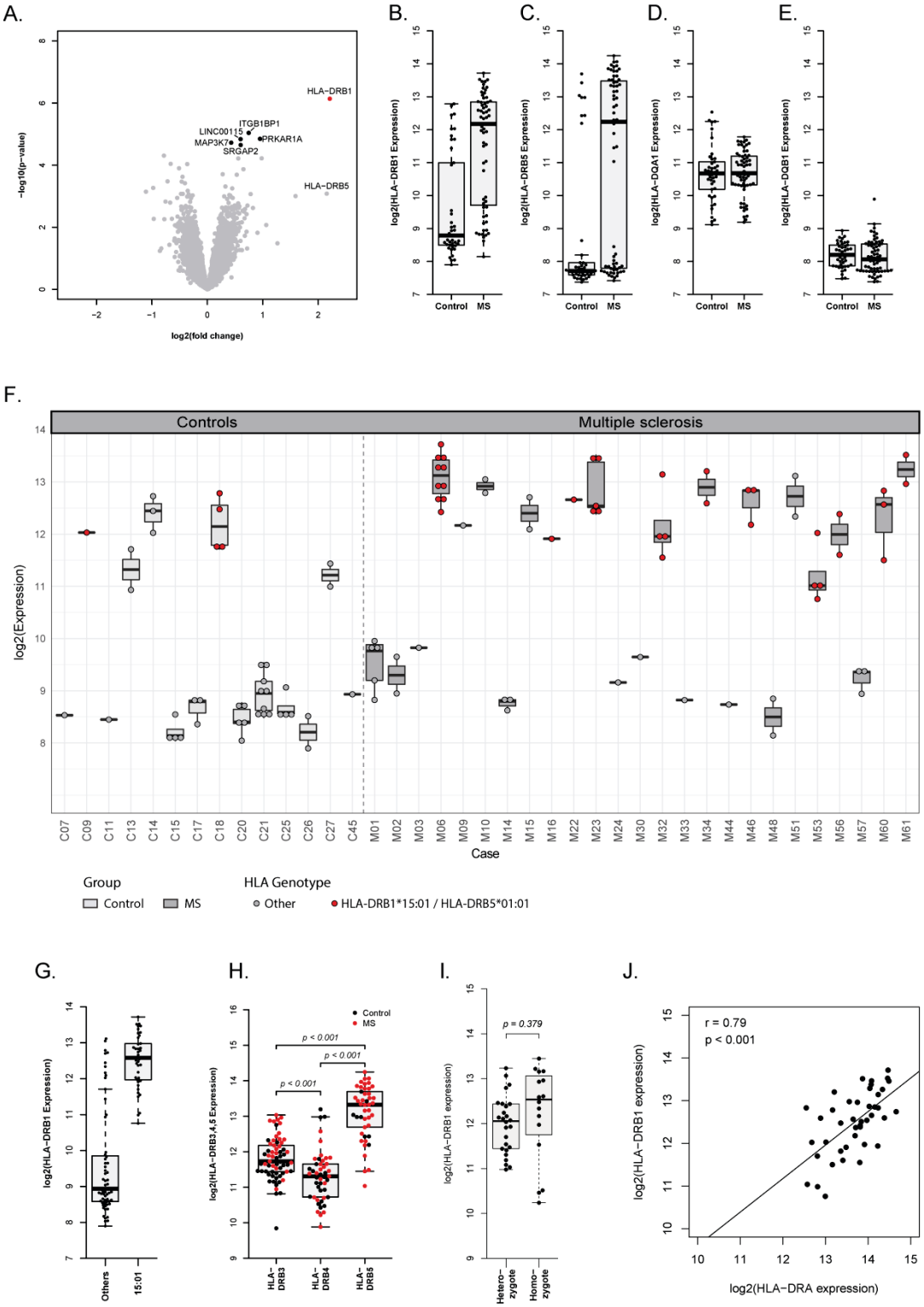

Figure 5. Differential gene expression in MS normal-appearing grey matter versus control case cortical grey matter

(A) Volcano plot of the differential gene expression analysis between MS normal-appearing grey matter and control grey matter (GM) revealed HLA-DRB1 as the most significant differentially regulated gene (FC=4.62, adj.p-value=0.013, marked in red). Differentially expressed genes with an adjusted p-value between 0.05 and 0.1 are marked in black. This was the case for ITGB1BP1 (FC=1.67, adj.p-value=0.065), PRKAR1A (FC=1.93, adj.p-value=0.065), LINC00115 (FC=1.5, adj.p-value=0.065), MAP3K7 (FC=1.34, adj.p-value=0.067), and SRGAP2 (FC=1.5, adj.p-value=0.067). Boxplots show the log2 gene expression of HLA-DRB1 (B), HLA-

DRB5 (C), and HLA-DQA1 (D) and HLA-DQB1 (E) between MS normal-appearing grey matter and CoGM. HLA-DRB1 is significantly differentially expressed between MS normal-appearing grey matter and control grey matter (B). Both, HLA-DRB1 (B) and HLA-DRB5 (C) show a bimodal expression pattern in MS and control tissue, whereas the expression of HLA-DQA1 (D) was normally distributed within the sample groups and HLA-DQB1 (E) was at the lower detection limit. (F) Boxplots show log2 of the HLA-DRB1 gene expression in all tissue samples and in all cases used for the microarray analysis. All cases with the HLA-DRB1*15:01 genotype show a high HLA-DRB1 expression (red dots). (G) HLA-DRB1 expression between samples from cases carrying *the HLA-DRB1*15:01* or other *HLA-DRB1* alleles. Boxplot shows that all *HLA-DRB1*15:01* tissue samples belong to the HLA-DRB1 high expresser group. (H) HLA-DRB3, 4, and 5 expressions of all samples. (I) Comparison of hetero- and homozygote carriers of the *HLA-DRB1*15:01* allele. (J) Correlation of HLA-DRB1 with HLA-DRA within the *HLA-DRB1*15:01* positive samples. (H, I) p-values are derived from a two-sided Welch t-test, (J) p-value is derived from a linear model.

*High cortical HLA-DRB1 expression is associated with the HLA-DRB1*15:01 haplotype*

The bimodal HLA-DRB1 expression pattern prompted us to investigate whether HLA-DRB1 expression in all tissue samples from one individual shows this mode of expression. This analysis revealed that single cases either expressed HLA-DRB1 at high or low levels in both MS and control cases (Figure 5F). As *HLA-DRB1*15:01* is strongest associated with MS risk (Patsopoulos, Barcellos et al. 2013, Moutsianas, Jostins et al. 2015) and HLA-DRB5 showed a similar expression distribution, we genotyped all cases for *HLA-DRB1*, *3*, *4* and *5* at a 3-field resolution (Table 3). As expected, we detected a trend towards higher frequency of the *HLA-DRB1*15:01* allele among the MS cases compared to control cases (Fisher's exact test, p=0.083, OR=4.5, 95%-CI=[0.8;50.2]) (for review see: Hollenbach and Oksenberg 2015). Gene expression analysis based on the *HLA-DRB1* genotype revealed that the bimodal distribution was linked to the *HLA-DRB1* genotype with individuals with the *HLA-DRB1*15:01* allele always showing high transcriptional expression of HLA-DRB1 (n=106 samples, Figure 5F, G). In contrast to HLA-DRB1, which is expressed in every case, only 11 MS and 1 control case turned out to carry the *HLA-DRB5* gene (Table 3). As expected, all individuals genotyped positively for *HLA-DRB5*01:01* allele were also positive for *HLA-DRB1*15:01* (Table 3). Compared to *HLA-DRB3* and *–DRB4* alleles in other DR haplotypes, *HLA-DRB5*01:01* always showed a higher expression ($p<0.001$, df=79.33, for DRB3, Figure 5H; $p<0.001$, df=89.58 for DRB4, Figure 5H). Notably, there were no significant differences in HLA-DRB1 gene expression levels between hetero- and homozygotic carriers of the *HLA-DRB1*15:01* allele (p=0.379, df=22.01, Figure 5I). Beside the cases carrying the *HLA-DRB1*15:01* allele, five MS and three control cases also showed high HLA-DRB1 expression (Figure 5F). Of these cases, one MS case was heterozygote for the *HLA-DRB1*04:01* allele and another case was heterozygote for the *HLA-DRB1*08:01:01G* allele. Interestingly, both alleles have been associated with risk of MS (Patsopoulos, Barcellos et al. 2013, Moutsianas, Jostins et al. 2015).

All three control cases were heterozygote for the *HLA-DRB1*03:01* allele, also previously shown to be associated with MS (Patsopoulos, Barcellos et al. 2013) (Table 3, risk genes marked in bold). Of the other three MS cases with high HLA-DRB1 expression, two did not carry a MS-associated allele (*HLA-DRB1*01:01:01*, **01:01:01G*, **01:03* and **07:01:01G*), and in one case genotyping failed.

We did not detect any systematic differences between the *HLA-DRB1*15:01* cases compared to the other cases concerning age at death, age at disease onset and disease duration (Figure 6 A-C). In addition, we did not detect any differences between the HLA-DRB1 high expressing cases compared to the low expressing cases concerning age at death, age at disease onset and disease duration (Figure 6 D-F).

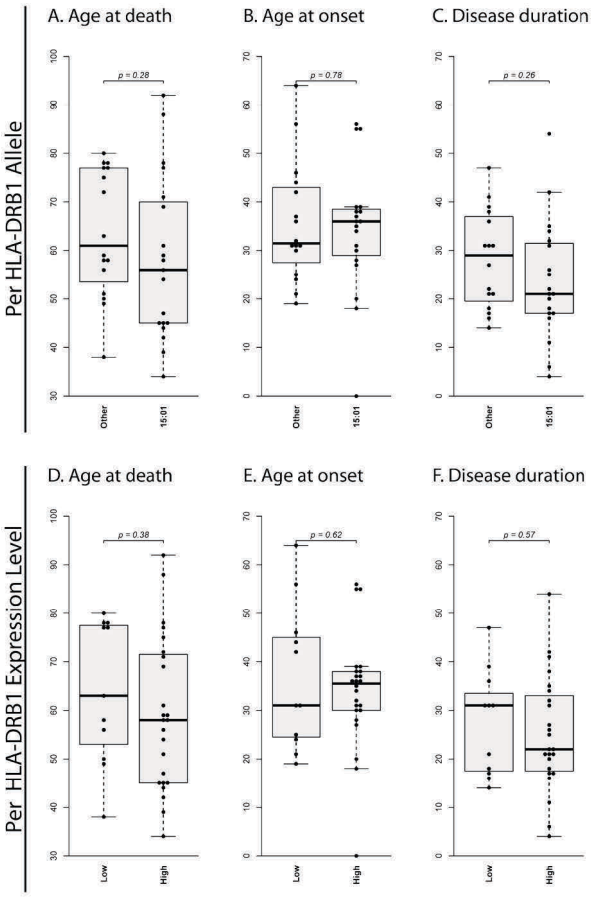

Figure 6. Sample population differences of HLA-DRB1*15:01 versus other alleles
Comparison of age, age at onset and disease duration between carriers of the *HLA-DRB1*15:01* and carriers of any other alleles. No statistically significant difference in the mean was detected when comparing **15:01* versus other allele carriers for age at death (p=0.28, df=32.8, mean (*HLA-DRB1*15:01*)=58.1, mean(other)=63.9), age at onset (p=0.78, df=32.7, mean (*HLA-DRB1*15:01*)=34.3, mean(other)=35.6) or disease duration (p=0.26, df=33, mean (*HLA-DRB1*15:01*)=23.8, mean(other)=28.1) or when comparing high versus low expressers for age at death (p=0.38, df=20.6, mean (high)=59.1, mean(low)=64.0), age at onset (p=0.62, df=16.1, mean (high)=34.1, mean(low)=36.6) or disease duration (p=0.57, df=21.0, mean (high)=25.0, mean(low)=27.4). p-Values are derived from a Welch two-sided t-test.

High HLA-DRB1 expression correlates with high expression of HLA-DRA

Functional HLA-DR molecules are heterodimers of a DRA-encoded alpha chain and a beta chain encoded by *DRB1* or *DRB3*,*4*,*5* respectively. Therefore, we investigated whether high HLA-DRB1 expression correlates with high HLA-DRA gene expression in *HLA-DRB1*15:01* carriers. Indeed high HLA-DRB1 gene expression correlated with high HLA-DRA ($r=0.79$, $p<0.001$) gene expression in *HLA-DRB1*15:01* cases, supporting the idea of a biologically functional upregulation of MHCII in MS normal-appearing grey matter of *HLA-DRB1*15:01* cases (Figure 5J).

HLA-DRB1 is expressed by microglia in human cortical grey matter

To determine which cell types are expressing HLA-DRB1 in normal-appearing grey matter, a confocal immunofluorescence colocalization analysis of fresh frozen and paraffin-embedded human brain tissues was performed (Figure 7). We detected that HLA-DRB1 colocalized with microglia in MS normal-appearing grey matter and control grey matter (Figure 7A). No colocalization could be detected in astrocytes (Figure 7B), neurons (Figure 7C), oligodendrocytes (Figure 7D) or blood vessels (Figure 7E).

*HLA-DRB1 protein expression is elevated in HLA-DRB1*15:01 positive cases*

Quantitative immunohistochemical analysis was performed to determine whether HLA-DRB1 gene and protein expression are associated with each other (Figure 8A). We detected a higher protein expression in high versus low HLA-DRB1 gene expressers ($p=0.052$, $df=46.9$, $n=49$) (Figure 8B) and a trend towards higher expression in MS and control cases carrying the HLA-*DRB1*15:01* allele compared to non-carriers ($p=0.097$, $df=60.5$, $n=74$). HLA-DRB1 protein expression varied considerably from case to case (Figure 8B).

*HLA-DRB1*15:01 genotype and increased expression of HLA-DRB1 is associated with increased cortical demyelination*

We hypothesized that the *HLA-DRB1*15:01* genotype and the increased HLA-DRB1 gene- and protein expression might be related to meningeal inflammation and cortical microglia activation, previously described in MS (Howell, Reeves et al. 2011), and hence might also correlate with increased levels of cortical demyelination.

We thus investigated all available tissue blocks from MS cases with cortical lesions and stained for MOG, delineated cerebral cortical area containing all six layers (identified by NeuN) (Figure 8C), and quantified the fraction of demyelinated versus whole cortical area (Figure 8D).

Areas of demyelination in MS cases carrying the *HLA-DRB1*15:01* allele, and respectively cases with a high HLA-DRB1 gene expression, were significantly larger than in *HLA-DRB1*15:01* negative cases (p=0.052, df=23, n=25) and, respectively, cases with low HLA-DRB1 gene expression (p=0.014, df=21, n=23) (Figure 8D).

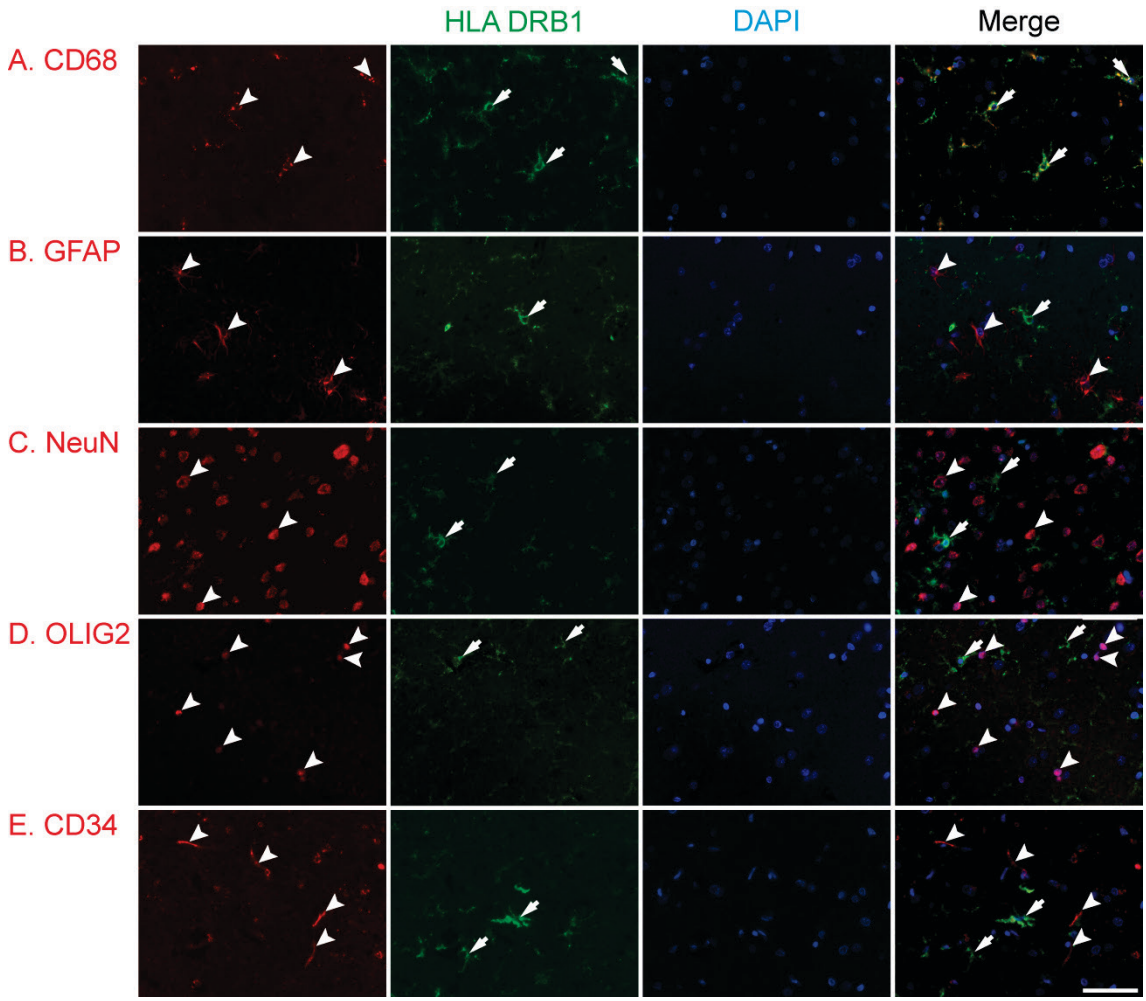

Figure 7. HLA-DRB1 colocalization in MS cortical grey matter
Immunofluorescent colocalization of HLA-DRB1 with cellular markers for resident cells of the cortical grey matter. HLA-DRB1 co-localized with CD68, a marker for microglia (A, arrows). No co-localization with astrocytes (B, GFAP, arrowhead), neurons (C, NeuN, arrowhead), oligodendrocytes (D, OLIG2, arrowhead) and blood vessels (E, CD34, arrowhead) could be found. Scale bar: 50µm.

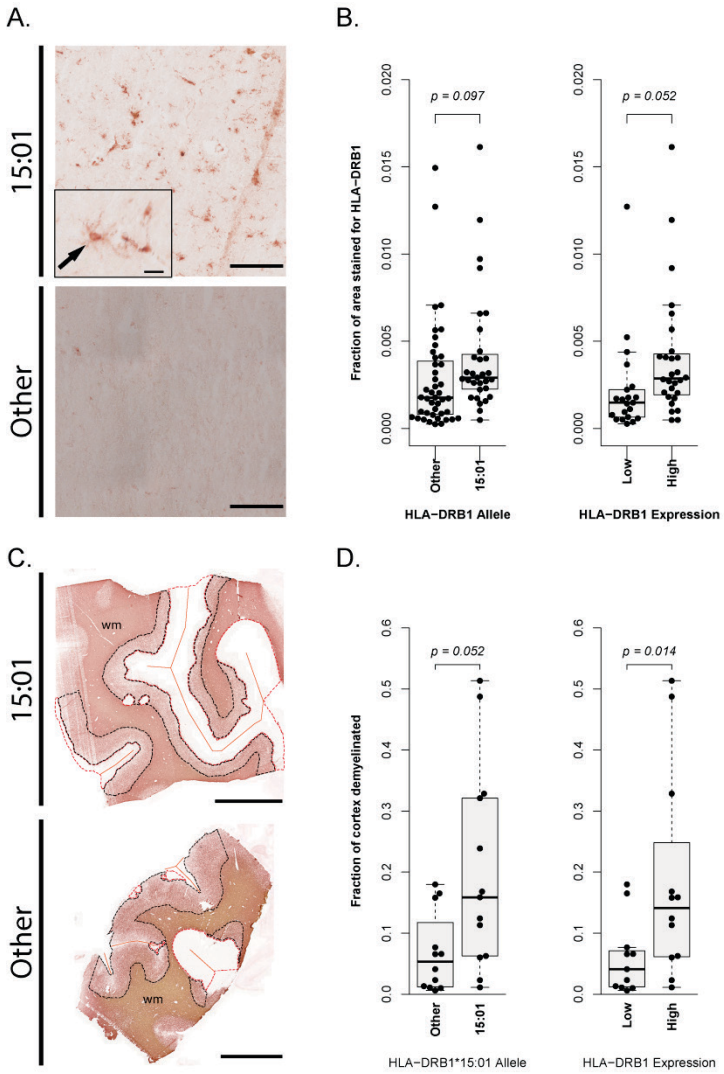

Figure 8. HLA-DRB1 protein expression in MS and control cases and cortical grey matter lesion size in MS cases associate with HLA-DRB1*15:01 allele

Representative image of immunohistochemical stainings for HLA-DRB1 protein in a *HLA-DRB1*15:01* positive (M6) and negative (M11) MS case (A). Most *HLA-DRB1*15:01* positive cases show an evenly distributed staining of cells with microglia-like morphology (arrow) throughout the cerebral cortex (top panel), whereas cases with other alleles may show similar staining or no staining at all (bottom panel, extreme case with no staining). Boxplots of the quantification of the HLA-DRB1 immunohistochemical staining (B) show MS and control cases carrying the *HLA-DRB1*15:01* allele (left plot) or with a high HLA-DRB1 gene expression (right plot). Higher overall HLA-DRB1 protein expression was detected in *HLA-DRB1*15:01* positive cases and high expressers compared to carriers of other alleles and low expressers, respectively. Detection of grey matter lesions in MS cases was performed by immunohistochemical staining for MOG (C shows representative images of a **15:01* positive (M28) and a negative (M3) MS case). Normal-appearing grey matter is demarcated by a black dotted line and grey matter lesions by a red dotted line; orange straight lines demarcate the meninges. Quantification of cortical grey matter lesion size as fraction of demyelinated versus total cortical grey matter is shown (D). Both *HLA-DRB1*15:01* carriers (left plot) and HLA-DRB1 high gene expressers (right plot) show a larger mean lesion size compared to carriers of other alleles or low expressers, respectively. (B, D) p-values are derived from a two-sided Welch t-test.

*HLA-DRB1*15:01 carrier status associates with higher expression of nine genes in cortical normal-appearing grey matter in both MS and controls*

We investigated the effect of the *HLA-DRB1*15:01* allele by analyzing the differential gene expression data after grouping the cases into *DRB1*15:01* positive or negative. We detected nine genes to be differentially regulated. Most interestingly, our data show an upregulation of interleukin 18 receptor 1 (IL18R1; FC=1.73, adj.p-value=0.004) and leukocyte immunoglobulin like receptor B1 (LILRB1; FC=1.54, adj.p-value=0.032). The highest fold change was detected for long intergenic non-protein coding RNA 01119 (LINC01119, FC=4.35, adj. p-value<0.0001). We further detected differentially expressed transcripts of protein O-fucosyltransferase 2 (POFUT2; FC=1.86, adj.p-value<0.001), G protein subunit beta 5 (GNB5; FC=-2.20, adj.p-value=0.003), epithelial stromal interaction 1 (EPSTI1; FC=1.50, adj.p-value=0.005), DExD/H-box helicase 60 (DDX60; FC=1.25, adj.p-value=0.010), N-acetylneuraminic acid phosphatase (NANP; FC=1.47, adj.p-value=0.012), and kinesin family member 25 (KIF25; FC=-1.37, adj.p-value=0.049).

Table 4. Differentially expressed genes between HLA-DRB1*15:01 carrier status and control versus MS

Symbol	Gene Name	log2FC	FC	adj. p. value
LINC01119	long intergenic non-protein coding RNA 1119	4.35	20.35	<0.001
POFUT2	protein O-fucosyltransferase 2	1.86	3.63	<0.001
GNB5	G protein subunit beta 5	-2.2	0.22	0.003
IL18R1	interleukin 18 receptor 1	1.73	3.33	0.004
EPSTI1	epithelial stromal interaction 1	1.5	2.83	0.005
DDX60	DExD/H-box helicase 60	1.25	2.37	0.010
NANP	N-acetylneuraminic acid phosphatase	1.47	2.76	0.012
LILRB1	leukocyte immunoglobulin like receptor B1	1.54	2.91	0.032
KIF25	kinesin family member 25	-1.37	0.39	0.049

Table shows the differentially expressed genes between HLA-DRB1*15:01 carriers and non-carriers and control versus MS status. Abbreviations: log2FC: Log2 of fold change; FC: Fold change.

8.1.5 Discussion

Our results demonstrate that HLA-DRB1 is significantly higher expressed in MS normal-appearing grey matter and shows a bimodal distribution with more MS cases showing a high expression compared to control cases. Genotyping of the HLA locus revealed an almost exclusive high expression of all *HLA-DRB1*15:01* allele carriers and of a few other MS-associated risk alleles. Consistent with the gene expression analysis, HLA-DRB1 protein expression is increased in *HLA-DRB1*15:01* positive cases in grey matter on microglia based on immunofluorescence colocalization. The *HLA-DRB1*15:01* genotype and high HLA-DRB1 gene expression are associated with larger grey matter lesions in MS. Further, it is important to

note that the second DR allele, *DRB5*01:01*, which is tightly linked with *DRB1*15:01* in the MS-associated DR haplotype is also expressed at higher levels.

These findings hint at a link between the strongest genetic risk factor for MS and an important pathological hallmark, namely demyelinated lesions in the cerebral cortex. We hypothesize that the *HLA-DRB1*15:01* genotype and the increased HLA-DRB1 and-DRB5 gene expression together with meningeal and parenchymal inflammation may lead to larger demyelinated lesions. A positive correlation between inflammation, cortical demyelination and the *HLA-DRB1*15* allele has already been described in autopsy tissue by Yates et al., who have detected more parenchymal, perivascular and meningeal T cell inflammation and larger motor cortical lesions in *HLA-DRB1*15* carriers compared to carriers of other alleles (Yates, Esiri et al. 2015). Even though magnetic resonance image detection of cortical grey matter lesions is improving, widespread subpial demyelination is still difficult to detect (Kilsdonk, Jonkman et al. 2016). A recent MRI study of 85 MS patients did not reveal a statistically significant difference between *HLA-DRB1*15:01* carriers and non-carriers, however, the authors point out the limited power due to the small number of cases (Yaldizli, Sethi et al. 2016). Further, meningeal inflammation and follicle-like structures in the meninges have been linked to microglia activity (Howell, Reeves et al. 2011) and larger subpial cortical grey matter lesions (Magliozzi, Howell et al. 2010). Regarding expression of the two *DR15* alleles, higher mRNA expression of *DRB5*01:01* compared to *DRB1*15:01* in MS lesions and normal-appearing white matter have already been observed previously supporting our findings; however, much fewer cases and neither grey matter nor the extent of demyelination had been studied (Prat, Tomaru et al. 2005). HLA class II molecules present processed peptides to CD4+ T lymphocytes. In MS, the strongest genetic association maps to the *HLA-DRB1* gene, while the association with *DRB5*01:01* has so far largely been ignored because the single nucleotide polymorphisms (SNP), which have been used for determining DR types from SNP typing are not sufficiently tightly spaced in the HLA region on chromosome 6 to allow assignment of the specific *HLA-DR3**, *-4** and *-5** alleles (Moutsianas, Jostins et al. 2015). The *HLA-DRB1*15:01* allele was reported to increase the risk for developing MS about threefold (International Multiple Sclerosis Genetics Consortium, Wellcome Trust Case Control Consortium et al. 2011). The higher HLA-DRB1 expression in the cortical grey matter in *HLA-DRB1*15:01* cases may therefore be involved in local activation of autoreactive CD4+ T cells. For CD4+ T cell activation to occur, an interaction between the T cell receptor (TCR) and MHC-class II/peptide (pMHC) complexes is required (for review see: Dustin 2008). The amount of antigen loaded on MHC-class II molecules of antigen presenting cells (APC) and the level of MHC-class II expression

determine the activation of CD4+ T cell activation and higher pMHC ligand densities enhance this process (Corse, Gottschalk et al. 2011). Similar to the ectopic expression of HLA-class II in autoimmune thyroid disease (Bottazzo, Pujol-Borrell et al. 1983), higher HLA-DRB1 expression by microglia in the brain may therefore affect the pMHC concentration and consequently lead to an increased probability of T cell activation and brain inflammation. This hypothesis is further supported by the finding that the level of HLA-DR expression in transgenic mice is an important prerequisite for developing spontaneous EAE (Quandt, Huh et al. 2012).

Besides their expression levels, the nature of the peptide repertoire that is presented by the two *HLA-DR* alleles in the MS-associated *DR15* haplotype, i.e. *DRB1*15:01 and DRB5*01:01* (Prat, Tomaru et al. 2005), probably also plays an important role for the activation of autoreactive T cells (Kondo, Cortese et al. 2001, Mohme, Hotz et al. 2013). Finally, autoreactive- and virus-specific, brain-infiltrating CD4+ T cells may recognize peptides in the context of both *DR* alleles of *the DR15* haplotype indicating that the expression of the two DR molecules may increase the likelihood of T cell activation further (Lang, Jacobsen et al. 2002, Sospedra, Muraro et al. 2006).

A bimodal expression pattern of HLA-DRB1 and -DRB5 has been described in lymphoblastoid cell lines (Alcina, Abad-Grau Mdel et al. 2012). The authors analyzed expression quantitative trait loci in the tag of the HLA-DRB1*15:01 allele associating with high HLA-DRB1, DRB5 and DQB1 gene expression. They concluded that a higher gene expression alone does not sufficiently explain the MS-associated risk of the *HLA-DRB1*15:01* allele. At present, it is not clear, which molecular pathomechanisms are responsible for the high versus lower expression in some individuals, but differences in gene regulation, for instance by different activation of the class II transactivator is one possibility (for review see: Reith, LeibundGut-Landmann et al. 2005).

Regarding the potential functional involvement of the *DRB1*15:01* haplotype, the higher DRB1- and DRB5 expression in MS brains raises questions beyond peptide presentation to autoreactive T cells. The brain is considered an immune privileged site, and besides shielding of the central nervous system from the peripheral immune system via specialized barriers, low MHC expression is considered an important aspect of this central nervous system immune privilege (for review see: Engelhardt, Vajkoczy et al. 2017). Aberrant and increased expression of HLA-DRB1 and -DRB5 may contribute to breaking immune tolerance in this tissue that is exquisitely vulnerable to damage and endowed with cells that are terminally differentiated and not replaceable. The interpretation of recent genome-wide association studies in MS, which

found almost exclusively immune system-related genes, has been that MS develops from outside, i.e. the peripheral immune system, in as opposed to starting by damage within the central nervous system and then involving peripheral immune cells, i.e. inside-out hypothesis (Barnett and Prineas 2004). Our data, although preliminary and not addressing functional aspects in human brain tissue, might indicate that increased HLA-DR expression in the brain, if it preceded peripheral immune T cell activation, could play a role both within and later also outside the brain.

Regarding gene expression in cortical grey matter, several studies have been performed with a relative small set of normal-appearing grey matter tissue samples (Dutta, McDonough et al. 2006, Torkildsen, Stansberg et al. 2010, Fischer, Wimmer et al. 2013) including ours (Zeis, Allaman et al. 2015). The present study with a much larger number of cases and tissues did not show the same gene expression alterations as the previous studies. Possible reasons are the different gene expression platforms, tissue preparation (fresh frozen versus paraffin-embedded), the statistical methods, and, most relevant, differences in the patient samples, which is a critical aspect in a heterogeneous disease like MS.

The gene expression analysis further revealed nine genes to be differentially expressed in *HLA-DRB1*15:01*-positive versus -negative samples. Among the detected genes, IL18R1 gene and protein expression have previously been shown to be elevated in MS in cerebrospinal fluid and peripheral blood mononuclear cells compared to controls (Gillett, Thessen Hedreul et al. 2010). The highest fold change was detected for LINC01119, a long intergenic non-protein coding RNA. Research on non-coding RNAs is rapidly evolving and some members have already been shown to play a role in immune system regulation (for review see: Wu, Pan et al. 2015). We further detected LILRB1, a receptor for class I MHC antigens expressed by different leukocyte lineages that may down-regulate monocyte activation signals. EPSTI1 (Nielsen, Ronnov-Jessen et al. 2002) and DDX60 (Schoggins, Wilson et al. 2011) have previously been shown to be differentially regulated upon interferon signaling in HLA-B27-transgenic rats, an animal model developing spontaneous autoimmune-mediated multisystem inflammatory disease (Fert, Cagnard et al. 2014). The other genes we detected were POFUT2 (Luo, Nita-Lazar et al. 2006), GNB5 (Shamseldin, Masuho et al. 2016), NANP (Maliekal, Vertommen et al. 2006) and KIF25 (Decarreau, Wagenbach et al. 2017). To the best of our knowledge, these genes have not been described to date in the context of MS or HLA-DRB as possibly linked to the HLA-DRB1*15:01 allele. The power of this particular analysis is however limited by the sample heterogeneity and needs further experimental investigation to evaluate the possible impact of the detected differential expression.

In conclusion, our results demonstrate elevated DR expression in the cortical grey matter of a subset of MS patients positive for the *HLA-DR15* haplotype and rarely also other *DR* types. HLA-DRB1 expression by microglia in the brain might play a role as vulnerability factor to develop or sustain MS. Further studies on DR expression in the brain, its causes and consequences would therefore be of great interest for a better understanding of MS pathogenesis.

8.1.6 Acknowledgments

We thank Prof. Dr. Richard Reynolds (UK Multiple Sclerosis Tissue Bank, Charing Cross Hospital London, UK) and Prof. Dr. Markus Tolnay (Pathology, University Hospital Basel, Switzerland) for providing human brain tissues. We also thank Sigrid Müller, Heidi Brodmerkel and Katja Schulz for technical assistance. Calculations were performed at sciCORE (http://scicore.unibas.ch/) Scientific Computing Center at University of Basel.

8.2 Study 2: Altered gene expression levels of olfactory receptors in neurons and blood vessels of multiple sclerosis cortical grey matter lesions

Lukas S. Enz, Gordana Jakimoski, Thomas Zeis, Daniela Schmid, Florian Geier, Guido Steiner, Ulrich Certa, Nicole Schaeren-Wiemers

Manuscript in preparation for publication.

Contributions of Lukas S. Enz:
Study design, sample selection and characterization, immunohistochemical characterization and analysis, immunofluorescence colocalization analysis, image and data analysis and interpretation, initial manuscript preparation and manuscript revisions.

Author contributions:
G.J.: Olfactory receptor immunohistochemical characterization and olfactory receptor immunofluorescence colocalization experiments. T.Z.: Microarray study design, sample selection and characterization and microarray analysis. D.S.: Microarray sample selection and characterization. F.G.: Data analysis and interpretation and statistics. G.S.: Microarray experiment design. U.C.: Microarray study design. N.S.W.: Study design, data analysis and interpretation and manuscript preparation.

8.2.1 Abstract

Multiple Sclerosis (MS) is a chronic inflammatory demyelinating disease of the central nervous system affecting white and grey matter. Among the characteristics of MS pathology are extended focal and diffuse cortical grey matter abnormalities, which have been linked to clinical signs such as cognitive impairment.

Objective: To explore molecular changes within chronic cortical grey matter lesions compared to normal-appearing cortical grey matter.

Method: We performed a histological analysis of the lesions of 48 MS cases. To investigate the molecular pathology, differential gene expression analysis of demyelinated cortical grey matter lesions and MS normal-appearing grey matter was performed. To further investigate three genes of interest, we performed immunofluorescent colocalization and quantification.

Results: We detected a total of 181 distinct lesions within the cortex of 48 MS cases. For the array we selected 37 samples containing cortical grey matter lesions and 41 samples from normal-appearing cortical grey matter. Among a total of 1'758 differentially expressed genes we detected higher expression of 68 unique olfactory receptors in tissue containing cortical grey matter lesions compared to normal-appearing grey matter. Quantitative immunohistochemical analysis of three selected olfactory receptors confirmed the higher expression in grey matter lesions on protein level. Immunofluorescence colocalization further demonstrated the three olfactory receptors to be expressed on neurons (OR5P2) on neurons and blood vessels (OR52I1/OR52I2) or on blood vessels (OR9K2).

Conclusions: Our data indicate that dysregulation of specific olfactory receptors is a common finding in MS grey matter lesions.

8.2.2 Introduction

Multiple Sclerosis (MS), the most common inflammatory neurologic disease affecting young adults, is a chronic demyelinating disease of the central nervous system. If untreated, MS leads to disability in a substantial proportion of patients (for review see: Jones and Coles 2010). The etiology of MS includes a complex genetic trait and several environmental risk factors, which act in concert and contribute to the main pathomechanisms including inflammation, de- and remyelination, axonal and neuronal loss, astroglia activation and metabolic changes (for reviews see: Mahad, Trapp et al. 2015, Olsson, Barcellos et al. 2017). The relative severity of these leads to the enormous heterogeneity of MS with respect to clinical signs, course, and response to treatment, but also pathological composition of lesions. The pathologic hallmark of MS is the formation of focal areas of myelin loss in the central nervous system called lesions.

Besides the most commonly described white matter lesions, extensive grey matter lesions can be found in MS cerebral cortex (Calabrese, Magliozzi et al. 2015).

Grey matter lesions are reported to occur in up to 90% of all MS patients with chronic MS and widespread subpial demyelination has been shown to be a feature unique to MS (Albert, Antel et al. 2007, Wegner and Stadelmann 2009, Junker, Wozniak et al. 2020). Early-stage MS grey matter lesions where shown to contain myelin-laden macrophages as well as perivascular CD3+ and CD8+ T-cell infiltration (Lucchinetti, Popescu et al. 2011), while chronic grey matter lesions characteristically lack significant infiltration of immune cells (Bø, Vedeler et al. 2003, for review see: Stadelmann, Albert et al. 2008), but show diffuse microglial activation (Magliozzi, Howell et al. 2010, Gardner, Magliozzi et al. 2013). Both, in early- and chronic-stage, grey matter lesions were shown to associate with meningeal inflammation (Howell, Reeves et al. 2011, Lucchinetti, Popescu et al. 2011). Further, they are characterized by more efficient myelin repair and less gliosis than white matter lesions (Stadelmann, Albert et al. 2008). Although grey matter lesion morphology has been studied thoroughly, many aspects of its pathogenesis are still unclear. In addition, the above characteristics have to be viewed with caution because very little longitudinal information from repeated biopsies exists and due to the fact that biopsies are usually performed, when patients present with unusual clinical features, for example large lesions with suspicion of underlying tumor.

Beside the well described demyelinated grey matter lesions also diffuse grey matter abnormalities in non-lesional normally myelinated areas have been observed (Dutta, McDonough et al. 2006, Dutta, McDonough et al. 2007, Kutzelnigg, Faber-Rod et al. 2007). At the molecular level, little is known about changes in normal-appearing cortical grey matter and grey matter lesions in MS. In the last years, several transcriptome studies of MS brain tissues have been performed, and a number of manifestations and possible pathomechanisms could be identified (e.g. mitochondrial dysfunction, metabolic changes in astrocytes, inflammation, oxidative stress) (Dutta, McDonough et al. 2006, Dutta, McDonough et al. 2007, Torkildsen, Stansberg et al. 2010, Fischer, Wimmer et al. 2013, Zeis, Allaman et al. 2015). A limitation of all these studies is the low number of tissue samples and cases and consequently the limited statistical power. The problem is further accentuated by the heterogeneity of MS, reflected by the variable clinical course, different clinical symptoms and imaging findings as well as variation in its pathology. During our own studies (Graumann, Reynolds et al. 2003, Zeis, Graumann et al. 2008, Zeis, Allaman et al. 2015, Zeis, Howell et al. 2018) we collected a large number of well characterized human brain tissue samples from control and MS cases. With these, we performed a comprehensive gene expression study with 78 tissue samples from

30 MS cases and compared the expression pattern of normal-appearing cortical grey matter and tissue containing grey matter lesions to understand if there are alterations that may underlie or contribute to the molecular pathology of the widespread cortical grey matter lesions.

8.2.3 Material and Methods

Tissue selection and characterization

MS- and control tissue samples were provided by the UK MS Tissue Bank (UK Multicentre Research Ethics Committee, MREC/02/2/39), funded by the MS Society of Great Britain and Northern Ireland registered charity 207495, or obtained from the archives of the Institute of Neuropathology at the University Medical Centre Göttingen. All cases were routinely screened by a neuropathologist to confirm diagnosis of MS and to exclude other confounding pathologies (Reynolds, Roncaroli et al. 2011). In total 48 MS cases were used for this study; detailed description of patient's data and examinations are shown in Table 5.

Ethical approvals

Ethical approvals for all human tissues used were given by the UK Multicentre Research Ethics Committee, MREC/02/2/39.

Immunohistochemical characterization

Routine pathological screening of the autopsy tissues was performed as described before (Reynolds, Roncaroli et al. 2011). Tissues were further characterized by staining for NeuN (Neurons, MAB377, Millipore, Billerica, Massachusetts, USA), OLIG2 (Oligodendrocytes, ab9610, Millipore, Billerica, Massachusetts, USA), MOG (Myelin, Clone Z12, kindly provided by Prof. R. Reynolds), CD68 (Microglia, ab845, Abcam, Cambridge, UK) (Figure 9). Cryostat sections (12 µm) from fresh frozen tissue blocks were stained as described before (Table 2).

RNA isolation and quality assessment

Total RNA from grey matter tissue was isolated using the Zymo ZR RNA Microprep Kit (Zymo Research, Irvine, CA, USA) as described before (Zeis, Allaman et al. 2015). Degraded (RIN < 6) and/or contaminated (260/280 nm ratio < 1.8; 230/280 nm ratio < 1.8) samples were excluded from the study.

Table 5. Patient data

Patient	Original Name	Sex	Cause of Death	p.m. time [h]	Age [a]	Disease Duration [a]	MS Type	# NAGM Microarray	# GML Microarray	Lesion Size [mm²]	NAGM Size [mm²]	Fraction Demyelinated [%]
M01	MS012	F	Breast carcinoma, Pneumothorax	8	56	31	SPMS	4	1	0.08	12.82	0.01
M02	MS013	F	NA	16	58	21	PPMS	1	5	3.78	20.16	0.16
M03	MS035	F	Myocardial infarction or acute abdomen	18	78	14	SPMS	1	3	1.32	6.68	0.17
M04	MS038	F	Respiratory failure	21	42	18	SPMS			0.42	0.88	0.32
M05	MS039	F	Septicaemia, urinary tract infection, multiple sclerosis	19	74	26	SPMS			0.16	2.55	0.06
M06	MS040	F	Bronchopneumonia	6	58	21	PPMS	7	2	2.49	37.38	0.06
M07	MS044	F	Pulmonary embolus, pneumonia	17	45	20	PPMS			0.05	3.57	0.01
M08	MS046	M	Dehydration, multiple sclerosis	18	40	23	SPMS			0.15	7.70	0.02
M09	MS049	M	Aspiration pneumonia, cerebrovascular accident, multiple sclerosis	8	75	38	RRMS			0	2.45	0
M10	MS050	F	Bronchopneumonia, multiple sclerosis	8	72	41	SPMS	1		0	0.47	0
M11	MS053	M	Bronchopneumonia	26	66	31	SPMS			0	1.23	0
M12	MS054	F	NA	11	69	31	NA		2	0.05	4.85	0.01
M13	MS056	M	Pneumonia, multiple sclerosis	11	63	39	SPMS		2	0.94	4.29	0.18
M14	MS057	F	General deterioration, lung infection	9	77	31	PPMS	3	2	0.27	6.33	0.04
M15	MS058	F	Multiple sclerosis	15	51	21	SPMS			0	3.26	0
M17	MS062	F	Respiratory infection	10	49	19	SPMS			0	1.18	0
M18	MS063	F	Aspiration, multiple sclerosis, peripheral vascular disease	13	66	30	NA			0.03	4.46	0.01
M20	MS066	F	Pneumonia, multiple sclerosis	21	86	56	SPMS			0.29	1.71	0.14
M22	MS070	F	Multiple sclerosis	21	77	22	PPMS			0	0.29	0
M23	MS071	F	Bronchus carcinoma, metastasized	5	78	42	SPMS	3	2	0.23	9.72	0.02
M24	MS076	F	Chronic renal failure, heart disease	31	49	18	SPMS	1		0.11	4.53	0.02
M26	MS080	F	Bowel blockage, post-operative complications, heart failure	24	71	35	SPMS		2	0.32	0.65	0.33
M27	MS082	F	Aspiration pneumonia	9	49	25	SPMS			0.48	0.80	0.37
M28	MS088	F	Bronchopneumonia	22	54	NA	NA		3	5.00	5.26	0.49
M29	MS089	F	Intercerebral bleeding, multiple sclerosis	17	71	26	SPMS			0	1.39	0
M30	MS103	F	Pneumonia	7	77	21	SPMS	1		0	7.38	0
M31	MS104	M	Advanced multiple sclerosis, urinary tract infection	12	53	11	SPMS			0.14	2.06	0.07
M32	MS106	F	Bronchopneumonia	18	39	21	NA	2		0.52	3.64	0.12
M34	MS111	M	Old age	9	92	54	PPMS	2		0	2.63	0
M36	MS122	M	Bronchopneumonia	16	44	16	SPMS		2	1.20	4.24	0.22
M40	MS136	M	Respiratory failure, sepsis, multiple sclerosis	10	40	9	SPMS			0	13.02	0
M42	MS153	F	Multiple sclerosis	12	50	NA	SPMS		2	1.92	5.52	0.26
M43	MS154	F	Pneumonia	12	34	NA	SPMS		1	0.14	7.98	0.02
M44	MS155	F	Small bowel obstruction, pleurisy, heart problem, multiple sclerosis	13	80	36	SPMS	1	2	0.32	3.83	0.08
M46	MS163	F	Multi-organ failure from septicaemia due to urinary tract infection, multiple sclerosis	28	45	6	RRMS	2	1	0	9.60	0
M47	MS176	M	Intestinal obstruction, chronic multiple sclerosis	12	37	27	PPMS			0.11	10.96	0.01
M48	MS192	F	Aspiration pneumonia, multiple sclerosis	24	78	47	SPMS	1		0.07	6.23	0.01
M51	MS231	F	Bronchopneumonia, multiple sclerosis	12	59	27	PPMS	1		0	5.30	0
M52	MS255	M	Bronchopneumonia, advanced multiple sclerosis	24	45	25	SPMS		1	0.35	2.78	0.11
M53	MS280	F	Septicaemia, bronchopneumonia, multiple sclerosis	16	47	17	SPMS	2		1.61	8.52	0.16
M54	MS289	M	Advanced Multiple Sclerosis	9	45	18	SPMS		3	2.35	2.22	0.51
M55	MS092	F	Multiple sclerosis	26	37	17	SPMS			2.77	8.83	0.24
M56	MS168	F	Bronchopneumonia	22	88	32	PPMS	1		0	3.74	0
M57	MS248	F	Chronic obstructive pulmonary disease, multiple sclerosis	17	58	16	PPMS	2		0.30	4.29	0.07
M58	M381	F	Multiple Sclerosis	7	80	37	SPMS			0	3.27	0
M59	MS387	F	Multiple Sclerosis	13	42	11	SPMS		1	1.17	5.78	0.17
M60	MS390	F	Respiratory failure	9	59	4	PPMS	3		0	7.51	0
M61	MS413	M	Pancreatic Cancer, respiratory failure	10	61	26	SPMS	2		0	5.42	0
		36 F 12 M		**Ø=14.7**	**Ø=60.4**	**Ø=25.9**	**31 SPMS 11 PPMS 2 RRMS 4 NA**	**41**	**37**	**Ø=0.61**	**Ø=5.82**	**Ø=0.09**

Table shows the patient data, number of samples used in the microarray and the measured normal-appearing grey matter and grey matter lesion tissue area. Abbreviations: CoGM: Control case cortical grey matter; CPMS:

Chronic progressive MS; NA: Data not available; NAGM: Normal-appearing cortical grey matter; p.m. time: Post-mortem time; PPMS: Primary progressive MS; PRMS: Progressive-relapsing MS; SPMS: Secondary progressive MS.

Microarray analysis and statistical analysis

From initially 43 normal-appearing grey matter and 39 grey matter lesion containing tissue samples of 63 MS patients, 4 (2 normal-appearing and 2 grey matter lesion) samples matching to a patient with unknown HLA status (M08) were excluded. This led to a total of 41 normal-appearing grey matter tissue samples from 20 MS cases and 37 grey matter lesion containing tissue samples from 18 MS cases used for the gene expression analysis between (Table 5). To minimize experimental bias microarray experiments were performed together. All samples used for the gene expression study originated from the UK MS Tissue Bank. Gene expression profiling was done using the Illumina cDNA-mediated annealing, selection, extension, and ligation (DASL) assay according to the manufacturer's protocol (Fan, Yeakley et al. 2004) (Part No. 15018210, Revision history D, April 2012, Illumina, San Diego, CA, USA). Beadchips were scanned by the iScan Array scanner (Illumina). All subsequent data analyses were performed using the statistical software R (R core development Team 2008; R version 3.5.0). Specifically, the Bioconductor packages beadarray (version 2.30.0) and illuminaHumanWGDASLv4.db (version 1.26.0) were used for reading-in data files and for probe annotation (probes n=48107). Between-array normalization was performed by variance stabilizing transformation followed by a quantile normalization using functions from the Bioconductor package lumi (version 2.32.0). Only probes mapping to an ENTREZ gene ID were retained. Probes with quality status 'bad' were removed. Bad quality probes are probe matches repeat sequences, intergenic or intronic regions, or is unlikely to provide specific signal for any transcript (according to illuminaHumanWGDASLv4 annotation). Since the resulting probes (n=25081) were still not unique, we selected the probe with the highest variance across all samples, neglecting sample values, which fall into the expression range of negative control probes. This way, each gene is represented by the probe, which contains most information on potential expression differences, but ignores probes, which appear artificially regulated due to false-negative regulation introduced by SNPs. This strategy gave rise to 17'908 unique gene-level probes.

Blasting of probe sequences

To check for alternative hybridization of the olfactory receptor probes of the microarray we utilized the basic local alignment search tool Blastn of the National Center for Biotechnology

Information (NCBI, Bethesda, Maryland, USA) (called November 2019) (Altschul, Gish et al. 1990, Zhang, Schwartz et al. 2000, Morgulis, Coulouris et al. 2008). The probe sequences used were:

OR5P2: GTGCCATCCAGCTTGGTTCAGCGGCTTTCTTTGCAACAGTCGAATGCGTC

OR52I1: *GGCAGGATATAGTGCCCTTGCACACCCAAGTGCTGCTAGCTGACCTGTAC*

OR52I2: *GTCCACTCCTACTGTGAGCACATAGCTTTGGCCAGGTTAGCATGTGCTGA*

OR9K2: *CACC-TGCAGCTCTCACCTGGGAGTTGTGAGTGTGCTGTATGGTGCTGTCT*.

Immunofluorescence colocalization and quantification

Immunofluorescent colocalization was performed as described before (Zeis, Graumann et al. 2008, Zeis, Allaman et al. 2015). Briefly, cryostat sections (12µm) from fresh frozen tissue blocks were fixed in 4% PFA for 10 minutes. Sections were then treated with 10mM cupric sulfate in 50mM ammonium acetate at pH 5.0 for 1 hour to diminish autofluorescence. The sections were blocked with 5 % normal donkey serum, 0.1 % Triton X-100, and 0.05 % Tween 20 in 1x PBS for 1 hour. After blocking, sections were incubated with the primary antibodies in in blocking buffer overnight at 4°C. The following antibodies were used: OR5P2 (ab129984), OR52I2 (ab129828), OR9K2 (ab188311) all from Abcam (Cambridge, UK). Sections were then incubated with the secondary antibodies in PBS overnight. After washing in PBS with 1:10000 DAPI, sections were mounted with fluorsave (Millipore) or with 20mM Tris, 0.5% N-propyl gallate, and 80% glycerol in ddH_2O and sealed with nail polish.

For quantification, the tissue was scanned with a Nikon TI2 microscope and further analyzed with ImageJ (Version 1.52, FIJI distribution, National Institute of Health, Bethesda, Maryland, USA) (Schindelin, Arganda-Carreras et al. 2012, Rueden, Schindelin et al. 2017). The images were individually thresholded manually and the function analyze particles was run, counting objects between 50 and 600 pixels for the NeuN staining and objects larger than 50 pixels for the ColIV stainings. The same procedure was repeated for the olfactory receptor stainings and the resulting images were overlapped. Neurons were counted as positive upon 70% overlap, whereas blood vessels were counted as positive upon minimum 40% overlap.

Statistical analysis

All statistical analyses were performed using R (R Development Core Team 2010). A p-value respectively FDR-adjusted p-value smaller 0.05 was considered statistically significant. Expression data were analyzed using R and the Bioconductor package limma (version 3.36.5). Statistical analysis was performed using a linear model with disease group and sex as factors.

Since some patients contributed multiple tissue samples (tissue blocks), we additionally distinguished these "technical" replicates from true biological replicates (patients) in the model to avoid a potential inflation of significance by pseudo-replication. Specifically, the duplicateCorrelation function of the limma package was used to estimate a consensus correlation between technical replicates and this value together with patient ID as a block factor entered into the model fit function. GO term enrichment analysis relied on the GO categories provided by MSigDB version 6.0 from Broad Institute. The limma function camera, which performs a competitive gene set enrichment test, was run with default parameter settings on the lesion vs normal-appearing contrast. GO terms with an FDR below 0.05 were considered significantly regulated. For all other statistical tests, a two-sided Welch t-test or a spearman correlation was used, as indicated.

Data availability

The gene expression data discussed in this publication have been deposited in NCBI's Gene Expression Omnibus under accession number GSE131279 (https://www.ncbi.nlm.nih.gov/geo/query/acc.cgi?acc=GSE131279).

8.2.4 Results

Chronic demyelinated grey matter lesions are frequent in multiple sclerosis brain tissue samples

We investigated a total of 110 tissue blocks from 48 MS cases for cortical grey matter lesions defined as areas with complete loss of immunohistochemical staining for MOG (Figure 9A-D). The total analyzed cortical area was 308.34mm^2. The total demyelinated lesion area was 28.99mm^2 and comprised of 181 distinct areas of cortical grey matter demyelination. 49.1% of the tissue blocks and 66.7% of cases had at least one cortical grey matter lesion.

Further characterization of the cortical grey matter lesions revealed 6.6% leukocortical lesions (4.9% of the lesion area, Figure 9A), 18.2% intracortical lesions (9.0% of the lesion area, Figure 9B), 68.5% subpial lesions (71% of the lesion area, Figure 9C) and 6.6% pancortical lesions (15.1% of the lesion area, Figure 9D) as defined by Peterson et al. and Bø et al. (Peterson, Bo et al. 2001, Bø, Vedeler et al. 2003). All detected grey matter lesions were chronic inactive lesions with no signs of ongoing inflammation identified by immunohistochemical staining against CD68 (Figure 9E).

Amongst the patients with cortical grey matter lesions, we detected a significant higher lesion load in secondary progressive cases (SPMS) compared to primary progressive cases (PPMS)

(fold change=2.7, p=0.013, df=21.58) (Figure 9F). The fraction of demyelinated cortical grey matter did not correlate with age (p=0.32, df=30), disease duration (p=0.25, df=27) or age at disease onset (p=0.52, df=27) and did not differ between female and male cases (p=0.78, df=8.6).

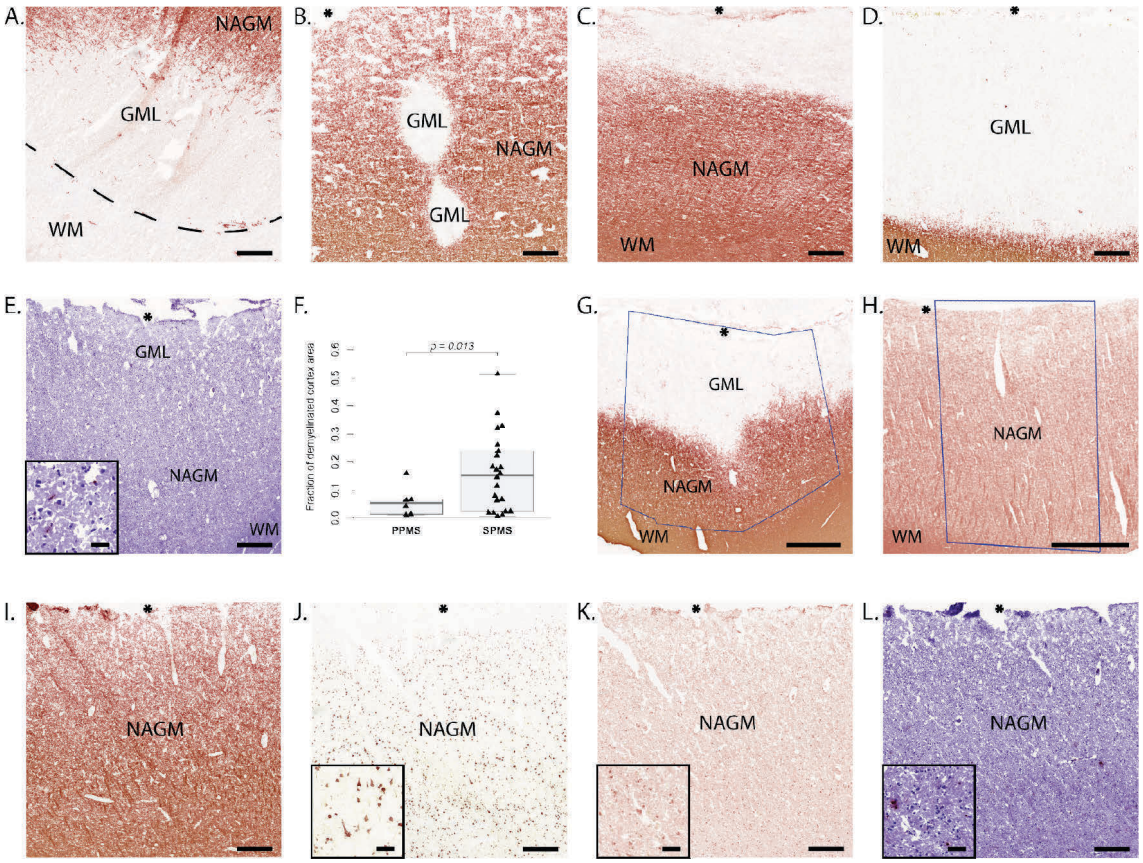

Figure 9. Tissue and lesion characterization and selection of region of interest
Representative images of grey matter lesions and normal-appearing grey matter (asterisks mark the meninges). (A) Leukocortical or type I cortical lesion in contact with white matter. (B) Intracortical or type II cortical lesion neither in contact with the white matter nor the brain surface. (C) Subpial or type III cortical lesion in contact with the brain surface. (D) Pancortical lesion or type IV grey matter lesion contacting the brain surface and the white matter. (E) CD68 staining in grey matter lesions showed no difference to normal-appearing grey matter with only few CD68+ (same region as in (G) is shown). (F) Boxplot comparing the fraction of demyelinated cortex between PPMS and SPMS. (G) Representative image of a MOG staining depicting a grey matter lesion region of interest isolated for the microarray marked with blue lines. Note that all layers of the cortex were isolated to ensure a comparable cellularity; therefore, grey matter lesions tissue almost always also included perilesional tissue. (H) Representative image of a normal-appearing grey matter region of interest chosen for the gene expression microarray. Normal-appearing grey matter was defined as no loss of MOG (I), NeuN (J) and OLIG2 (K) staining and no increase in CD68 (L); i.e. occasional CD68+ staining intra- or perivascular and only few CD68+ staining in the tissue. Scale bars A-E: 250µm, G-H: 1000µm, I-L: 250µm, insets I-L: 50µm.

Differential gene expression analysis reveals 1'758 genes to be differentially regulated in demyelinated grey matter lesions compared to normal-appearing grey matter

We investigated the gene expression in cortical grey matter lesions and normal-appearing grey matter of 30 MS cases in a total of 78 regions of interest, comprising of 37 areas containing cortical grey matter lesions and 41 normal-appearing grey matter areas. To ensure isolation of comparable cortical tissue, we isolated all six cortical layers for each region of interest. This implies that tissue designated as cortical grey matter lesion usually also contains perilesional tissue and not solely demyelinated areas (Figure 9G, H). Normal-appearing grey matter was defined as tissue without signs of demyelination identified by MOG (Figure 9I), neuronal degeneration identified by NeuN (Figure 9J), oligodendrocyte loss identified by Olig2 (Figure 9K), and without signs of inflammation such as microglia activation and macrophage infiltration identified by CD68 (Figure 9L).

The microarray analysis revealed, after all quality control steps, a total of 17'908 genes to be investigated. Differential gene expression analysis between MS grey matter lesions and MS normal-appearing grey matter identified 1'047 genes to be significantly higher expressed and 711 genes to be significantly lower expressed in tissue containing grey matter lesions (Figure 10A).

The most significant differentially upregulated genes included three olfactory receptors (OR2AK2, OR5P2 and OR6V1), a potassium channel protein (KCNG1), keratin and keratin associated proteins (KRT33B and KRTAP5-6) and microRNAs (MIR631, MIR296, MIR874 and MIR647) (Table 6A).

The most significant differentially downregulated genes included, amongst other genes, the myelin regulatory protein sirtuin 2 (SIRT2) and a potassium channel protein (KCNQ5) (Table 6B).

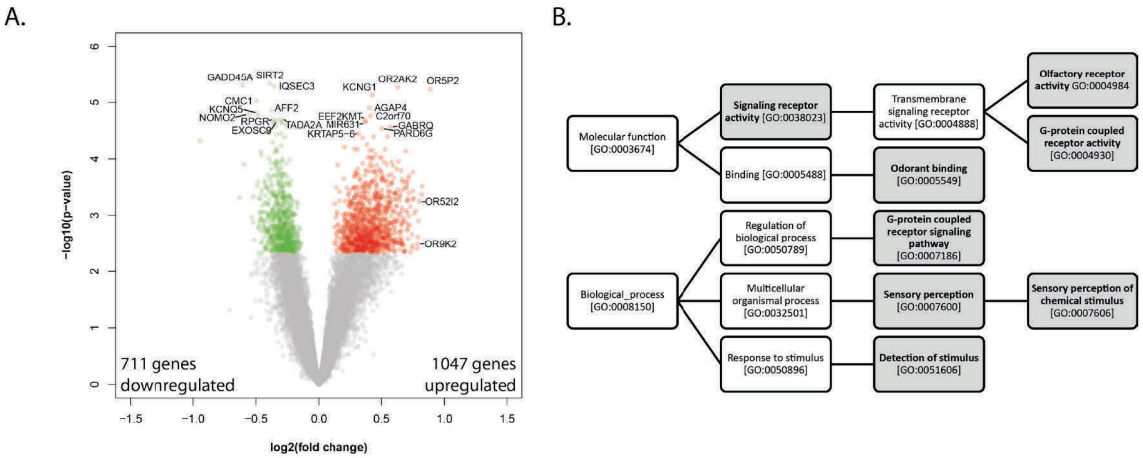

Figure 10. Differential gene expression MS versus control cases

(A) Volcano plot of the differential gene expression analysis between grey matter lesions and normal-appearing grey matter. Upregulated genes with an adjusted p-value lower than 0.05 are marked in red, downregulated genes with an adjusted p-value lower than 0.05 are marked in green. The top ten differentially up- respectively downregulated genes and OR52I2 and OR9K2 are marked with their symbols. (B) Diagram showing the hierarchy of the eight statistically significant GO terms containing ORs.

Table 6. Differentially expressed genes

A. Top 25 upregulated genes by p-value

Symbol	GeneName	Log2(Fold change)	Fold change	adj.p.val
OR2AK2	olfactory receptor family 2 subfamily AK member 2	0.63	1.55	0.021
OR5P2	olfactory receptor family 5 subfamily P member 2	0.89	1.85	0.021
KCNG1	potassium voltage-gated channel modifier subfamily G member 1	0.43	1.34	0.021
AGAP4	ArfGAP with GTPase domain, ankyrin repeat and PH domain 4	0.4	1.32	0.021
C2orf70	chromosome 2 open reading frame 70	0.41	1.33	0.021
EEF2KMT	eukaryotic elongation factor 2 lysine methyltransferase	0.37	1.29	0.021
MIR631	microRNA 631	0.37	1.3	0.021
GABRQ	gamma-aminobutyric acid type A receptor theta subunit	0.57	1.49	0.021
PARD6G	par-6 family cell polarity regulator gamma	0.5	1.42	0.022
KRTAP5-6	keratin associated protein 5-6	0.32	1.25	0.022
KRT33B	keratin 33B	0.55	1.46	0.022
PARP10	poly(ADP-ribose) polymerase family member 10	0.44	1.35	0.022
MECR	mitochondrial trans-2-enoyl-CoA reductase	0.35	1.28	0.022
MED16	mediator complex subunit 16	0.39	1.31	0.027
MIR296	microRNA 296	0.21	1.15	0.027
OR6V1	olfactory receptor family 6 subfamily V member 1	0.29	1.22	0.027
LY6G6D	lymphocyte antigen 6 family member G6D	0.53	1.44	0.027
TMEM234	transmembrane protein 234	0.31	1.24	0.027
ERMAP	erythroblast membrane associated protein (Scianna blood group)	0.43	1.35	0.027
P2RY1	purinergic receptor P2Y1	0.41	1.33	0.027
DSCR10	Down syndrome critical region 10 (non-protein coding)	0.69	1.62	0.027
MIR874	microRNA 874	0.45	1.37	0.029
MIR647	microRNA 647	0.39	1.31	0.029
UBXN11	UBX domain protein 11	0.49	1.4	0.029
MRPL4	mitochondrial ribosomal protein L4	0.42	1.34	0.029

B. Top 25 downregulated genes by p-value

Symbol	GeneName	Log2(Fold change)	Fold change	adj.p.val
SIRT2	sirtuin 2	-0.39	-1.31	0.021
GADD45A	growth arrest and DNA damage inducible alpha	-0.61	-1.52	0.021
IQSEC3	IQ motif and Sec7 domain 3	-0.36	-1.28	0.021
CMC1	C-X9-C motif containing 1	-0.5	-1.41	0.021
AFF2	AF4/FMR2 family member 2	-0.38	-1.3	0.021
KCNQ5	potassium voltage-gated channel subfamily Q member 5	-0.49	-1.4	0.021
NOMO2	NODAL modulator 2	-0.56	-1.47	0.021
TADA2A	transcriptional adaptor 2A	-0.3	-1.23	0.021
RPGR	retinitis pigmentosa GTPase regulator	-0.36	-1.28	0.021
EXOSC9	exosome component 9	-0.34	-1.26	0.021
ATP1A1	ATPase Na+/K+ transporting subunit alpha 1	-0.29	-1.23	0.021
WRNIP1	Werner helicase interacting protein 1	-0.36	-1.29	0.021
NSUN4	NOP2/Sun RNA methyltransferase family member 4	-0.3	-1.23	0.021
FGF7P3	fibroblast growth factor 7 pseudogene 3	-0.26	-1.2	0.021
PITRM1	pitrilysin metallopeptidase 1	-0.35	-1.27	0.021
PSRC1	proline and serine rich coiled-coil 1	-0.41	-1.33	0.022
USP13	ubiquitin specific peptidase 13	-0.4	-1.32	0.022
SNX14	sorting nexin 14	-0.4	-1.32	0.022
MOSPD1	motile sperm domain containing 1	-0.3	-1.23	0.022
VPS13D	vacuolar protein sorting 13 homolog D	-0.34	-1.26	0.022
HMGXB4	HMG-box containing 4	-0.27	-1.21	0.022
CTXN3	cortexin 3	-0.94	-1.92	0.025
CCDC25	coiled-coil domain containing 25	-0.37	-1.29	0.025
CFAP221	cilia and flagella associated protein 221	-0.3	-1.23	0.027
IMPA1	inositol monophosphatase 1	-0.34	-1.27	0.027

Table shows the top 25 differentially up- (A) respectively downregulated (B) genes detected with the DASL microarray between tissue containing grey matter lesions and normal-appearing grey matter.

Gene ontology terms analysis reveals groups of olfactory receptors and keratin to be upregulated in grey matter lesion compared to normal-appearing grey matter

To identify functional groups of differentially regulated genes in our sample, we performed a gene set enrichment analysis using a curated set of gene ontology (GO) terms provided by the Molecular Signatures Database (MSigDB version 6.0, Broad Institute). This analysis revealed a total of 147 GO terms to be differentially regulated when comparing tissue containing grey

matter lesions versus normal-appearing grey matter samples. Amongst the top ten significant GO terms eight included olfactory receptors and two included keratin and keratin-associated genes (Figure 10B, Table 7).

Table 7. Top 10 overrepresented gene sets by p-value

Gene set	NGenes	AbsLog2FC	Fold change	adj.P.Val
Olfactory receptor activity	352	0.27	1.2	2.94E-25
Sensory perception of chemical stimulus	438	0.24	1.18	4.43E-20
Odorant binding	83	0.27	1.21	4.69E-14
G protein coupled receptor activity	769	0.20	1.15	2.56E-11
Detection of stimulus	586	0.21	1.16	4.32E-11
Keratin filament	71	0.19	1.14	1.83E-10
Sensory perception	825	0.20	1.15	4.32E-08
Intermediate filament	164	0.18	1.14	5.49E-07
G protein coupled receptor signaling pathway	1062	0.19	1.14	3.64E-06
Signaling receptor activity	1241	0.18	1.13	2.67E-05

Table shows the top ten significant overrepresented gene ontology gene sets between normal-appearing grey matter and tissue containing grey matter lesions. Marked in bold are the GO terms containing olfactory receptor genes. Abbreviations: AbsLog2FC: log2 of the absolute fold change across all genes.

Inflammation related GO terms are not significantly regulated between tissue containing grey matter lesions and normal-appearing grey matter

As grey matter lesions have previously been shown to have a changed cellularity in comparison to normal-appearing grey matter, we searched specifically for overrepresented GO terms containing the terms oligodendrocyte, astrocyte, neuron, microglia, macrophage, B-cell, T-cell and lymphocyte. This analysis revealed one significantly regulated GO term containing myelin: myelin sheath (AbsLog2FC=0.13, adj. p. value=0.001), two terms containing neuron: neuron fate specification (AbsLog2FC=0.15, adj. p. value=0.04) and spinal cord association neuron differentiation (AbsLog2FC=0.19, adj. p. value=0.04) and two terms containing lymphocyte: lymphocyte migration (AbsLog2FC=0.18, adj. p. value=0.015) and lymphocyte chemotaxis (AbsLog2FC=0.18, adj. p. value=0.03). No overrepresentation was detected for terms containing oligodendrocyte, astrocyte, microglia, macrophage, B-cell, T-cell, immuno- and immune-.

68 olfactory receptors are higher expressed in tissue containing grey matter lesions

The results of the gene set enrichment analysis prompted us to further investigate the class of olfactory receptors. The gene expression analysis detected 361 olfactory receptor genes and pseudogenes, 68 of these were found to be significantly upregulated in tissue containing grey matter lesions compared to normal-appearing grey matter. 22 olfactory receptors were upregulated with a fold-change of at least 1.5 (Table 8A). No olfactory receptor was found to

be significantly lower expressed in tissue containing cortical grey matter lesions. Obligate functional components and olfactory receptor associated proteins include the adenylate cyclase 3 ADCY3 the G-protein subunit alpha L GNAL, the receptor transporters RTP1, RTP2, the receptor accessory protein REEP1 and the UDP-glucuronosyltransferase UGT1A6 (Garcia-Esparcia, Schluter et al. 2013). Of these transcripts, only RTP2 was found to be differentially expressed between tissue containing grey matter lesions and normal-appearing grey matter tissue samples (Table 8B).

For our further investigations we focused on the top three regulated olfactory receptors with the highest fold-change, statistically significant differential regulation, and for which antibodies were available for further evaluation, namely the receptors OR5P2, OR52I2 and OR9K2.

Table 8. Differentially expressed olfactory receptors and associated genes

A. Differentially expressed olfactory receptors

Symbol	GeneName	Log2(Fold change)	Fold change	adj.p.Val
OR5P2	olfactory receptor family 5 subfamily P member 2	0.89	1.85	0.021
OR52I2	olfactory receptor family 52 subfamily I member 2	0.8	1.74	0.030
OR4A5	olfactory receptor family 4 subfamily A member 5	0.79	1.73	0.040
OR9K2	olfactory receptor family 9 subfamily K member 2	0.79	1.73	0.043
OR1L4	olfactory receptor family 1 subfamily L member 4	0.75	1.68	0.044
OR11H12	olfactory receptor family 11 subfamily H member 12	0.74	1.67	0.046
OR8K5	olfactory receptor family 8 subfamily K member 5	0.72	1.65	0.037
OR4E2	olfactory receptor family 4 subfamily E member 2	0.71	1.64	0.041
OR1M1	olfactory receptor family 1 subfamily M member 1	0.71	1.63	0.037
OR2W1	olfactory receptor family 2 subfamily W member 1	0.71	1.63	0.038
OR5AK2	olfactory receptor family 5 subfamily AK member 2	0.69	1.61	0.047
OR5V1	olfactory receptor family 5 subfamily V member 1	0.68	1.6	0.048
OR5B3	olfactory receptor family 5 subfamily B member 3	0.68	1.6	0.047
OR4F4	olfactory receptor family 4 subfamily F member 4	0.68	1.6	0.048
OR52I1	olfactory receptor family 52 subfamily I member 1	0.67	1.59	0.043
OR8U8	olfactory receptor family 8 subfamily U member 8	0.66	1.58	0.041
OR5H15	olfactory receptor family 5 subfamily H member 15	0.66	1.58	0.043
OR56A4	olfactory receptor family 56 subfamily A member 4	0.65	1.56	0.041
OR4C15	olfactory receptor family 4 subfamily C member 15	0.65	1.55	0.043
OR2AK2	olfactory receptor family 2 subfamily AK member 2	0.63	1.55	0.021
OR52J3	olfactory receptor family 52 subfamily J member 3	0.63	1.54	0.041
OR51F2	olfactory receptor family 51 subfamily F member 2	0.62	1.53	0.043

B. Olfactory receptor associated genes

Symbol	GeneName	Log2(Fold change)	Fold change	adj.p.Val
RTP2	receptor transporter protein 2	0.33	1.26	**0.047**
UGT1A6	UDP-glucuronosyltransferase family 1 member A6	0.31	1.24	0.062
RTP1	receptor transporter protein 1	-0.16	-1.12	0.163
ADCY3	adenylate cyclase 3	-0.09	-1.07	0.41
OBP2A	odorant binding protein 2A	0.06	1.05	0.601
GNAL	G protein subunit alpha L	-0.06	-1.04	0.744
REEP1	receptor accessory protein 1	-0.03	-1.02	0.806

C. Correlations of olfactory receptor associated genes

	OR5P2		**OR52I1/OR52I2**		**OR9K2**	
	r	p-value	r	p-value	r	p-value
ADCY3	-0.23	**0.045**	-0.27	**0.017**	-0.13	0.25
GNAL	-0.07	0.541	0.11	0.34	-0.05	0.64
OBP2A	0.24	**0.038**	**0.35**	**0.002**	0.26	**0.023**
REEP1	**-0.33**	**0.004**	**-0.38**	**<0.001**	**-0.32**	**0.004**
RTP1	-0.25	**0.024**	**-0.44**	**<0.001**	**-0.36**	**0.001**
RTP2	**0.65**	**<0.001**	**0.68**	**<0.001**	**0.78**	**<0.001**
UGT1A6	**0.65**	**<0.001**	**0.87**	**<0.001**	**0.85**	**<0.001**

(A) Table shows the olfactory receptors expressed differentially higher in grey matter lesions compared to normal-appearing grey matter with a fold change of at least 1.5 (log2(fold change) of at least 0.585), sorted by the fold change. (B) Differential gene expression between grey matter lesions and normal-appearing grey matter of some olfactory receptor associated genes, sorted by the adjusted p-value. Significant p-value is marked in bold. (C) Pearson-correlation of the olfactory receptor associated genes with the three olfactory receptors of interest. Correlation coefficients with an absolute value larger than 0.3 and significant p-values are marked in bold.

Gene expression profiles and confounding factors of OR5P2, OR52I2 and OR9K2

The olfactory receptor OR5P2 was the olfactory receptor with the highest fold change (p=0.021, log2FC=0.89, Figure 11A), followed by OR52I2 (p=0.03, log2FC=0.8, Figure 11B) and OR9K2 (p=0.043, log2FC =0.79, Figure 11C). All three olfactory receptors showed a significant negative correlation with the RNA integrity number (RIN) (OR5P2: r=-0.28,

p=0.024, df=76, OR52I2: r=-0.43, p<0.001, df=76, OR9K2: r=-0.42, p=0.005, df=76). The correlation is however weak and does not explain the difference observed between normal-appearing and lesion-containing tissue samples. OR5P2 gene expression levels further correlated weak but statistically significant with the post-mortem interval (r=-0.05, p=0.02, df=76). OR52I2 and OR9K2 expression levels did not correlate with the post-mortem interval. All three ORs of interest did not significantly correlate with disease duration or age and did not significantly associate with sex or frontal versus parietal brain lobe.

As the olfactory receptor gene sequences may show a high degree of similarity, we retrospectively investigated the primers used for the microarray concerning their specificity. We did not detect any alternative hybridization target for OR5P2 and OR9K2. For OR52I2 we detected that the probe sequence showed a 98% similarity with 100% query cover for OR52I1, making it highly likely that the probe does not properly distinguish between these two target sequences. The probe for OR52I1 showed 96% identity with a 100% query cover for OR52I2. OR52I1 was also differentially higher expressed in tissue containing grey matter lesions compared to normal-appearing grey matter (log2FC=0.67, adj.p.value=0.043) and the gene expression of the two genes correlated strongly (r=0.94, df=76, p<0.001). We therefore from now on write OR52I1/OR52I2 instead of OR52I2.

The gene expression levels of the three olfactory receptors of interest showed a statistically significant positive correlation with the olfactory binding protein OBP2A and with the obligate olfactory receptor pathway components RTP2 and UGT1A6 (Table 8C). However, they also correlated negatively with REEP1 and RTP1 (Table 8C).

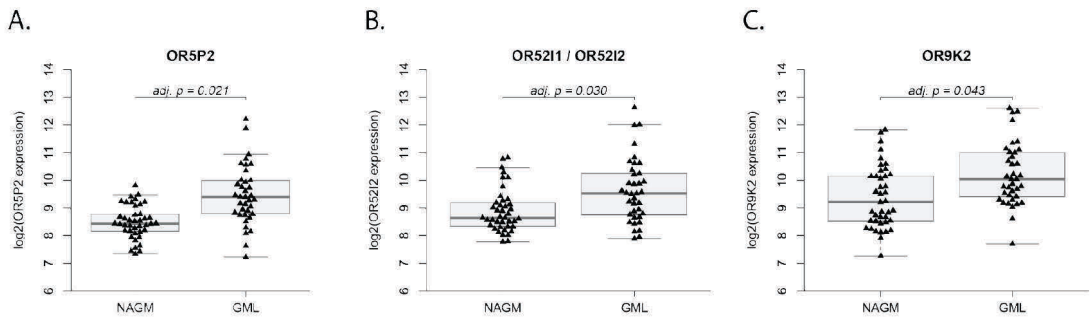

Figure 11. Gene expression levels of the selected olfactory receptors

Plots show the gene expression levels of the selected ORs (A) OR5P2, (B) OR52I1/OR52I2 and (C) OR9K2. All three selected ORs demonstrate a higher gene expression level in tissues containing grey matter lesions compared to normal-appearing grey matter. Abbreviations: GML: Tissue containing grey matter lesions; NAGM: Normal-appearing grey matter tissue.

Histological protein colocalization reveals OR5P2 on neurons, OR52I1/OR52I2 on neurons and blood vessels, and OR9K2 on blood vessels

Immunofluorescence colocalization experiments on cortical grey matter from MS normal-appearing and lesion containing tissue samples demonstrated OR5P2 expression on neurons (Figure 12A, B), OR52I1/OR52I2 expression on blood vessels and neurons (Figure 12C, D) and OR9K2 expression on blood vessels (Figure 12E, F) in all tissue types. Very few glia cells were also detected to express the olfactory receptors of interest. As not all neurons and not all blood vessels appeared to be stained for the respective olfactory receptor, we analyzed further tissue samples and quantified the percentage of double positive neurons and double positive blood vessels. For this analysis we chose to investigate subpial grey matter lesions and normal-appearing grey matter from 12 tissue blocks of 10 MS cases.

Within tissue containing grey matter lesions we detected 52.3% of the NeuN positive cells to be positive for OR5P2, differing significantly from 38.0% detected in normal-appearing grey matter ($p=0.037$, $df=19.7$). For OR52I1/OR52I2 we detected a mean of 47.2% of NeuN cells to be double positive, not differing significantly from 33.5% detected in normal-appearing grey matter ($p=0.15$, $df=21.3$).

Co-localizing experiments with collagen IV revealed a mean of 24.7% of blood vessels to be positive for OR52I1/OR52I2 in tissue containing grey matter lesions. This was significantly higher compared to 12.4% detected in normal-appearing grey matter ($p=0.01$, $df=26.0$). For OR9K2 we detected an average of 60.8% of blood vessels to be double-positive in tissue containing grey matter lesion. This also showed to be significantly higher compared to 28.9% detected in normal-appearing grey matter ($p<0.001$, $df=20.7$).

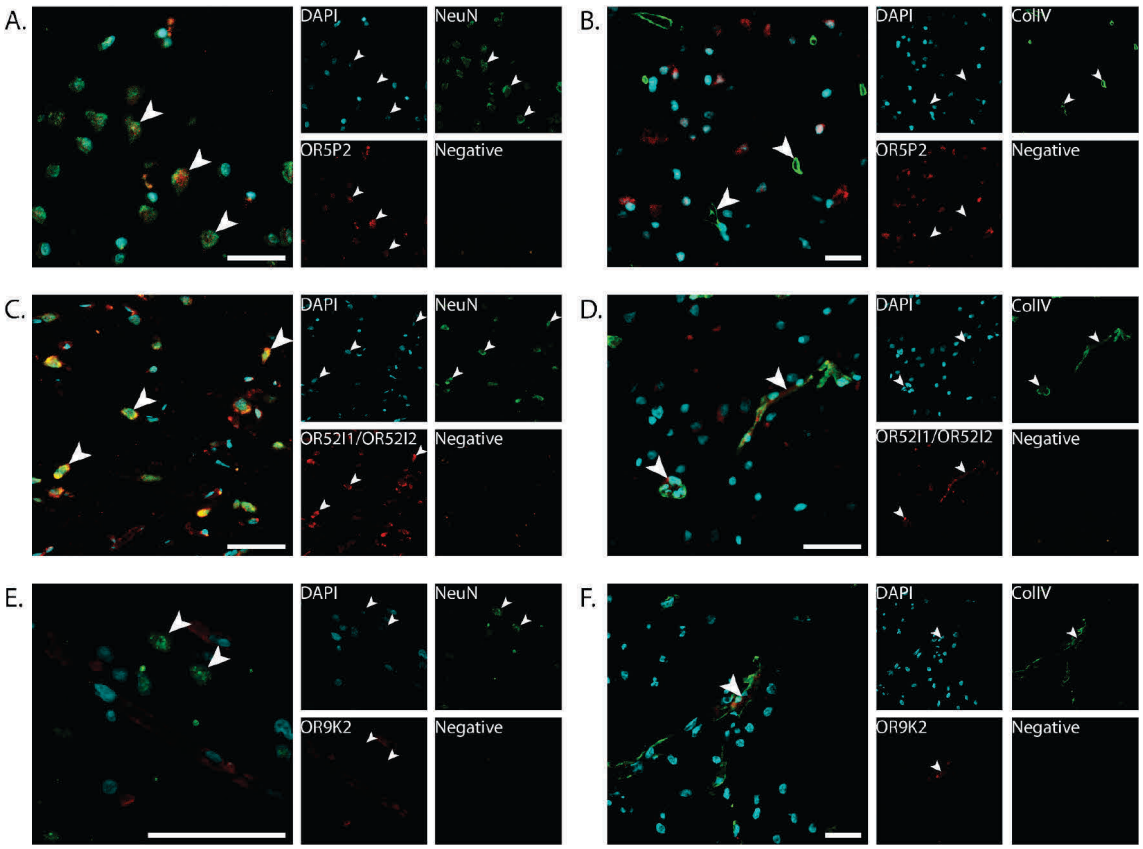

Figure 12. Cellular identity of OR5P2, OR52I1/OR52I2 and OR9K2 protein expression
(A) OR5P2 colocalizes with neurons (arrows), marked with NeuN, (B) but not with with blood vessels (arrows), marked with ColIV. (C) OR52I1/OR52I2 colocalizes with neurons (arrows) and (D) with blood vessels (arrows). (E) OR9K2 doesn't colocalize with neurons (arrows), (F) but demonstrated a punctuated expression pattern on blood vessels (arrows). As human cortex regularly shows false-positive signal due to autofluorescence of hemosiderin within the neurons, the Cy3 channel was scanned without secondary antibody. Scale bars: 50µm.

The difference in neuronal expression is driven by the tissue containing the subpial demyelination, whereas the vascular expression is higher throughout the cortex

We were then further intrigued to investigate the question, whether the differences in the fraction of neurons and blood vessels expressing the olfactory receptors is driven by the subpial lesion in the upper layers of the cortex, or instead by the perilesional lower cortical layers. Visual investigation of the fluorescence double-labeling did not give an apparent answer to this. We thus compared the top half of the cortex (corresponding to the neuronal layers I to III), containing the subpial lesions in the grey matter lesion containing samples, to the top half of normal-appearing cortex. Analogously, we compared the lower half of the cortex (neuronal layers IV to VI), containing perilesional, myelinated areas in the tissue containing lesions, to the lower half of normal-appearing grey matter.

This investigation revealed a statistically significant difference between the number of OR5P2 positive neurons in the upper layers of the cortex in the lesion containing tissue compared to

the normal-appearing grey matter (Figure 13A, C, Table 9). There was no statistically significant difference between the tissue samples from the lower half of the cortex. For OR52I1/OR52I2 colocalization within neurons, we also detected a significant increase in the upper layers, but not in the lower layers (Figure 13A, C, Table 9).

Concerning colocalization with blood vessels, we detected a significant higher numbers of olfactory-receptor positive blood vessels in the upper as well as the lower layers for OR52I1/OR52I2 and for OR9K2 (Figure 13B, D, Table 9).

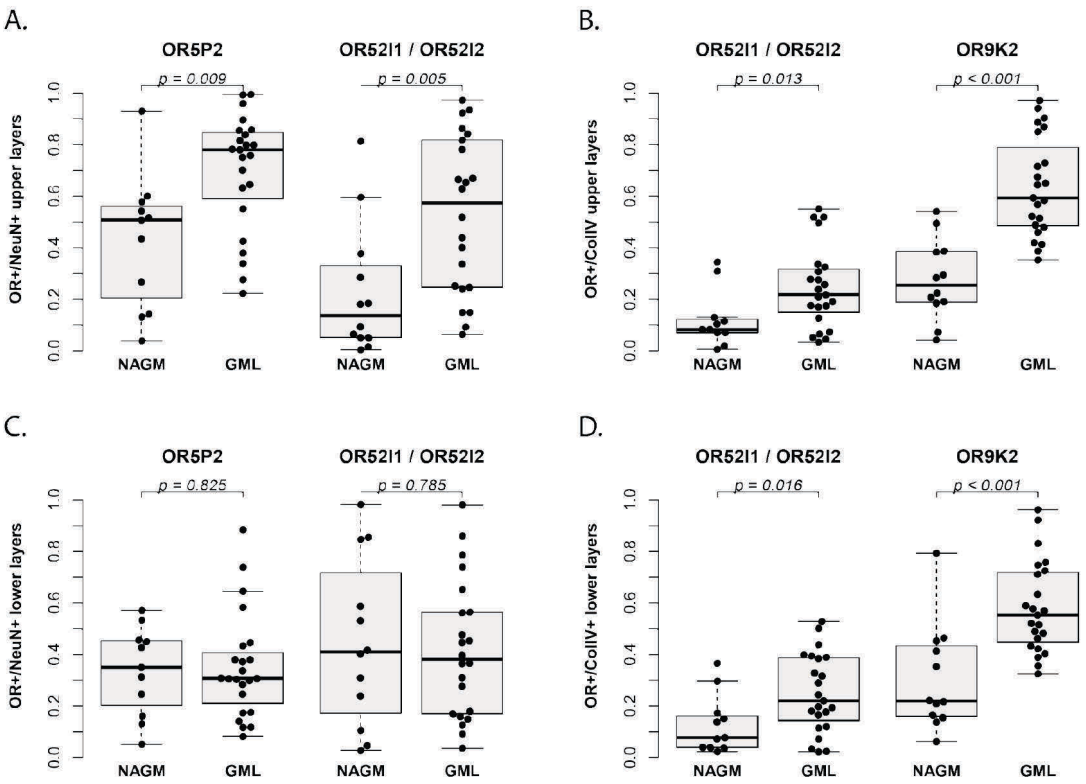

Figure 13. Quantification of the neurons and blood vessels positive for the respective olfactory receptor
(A) Boxplots showing the percentage of NeuN+ cells colocalizing with the respective olfactory receptor in the upper half of the cortex. (B) Boxplots showing the percentage of ColIV+ blood vessels colocalizing with the respective olfactory receptor in the upper half of the cortex. (C) Boxplots showing the percentage of NeuN+ cells colocalizing with the respective olfactory receptor in the lower half of the cortex. (D) Boxplots showing the percentage of ColIV+ blood vessels colocalizing with the respective olfactory receptor in the lower half of the cortex. p-values are derived from a two-sided Welch t-test pooling all samples of NAGM and GML respectively. Abbreviations: GML: Tissue containing grey matter lesions; NAGM: normal-appearing grey matter.

Table 9. Fraction of neurons and blood vessels positive for the respective olfactory receptor

			Mean NAGM	Mean GML	p-value	degrees of freedom
OR5P2	Neurons	Top cortical Layers	42.6%	69.7%	**0.009**	17.6
		Bottom cortical layers	33.5%	35.0%	0.82	23.2
OR52I1/OR52I2	Neurons	Top cortical Layers	22.5%	52.8%	**0.005**	26.4
		Bottom cortical layers	44.5%	41.5%	0.78	19.2
	Blood vessels	Top cortical Layers	12.1%	24.5%	**0.013**	27.6
		Bottom cortical layers	12.8%	24.9%	**0.016**	25.9
OR9K2	Blood vessels	Top cortical Layers	27.5%	63.5%	**<0.001**	27.1
		Bottom cortical layers	30.3%	58.1%	**<0.001**	20.0

Table shows the fraction of neurons (derived from NeuN staining) and blood vessels (derived from ColIV staining) positive for the respective olfactory receptor OR5P2, OR52I1/OR52I2 or OR9K2. The given p-values and degrees of freedom are derived from two-sided Welch t-tests to compare normal-appearing grey matter and grey matter lesions. Abbreviations: GML: Tissue containing grey matter lesions; NAGM: Normal-appearing grey matter tissue.

8.2.5 Discussion

We were interested in the molecular changes within chronically demyelinated cortical grey matter lesion areas compared to non-demyelinated, normal-appearing cortical grey matter areas in MS brain tissues. Grey matter lesions in MS have been studied increasingly over the past two decades (Kidd, Barkhof et al. 1999) and both the number and distribution of lesion types in our study group are in line with previous publications (Bø, Vedeler et al. 2003). All our examined grey matter lesions showed no sign of inflammation, which is a common finding in chronic cortical grey matter lesions and is in contrast to chronic active white matter lesions (Bø, Vedeler et al. 2003).

First, we investigated the fraction of demyelinated area in the MS cerebral cortex. Our study revealed a significant higher fraction of demyelinated cortex in secondary progressive MS cases compared to primary progressive cases. We were not able to find any publication concerning the fraction of cortical demyelination in primary progressive compared to secondary progressive MS cases. It has recently been pointed out in a review article that no difference in the cortical demyelination between these two disease courses has been described to date (for review see: Lassmann 2019). As our study population however included only six primary progressive cases with grey matter lesions, this should be further systematically investigated with more cases.

Whereas we did not find any difference between the demyelinated cortical areas between the sexes, in a large study, analyzing autopsy tissue of 182 MS cases, a higher proportion of men with grey matter lesions was identified compared to women (Luchetti, Fransen et al. 2018), but they did not investigate the lesion size within the cortical grey matter.

Among the 1'758 differentially expressed genes between normal-appearing grey matter and grey matter containing demyelinated lesions we found a group of 68 olfactory receptors to be differentially higher expressed. ORs are members of the class A rhodopsin-like family of G protein-coupled receptors and may bind a multitude of chemical compounds and are known to be expressed in many different tissue types such as the olfactory bulb, testis, kidney, heart and lung (Zhang, De la Cruz et al. 2007). ORs have previously been shown to be differentially expressed in various neurodegenerative diseases such as Parkinson's disease (Garcia-Esparcia, Schluter et al. 2013), Alzheimer's disease, progressive supranuclear palsy, Creutzfeldt-Jakob disease (Ansoleaga, Garcia-Esparcia et al. 2013), chronic schizophrenia (Ansoleaga, Garcia-Esparcia et al. 2015) and in the Alzheimer disease related mouse model APP/PS1 (Ansoleaga, Garcia-Esparcia et al. 2013). These diseases, together with MS, have in common a neurodegenerative component in their pathology. The olfactory receptors previously studied within the human cerebral cortex were all detected to be expressed in neurons and differ from the three receptors of interest we have studied here (Ansoleaga, Garcia-Esparcia et al. 2013, Garcia-Esparcia, Schluter et al. 2013, Ansoleaga, Garcia-Esparcia et al. 2015).

We were able to localize the protein expression of OR5P2 and OR52I1/OR52I2 on neurons and demonstrated the presence of OR52I1/OR52I2 and OR9K2 on cortical blood vessels. A more detailed investigation of the protein expression pattern revealed only a fraction of the neurons and blood vessels to be positive for the respective OR. We revealed a higher fraction of neurons to be positive for OR5P2 and OR52I1/OR52I2 within the subpial demyelinated area compared to the perilesional lower layers. This stands in contrast to the upregulation of OR52I1/OR52I2 and OR9K2 in the blood vessels in both the upper, demyelinated and lower, normally myelinated areas.

Blasting for OR52I2 revealed an important issue when studying this family of receptors, which is the high similarity of their sequences. Neither the microarray nor the antibody used for the immunofluorescent detection may distinguish between OR52I2 and OR52I1. A more detailed analysis of which receptor gave rise to our results would require for example deep-sequencing analysis or in situ RNA hybridizations.

The presence of proteins involved in transporting olfactory receptors to the cell surface, such as RTP1, RTP2 and REEP1 and of the UDP-glucuronosyltransferase UGT1A6 and of obligate downstream components of the OR signaling pathway such as ADCY3 and GNAL have been demonstrated in neurons in the human cerebral cortex previously (Garcia-Esparcia, Schluter et al. 2013). This supports the hypothesis of a functional expression of ORs within the human cortex. Though we only detected RTP to be significantly differentially higher expressed in

tissue containing grey matter lesions compared to normal-appearing grey matter in our samples, this does not contradict a functional upregulation of the ORs studied here, as the protein expression may not be the bottle neck of the olfactory receptor signaling pathway.

In general, the neurons of the olfactory epithelium, where these receptors were first discovered, express one olfactory receptor per neuron exclusively. As we detected around 50% of the neurons to be positive for OR5P2 and OR52I1/OR52I2 within our samples respectively, our data suggests that the protein expression is not exclusive per neuron within the cerebral cortex, without directly demonstrating this, as all antibodies available were produced in the same species. The same argument without direct proof has been made previously for other olfactory receptors located on cortical neurons (Garcia-Esparcia, Schluter et al. 2013).

The role of olfactory receptors in the human brain remains elusive, but the presence of these receptors on neurons might indicate that there is the possibility of a local stimulation by neighboring cells or maybe a self-stimulation. The expression in blood vessels is highly suggestive of a ligand within the blood stream, but no description of such mechanisms is known to us. It has previously been pointed out that the widespread expression of many olfactory receptors may point towards a cardinal physiological role within the signaling environment of the brain, which remains to be investigated in detail (Ansoleaga, Garcia-Esparcia et al. 2013).

Odorant-binding proteins are extracellular proteins, which aid in olfactory perception by binding lipophilic molecules and transporting them to the olfactory receptors. In mammals, these proteins belong to the lipocalin super family. Though highly speculative, odorant-binding proteins might link the olfactory receptors to iron-homeostasis and oxidative stress: In mice, it has been suggested that odorant-binding proteins may scavenge for free-iron (Stopkova, Dudkova et al. 2014). Changes in iron homeostasis have been linked to demyelination and neurodegeneration in MS (Hametner, Wimmer et al. 2013, Haider, Simeonidou et al. 2014, Magliozzi, Hametner et al. 2019). Further, the bovine odorant-binding protein has been shown to protect from chemically induced oxidative stress (Macedo-Marquez, Vazquez-Acevedo et al. 2014). Whether similar mechanisms might take place within the human brain and whether this also involves olfactory receptors remains subject for further investigations and is highly speculative at this point.

Using human brain tissue from autopsies for gene expression studies to further increase our understanding of human brain diseases is an invaluable tool, allowing us to gain insights on human diseases not otherwise possible. The limitations of this approach however need to be carefully explored and confounding factors such as the presence of other neurological diseases, age-related changes and post-mortem related degradation need to be considered. While we

excluded any tissue showing signs of any other neurological pathology and excluded samples showing a low RNA quality, we still detected a relatively weak, but statistically significant negative correlation of the RNA integrity index with OR5P2, OR52I1/OR52I2 and OR9K2. This correlation might derive from a relative stability towards post mortem decay of these transcripts, leading to an artificially higher expression. This effect however is not strong enough to account for the higher expression we detected in samples containing lesions compared to normal-appearing grey matter.

In summary, we hypothesize that the differential expression of olfactory receptors within chronic grey matter lesion containing tissue might either be a correlate of ongoing tissue damage and degeneration, or might be part of adaptation mechanisms secondary to damage, potentially overlapping with tissue damage and difficult to discern. Alternatively, they could be involved in neuroprotective mechanisms. Our study adds a new piece to the puzzle, demonstrating the expression of olfactory receptors on neurons and blood vessels in chronic cortical grey matter lesion pathology. Even though the (patho-)-mechanisms behind the olfactory receptor expression remains elusive, this might be a putative link of MS to other neurodegenerative diseases and be part of more general mechanisms.

With an increasing number of studies being performed on olfactory receptors in various tissues, novel model systems are being designed to study their physiological roles. One specific model makes use of modified HEK293 cells, termed Hana3a cells, which stably express obligate olfactory receptor pathway components (Trimmer, Snyder et al. 2014). By transducing this cell line with an olfactory receptor, the receptor is functionally expressed at the cell surface and the activity of the receptor can be tested with, for example, a double luciferase assay (Trimmer, Snyder et al. 2014). We are currently setting up experiments to investigate the hypothesis of OR5P2, OR52I1/OR52I2 and OR9K2 ligands within the blood stream using this model system.

8.2.6 Acknowledgments

We thank Prof. Dr. Richard Reynolds (UK Multiple Sclerosis Tissue Bank, Charing Cross Hospital London, UK) for providing human brain tissues. We also thank Prof. Christine Stadelmann (University Hospital, Göttingen, Germany) for fruitful discussions and Stephanie Jaggi for technical assistance. This study was supported by the Roche Translational Medicine Hub, by the Swiss National Science Foundation (31003A_159528/1), by the Swiss Multiple Sclerosis Society, and by the French MS Society (ARSEP) all to N.S.W. and by the Swiss National Science Foundation MD-PhD grant 323530_171139, 2016-2019 to L.S.E.

Calculations were performed at sciCORE (http://scicore.unibas.ch/) scientific computing center at University of Basel.

8.3 Study 3: A novel animal model for meningeal inflammation and chronic inflammatory demyelination of the cerebral cortex

Lukas S. Enz, Anne Winkler, Claudia Wrzos, Boris Dasen, Christine Stadelmann, Nicole Schaeren-Wiemers

Manuscript in preparation for publication.

Contributions of Lukas S. Enz:
Study design, cloning of plasmids, lentivirus production and testing, stereotactic injections, image analysis, data analysis and interpretation, initial manuscript preparation and manuscript revisions.

Author contributions:
A.W.: Study design, stereotactic injections, immunohistochemistry, data analysis and interpretation, and manuscript revisions. C.W.: Study design, stereotactic injections and immunohistochemistry. B.D.: Cloning of plasmids, Lentivirus production. C.S.: Study design, data analysis and interpretation, and manuscript revisions. N.S.W. Study design, data analysis and interpretation, and manuscript revisions.

8.3.1 Abstract

The development of a model for chronic cortical demyelination is important to study chronic changes such as failure of remyelination, chronically disturbed functions of oligodendrocytes, neurons and astrocytes, brain atrophy and cognitive impairments observed in patients with Multiple Sclerosis.

Objective: We describe the generation of an animal model to study the effects of chronic cortical demyelination and meningeal inflammation.

Method: To model cortical demyelination and chronic meningeal inflammation as seen in Multiple Sclerosis, we immunized female Lewis rats against myelin oligodendrocyte glycoprotein and injected lentiviruses to overexpress the cytokines Tnf and Ifng in the cortical brain parenchyma.

Results: Immunization and lentiviral injection gave rise to widespread subpial demyelination and meningeal inflammation, stable for at least 10 weeks.

Conclusions: Our new model will in the future allow to investigate molecular, cellular and functional investigations for a better understanding of the adaptation mechanisms of the brain cortex to a chronically demyelinated and inflamed environment as seen in Multiple Sclerosis.

8.3.2 Introduction

Multiple sclerosis (MS) is the most common chronic inflammatory and neurodegenerative disease of the central nervous system. The pathologic hallmark of MS is the formation of focal areas of myelin loss termed lesions. Besides the most commonly described white matter lesions, extensive grey matter lesions are found in MS cerebral cortex (Brownell and Hughes 1962, Kidd, Barkhof et al. 1999, Peterson, Bo et al. 2001). Grey matter lesions are reported to occur in up to 90% of all MS patients with chronic MS (Albert, Antel et al. 2007, Wegner and Stadelmann 2009). Early-stage MS grey matter lesions where shown to contain myelin-laden macrophages as well as perivascular CD3+ and CD8+ T-cell infiltration (Lucchinetti, Popescu et al. 2011), while chronic grey matter lesions characteristically lack significant infiltration of immune cells (Bø, Vedeler et al. 2003), but show diffuse microglial activation (Magliozzi, Howell et al. 2010, Gardner, Magliozzi et al. 2013). Both, in early- and chronic-stage, grey matter lesions were shown to associate with meningeal inflammation (Howell, Reeves et al. 2011, Lucchinetti, Popescu et al. 2011). Cortical demyelination has been shown to associate with loss of neurons, axons, synapses and glia cells (Wegner, Esiri et al. 2006, Dutta, Chang et al. 2011). Grey matter lesions are further characterized by more efficient myelin repair and less gliosis compared to white matter lesions (Albert, Antel et al. 2007).

Cortical atrophy and demyelination are associated with B-cell follicle-like structures in the meninges (Magliozzi, Howell et al. 2010) and have been linked to higher levels of interferon gamma (IFNG) and tumor necrosis factor alpha (TNF) in the meninges and in the cerebrospinal fluid (Gardner, Magliozzi et al. 2013). Although grey matter pathology in MS has received a rapidly growing interest over the past two decades, many aspects of the chronic pathological processes and the adaptations to a chronically demyelinated environment remain elusive.
Long-standing cortical demyelination may contribute to neuronal damage and degeneration. It is estimated that 40-70% of MS patients suffer from deficits of memory and attention, reduction of cognitive flexibility and impairment of executive functions. These symptoms are therapeutically very difficult to address and are mechanistically poorly understood, but it is strongly suspected that these cognitive symptoms are associated with changes in the cortical grey matter such as demyelinated lesions and atrophy (Rudick, Lee et al. 2009). Beside the well described demyelinated grey matter lesions also diffuse grey matter abnormalities in non-lesional normally myelinated areas, such as diffuse microglia activation, diffuse axonal injury and astrocyte gliosis have been observed (Kutzelnigg, Lucchinetti et al. 2005).

To study the pathomechanisms and functional consequences of chronic grey matter demyelination and meningeal inflammation in detail, an animal model replicating the key phenotypes is required. Such an animal model has been established by Merkler et al. in 2006 by immunizing Lewis rats with recombinant myelin oligodendrocyte glycoprotein (MOG) and incomplete Freunds adjuvant (IFA) (Merkler, Ernsting et al. 2006). This animal model was characterized by highly reproducible focal cortical demyelination and inflammation, followed by rapid resolution and remyelination. This model however did not give rise to a chronic cortical pathology, thereby not reproducing key features of chronic cortical grey matter pathology in MS such as failure of remyelination, chronic disturbances of the physiological functionality of the different cell populations, cortical atrophy and possible cognitive dysfunctions as seen in MS. To date, a model for chronic grey matter lesions does not exist, hampering mechanistically oriented research towards chronic changes, cognitive impairment and grey matter atrophy. We here report the establishment of an animal model for studying the effects of chronic cortical grey matter demyelination and meningeal inflammation.

8.3.3 Material and Methods

Subcloning of lentiviral plasmids

The lentiviral plasmid pULTRA was used as backbone and was acquired via Addgene (Addgene plasmid #24129, Addgene, Watertown, MA, USA) as a gift from Malcolm Moore (Lou, Fujisawa et al. 2012). The sequence for Tnf (Reference sequence: NM_012675.3, nucleotides 5'-145-852-3') was acquired from rat cDNA and the sequence for Ifng (Reference sequence: NM_138880.2, nucleotides 5'-10-480-3') was amplified by polymerase chain reaction from a cDNA ORF Clone plasmid (RG80234-UT, Sino Biological, Wayne, PA, USA). Primers for the polymerase chain reaction of Tnf and Ifng were designed with specific restriction enzyme sequences at the 5' and 3' sites (Table 10). The polymerase chain reaction products were purified by gel-electrophoresis and a gel DNA recovery kit according to the manufacturer's protocol (D4007, Zymo Irvine, CA, USA). The sequence for LacZ was acquired by restriction digest with BamHI (R3136S, New England Biolabs, Ipswich, MA, USA) of the plasmid LV-Lac acquired as a gift from Inder Verma (Addgene plasmid #12108 (Pfeifer, Brandon et al. 2001)). Restriction digests were performed in CutSmart buffer (B7204S, New England Biolabs, Ipswich, MA, USA), using 6 units restriction enzyme per microgram cDNA at 37°C for 3 hours. Subcloning of tzhe cDNAs occurred into the pULTRA backbone with the Rapid DNA Dephos & Ligation Kit (4898117001, Hoffmann-La Roche, Basel, CH) according to the manufacturer's protocol and, for amplification, the plasmids were transformed into Stbl3 bacteria (C737303, Thermo Fisher Scientific, Waltham, MA, USA). The plasmids were purified with the miniprep classic kit (D4015, Zymo Irvine, CA, USA) and sent to Microsynth (Balgach, Switzerland) for sequencing.

Table 10. Primers and restriction enzymes used for cloning

Primer Name	Primer Sequence	Enzyme / Cat. Number
5'-XbaI-ATG-Tnf-3'	ATGTTCTCTAGAATGAGCACGGAAAGCATGATCC	XbaI, R0145S
5'-BamHI-STOP-Tnf-3'	AGTTAGGATCCTCACAGAGCAATGACTCCAAAGTAGAC	BamHI, R3136S
5'-NheI-ATG-Ifng-3'	GATCATGCTAGCATGAGTGCTACACGCCGCGTCTTGG	NheI, R3131S
5'-EcoRI-STOP-Ifng-3'	GATCATGAATTCTCAGCACCGACTCCTTTTCCGCTTCCTTAG	EcoRI, R3101S

Table shows the primers and restriction enzymes used for cloning Tnf and Ifng. All restriction enzymes were acquired from New England Biolabs (Ipswich, MA, USA).

HEK293T cells

HEK293T cells were used for lentivirus production and lentiviral quality control. Cells were kept in high glucose DMEM (D6429, Sigma-Aldrich, St. Louis, MO, USA) containing 10% fetal bovine serum (F9665, Sigma-Aldrich) and 1% antibiotics and antimycotics (A5955, Sigma-Aldrich). Splitting of the cells was performed when necessary by removing the culture

medium, rinsing with calcium-free Dulbecco's Phosphate Buffered Saline (D8537, Sigma-Aldrich), mobilizing cells with 0.25% Trypsin-EDTA solution (T4049, Sigma-Aldrich), inactivating trypsin activity with 1ml culture medium and distributing cells to new flasks.

Lentivirus production

Lentiviruses containing the sequence for enhanced green fluorescent protein (eGFP) and either LacZ, Tnf or Ifng were produced in HEK293T cells. The lentiviral helper plasmids pMD2.VSV-G, (Addgene plasmid #12259), pMDLg/pRRE (Addgene plasmid #12251) and pRSV-Rev (Addgene plasmid #12253) were acquired from Addgene (Watertown, MA, USA) as a gift from Didier Trono (Dull, Zufferey et al. 1998). Per T75 flask of 70% confluent HEK293T cells a 1.5ml tube with 0.75ml Opti-MEM Medium (31985062, Thermo Fisher Scientific) was mixed with 5µg of each helper plasmid and 6.5µg of the lentiviral plasmid. Further, one 15ml tube with 0.75ml Opti-MEM medium was mixed with 60 µl Lipofectamine 2000 Transfection Reagent (No. 11668027, Thermo Fisher Scientific). The diluted plasmids were mixed with the Lipofectamine solution, vortexed and incubated for five minutes at room temperature. The DNA-lipid complex was then added to the T75 flasks and incubated for 18 hours, removed and replaced with 7ml fresh HEK293T culture medium. After 48 hours, the cell culture medium was harvested to a 15ml tube and centrifuged 15 minutes at 3'000g to pellet cells and debris. The supernatant was then filtered through a 0.45µm filter on a syringe. To concentrate the viral particles, 2.3ml Lenti-X-concentrator was added to the filtrate (631232, Takara, Kyoto, Japan). The mixture was gently inversed several times, incubated at 4°C for 5 hours, centrifuged at 1'500g for 45 minutes at 4°C, the supernatant was carefully removed and the pellet was resuspended in 70µl phosphate buffered saline. The lentiviral particles were aliquoted and stored at -80°C.

Lentivirus quantification

Concentration of lentiviral particles was determined by estimating the concentration of lentivirus-associated p24 protein with the QuickTiter Lentivirus Titer Kit according to the manufacturer's protocol (VPK-107, Cell Biolabs, Inc., San Diego, CA, USA). For calculating the approximate number of transfective units, the conservative assumption of 1'000 P24 proteins per lentiviral particle was applied (range suggested by the manufacturer: 100-1'000).

Lentivirus quality control

To confirm the production of functional lentiviruses, Tnf and Ifng production and secretion was verified by enzyme-linked immune-sorbent assay (ELISA). HEK293T cells were seeded into 6 well plates at a density of 200'000 cells per well, and cultivated for 18 hours before transduction with one viral particle per cell of either LV-Tnf or LV-Ifng. Medium was exchanged three times per week and cells were transferred to fresh flasks three times before assuming the supernatant and cells to be free of active lentiviral particles. Cell culture medium was then replaced with 1ml fresh medium without serum and 24 hours later cytometry and ELISA were performed.

For cytometry cells were washed with PBS without calcium and magnesium, dissolved with Trypsin-EDTA and diluted in culture medium. Cells were then centrifuged for 5 minutes with 350g at 4°C, the supernatant was discarded and the cell pellet was dissolved in PBS without calcium and magnesium. Cells were again centrifuged, the supernatant was discarded, and the cell pellet was resuspended in 300µl 5mM EDTA in PBS without calcium and magnesium

For Tnf and Ifng ELISA an unlabeled Tnf capture antibody (dilution 1:167, 506102, Biolegend, San Diego, CA, USA), or an unlabeled Ifng capture antibody (diluted 1:500, 507802, Biolegend) respectively was diluted in coating buffer (421701, Biolegend), and 100µl per well were distributed in a 96-well plate (423501, Biolegend). After 18 hours incubation at 4°C, the plate was washed with 0.05% Tween-20 in PBS three times and 200µl blocking solution (421203, BioLegend) was added per well for 1 hour. The plate was then washed as before, and incubated for 3 hours with 100µl pure or 1:100 diluted supernatants from the HEK293 cell culture transfected with LV-Tnf or LV-Ifng. The plate was washed and the biotin-labeled detection antibody against Tnf (diluted 1:1000, 516003, Biolegend, San Diego, CA, USA) or Ifng (diluted 1:500, 518803, Biolegend, San Diego, CA, USA), respectively, was added for 1 hour. Plate was washed and 100µl per well Avidin-Horse radish peroxidase conjugate was added (diluted 1:1000 in blocking buffer, 405103, Biolegend). The plate was washed and 200µl substrate solution (421101, Biolegend) was added per well. Upon sufficient color development 100µl stop solution (423001, Biolegend) was added. Absorption was measured at 450nm.

Animals

For the experiments, adult (185-250 g) female inbred Lewis rats were purchased from Janvier Labs (Saint-Berthevin, France). Animal housing and all animal experiments were performed at the Universitätsmedizin Göttingen, Institute for Neuropathology, 37075 Göttingen, Germany. The rats were housed in cages with up to 5 animals each under constant temperature and humidity, a 12/12 h light/dark cycle and with free access to food and water. All animal

experiments were performed in accordance with the European Communities Council Directive of September 22, 2010 (2010/63/EU) and were approved by the Government of Lower Saxony, Germany. The animals were not asked for consent.

Immunization and intracerebral stereotactic injection

The immunization and intracerebral stereotactic injection were performed as described before (Merkler, Ernsting et al. 2006). Briefly, adult female Lewis rats were anaesthetized with isoflurane and immunized subcutaneously with 50µg recombinant MOG corresponding to the N-terminal sequence of rat MOG 1-125, expressed in Escherichia coli and purified as described before (Adelmann, Wood et al. 1995) and emulsified in incomplete Freund's adjuvant (F5506, Sigma-Aldrich). For control experiments, rats were injected with PBS emulsified in incomplete Freund's adjuvant.

18 days after immunization, intracerebral stereotactic injection was performed. For this, rats were anaesthetized by intraperitoneal injection of Ketamin/Xylazine and fixed in a stereotactic frame. A one-centimetre-long incision of the skin on the midline of the skull was made to expose the bregma and a hole was drilled 2 mm lateral of and 1 mm caudal of the bregma. Using a finely calibrated glass capillary, 2.5µl solution was carefully injected into the cortex, containing either LV-Tnf and LV-Ifng mixed 1:1, LV-LacZ or the recombinant cytokines Tnf (250 ng; P16599, R&D Systems, Abingdon, UK) and Ifng (150 U; 400-20, PeproTech, London, UK). Monastral blue was added as a marker dye. After the injection, the glass capillary was retracted and the skin was closed with a suture. Rats were perfused after 5 days, 4 weeks, 7 weeks or 10 weeks to investigate lesion evolution. Therefore, the animals were anaesthetized with isoflurane, lethally injected with Ketamin/Xylazine and perfused transcardially with PBS followed by 4% paraformaldehyde. Subsequently, the heads were postfixed in 4% paraformaldehyde at 4°C for 2 days before removing the brain and embedding it in paraffin.

Enzyme-linked immunosorbent assay for MOG titers

The measurement of the serum anti-MOG antibody titers, an ELISA was performed as described before (Kerschensteiner, Stadelmann et al. 2004, Merkler, Ernsting et al. 2006). Values above 2-fold of the background levels were considered to be positive.

Immunohistochemistry

Immunohistology was performed on 3µm thin formalin-fixed, paraffin embedded (FFPE) sections using antibodies for macrophages/ activated microglia (CD68, clone ED1, Bio-Rad

AbD Serotec, Oxford, UK), CD3+ T-cells (clone CD3-12Bio-Rad AbD Serotec, Oxford, UK), CD45R+ B-cells (clone HIS24, BD Biosciences, Franklin Lakes, USA), myelin basic protein (MBP, Abcam, Cambridge, UK), anti-neuronal nuclei (NeuN, Abcam, Cambridge, UK), oligodendrocyte lineage factor 2 (OLIG2, clone 211F1.1, Merck Millipore, Darmstadt, Germany), mature oligodendrocytes (P25/TPPP, clone EPR3316, Abcam, Cambridge, UK), (pre-)myelinating oligodendrocytes (BCAS1, Santa Cruz, Heidelberg, Germany), FITC (HRP conjugated, Dako Deutschland GmbH, Hamburg, Germany) and green fluorescent protein (GFP, clone 6AT316, Abcam, Cambridge, UK).

Image analysis

All stained tissue sections were scanned with an Olympus VS120-L100-W scanner fitted with a VC50 camera (Olympus, Shinjuku, Tokio, Japan) with a 200x magnification at a resolution of 0.345 micrometer per pixel.

For CD3 and CD45R stainings, the cells were counted manually using the NIS-Elements software (Version 5.11.00, Nikon, Tokyo, Japan). For demyelination, areas were delineated manually using the CellSense software (Version 1.6, Olympus, Tokyo, Japan).

Statistical analysis

Statistical analysis was performed with R. To compare means of two groups two-sided Welch t-tests were performed. For correlations, pearson correlations were calculated. A p-value below 0.05 was considered statistically significant.

Data availability

All data generated or analyzed during this study will be included in the published article and its supplementary information files.

8.3.4 Results

Establishment of the lentiviral based animal model

The DNA sequences encoding for Tnf, Ifng and LacZ were cloned into the pULTRA plasmid to produce the plasmids pULTRA-Tnf, pULTRA-Ifng and the control plasmid pULTRA-LacZ (Figure 14A). From these plasmids, the lentiviruses LV-Tnf, LV-Ifng and LV-LacZ were produced in HEK293T cells. ELISA quantification of lentiviral-associated P24 protein revealed an average of $8.2x10^6$ transfective units per ml over all batches and viruses. Biological activity

of each batch of lentiviruses was confirmed by transducing HEK293T cells and subsequent qualitative ELISA measurement of Tnf and Ifng protein from the supernatant.

The lentiviruses were stereotactically injected into MOG-immunized animals (LV-Tnf mixed 1:1 with LV-Ifng or only LV-LacZ) or into non-immunized animals (LV-Tnf mixed 1:1 with LV-Ifng). A further control group of MOG-immunized animals were injected with recombinant protein Tnf and Ifng (Figure 14B). The animals were perfused 5 days or 4, 7, or 10 weeks after the injection.

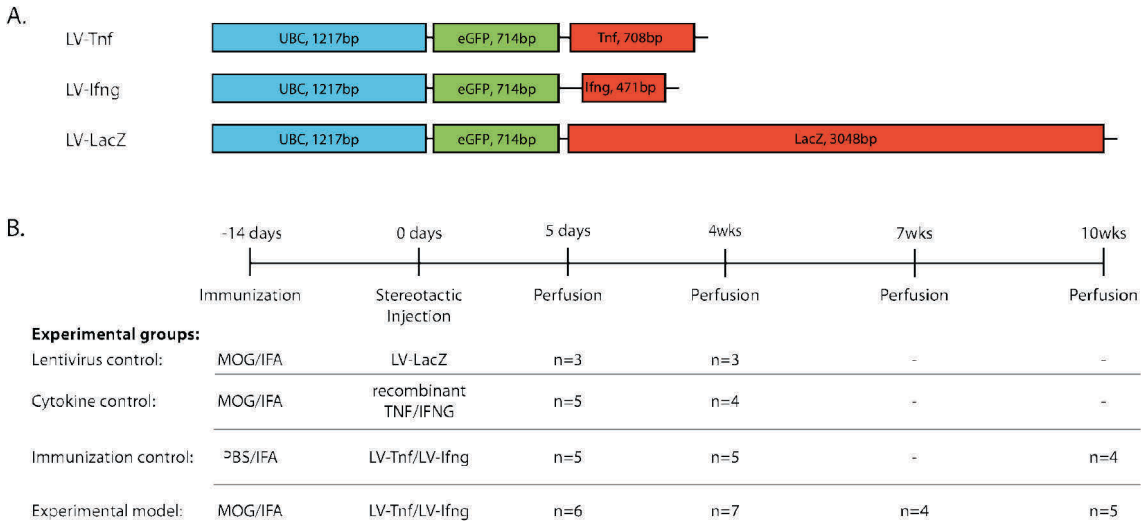

Figure 14. Lentiviral constructs and experimental design

(A). Schematic drawing of the lentiviral constructs depicting the human ubiquitin C promoter (UBC), and the sequences for enhanced green fluorescent protein (eGFP), tumor necrosis factor (*Tnf*), interferon gamma (*Ifng*), beta galactosidase (*LacZ*). (B). Experimental timeline and table depicting the four experimental groups with the respective number of animals in the final analysis per group and time point. Animals are pooled from two independent experiments. MOG: recombinant myelin-oligodendrocyte glycoprotein, PBS: phosphate buffered saline, IFA: incomplete freund's adjuvants.

Immunization against MOG is required for cortical demyelination

5 days after the stereotactical injection, cortical demyelination was detected by staining against MBP in all study groups previously immunized against MOG (Figure 15A-D). All cortical demyelination detected was subpial, stretching from the midline lateral. The fraction of the cortex which was demyelinated ranged from 0-19.5% of the total cortical area (Figure 15F). The percent of cortex demyelinated was largest in the animals injected with LV-Tnf and LV-Ifng with a mean of 13.3% (n=6), followed by the animals injected with the cytokines with a mean of 5.6% (n=5) and the animals injected with LV-LacZ with a mean of 4.8% (n=3). The non-immunized animals injected with LV-Tnf and LV-Ifng did not show any demyelination (n=5, Figure 15C).

Subpial demyelination is long-standing in animals after LV-*Tnf and* LV-*Ifng injection*

4 weeks after the stereotactical injection, the subpial demyelination was still largest in the MOG-immunized animals injected with LV-Tnf and LV-Ifng with a mean of 5.5% (n=7, Figure 15F). The demyelinated area was significantly smaller compared to the same treatment group after 5 days (p=0.01, df=5, Figure 15F). After 7 weeks, the demyelinated area was 5.0% of the total cortical area and after 10 weeks 5.6%, with no statistically significant difference between 4, 7 and 10 weeks. 4 weeks or longer after the stereotactic injections demyelination was still detected in both hemispheres (Figure 15E). Residual subpial demyelination was detected in the animals injected with the recombinant proteins after 4 weeks with a mean of 0.9% of the cortex demyelinated (n=4) and in the animals injected with LV-LacZ with a mean of 1.3% of the cortex demyelinated (n=3, Figure 15F).

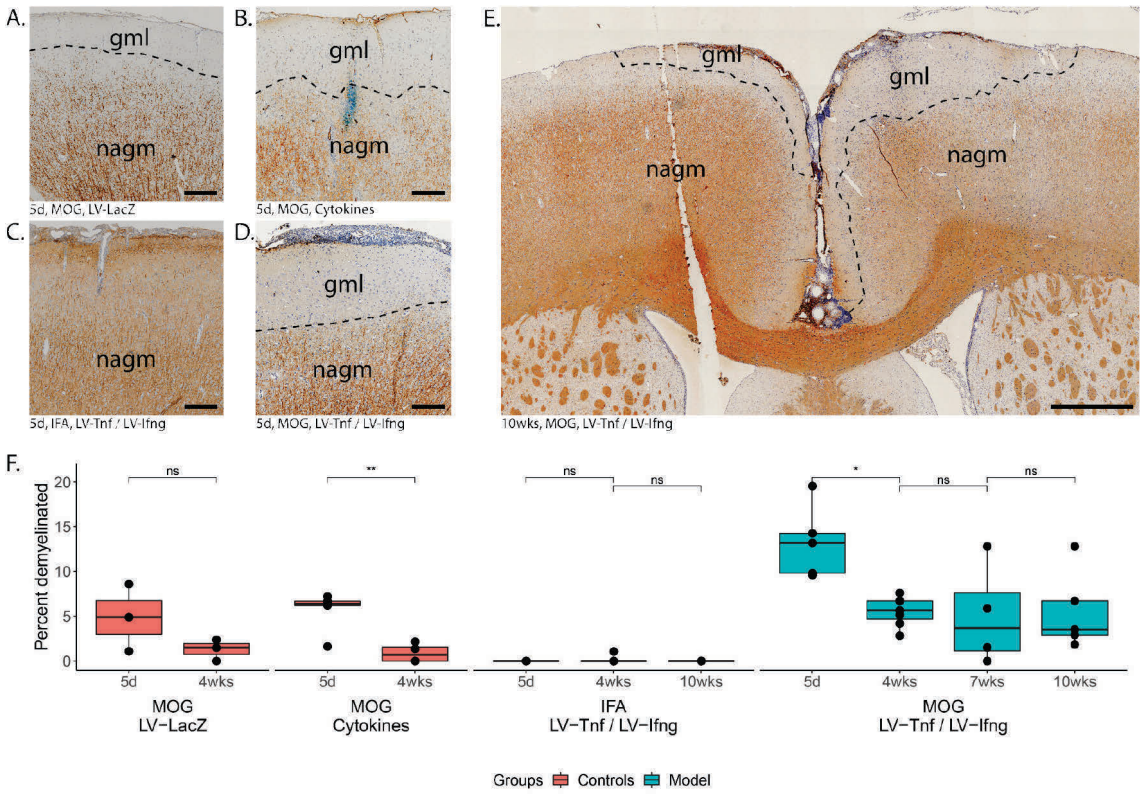

Figure 15. Subpial demyelination

Representative images of anti-MBP stainings demonstrating the subpial demyelination 5 days after the intracerebral injection of (A) LV-LacZ, (B) recombinant protein Tnf and Ifng, (C) LV-Tnf and LV-Ifng in non-immunized animals and (D) LV-Tnf and LV-Ifng in MOG-immunized animals. (E) overview image depicting the subpial demyelination present 10 weeks after the intracerebral injection. (F) Boxplots showing the percent of cortex demyelinated across both hemispheres for all groups studied. Abbreviations: gml: grey matter lesion; nagm: normal-appearing grey matter. A two-sided Welch t-test was performed to compare between the time points: ns: not significant; *: p-value <0.05; **: p-value <0.01.

Meningeal inflammation is dependent on LV-Tnf and LV-Ifng

5 days after the stereotactical injection, a widespread meningeal infiltrate was detected in both study groups injected with LV-Tnf and LV-Ifng, irrespective of the immunization. The mean maximum thickness of the meninges was 99.1µm in these study groups compared to 16.8µm in all other study groups. The meningeal infiltrate always involved the longitudinal fissure and spread lateral for 4'243µm on average in the non-immunized LV-Tnf/LV-Ifng-injected group and 5'148µm in the MOG-immunized LV-Tnf/LV-Ifng-injected group (Figure 16). In all other study groups there was no or almost no infiltration of the meninges with immune cells.

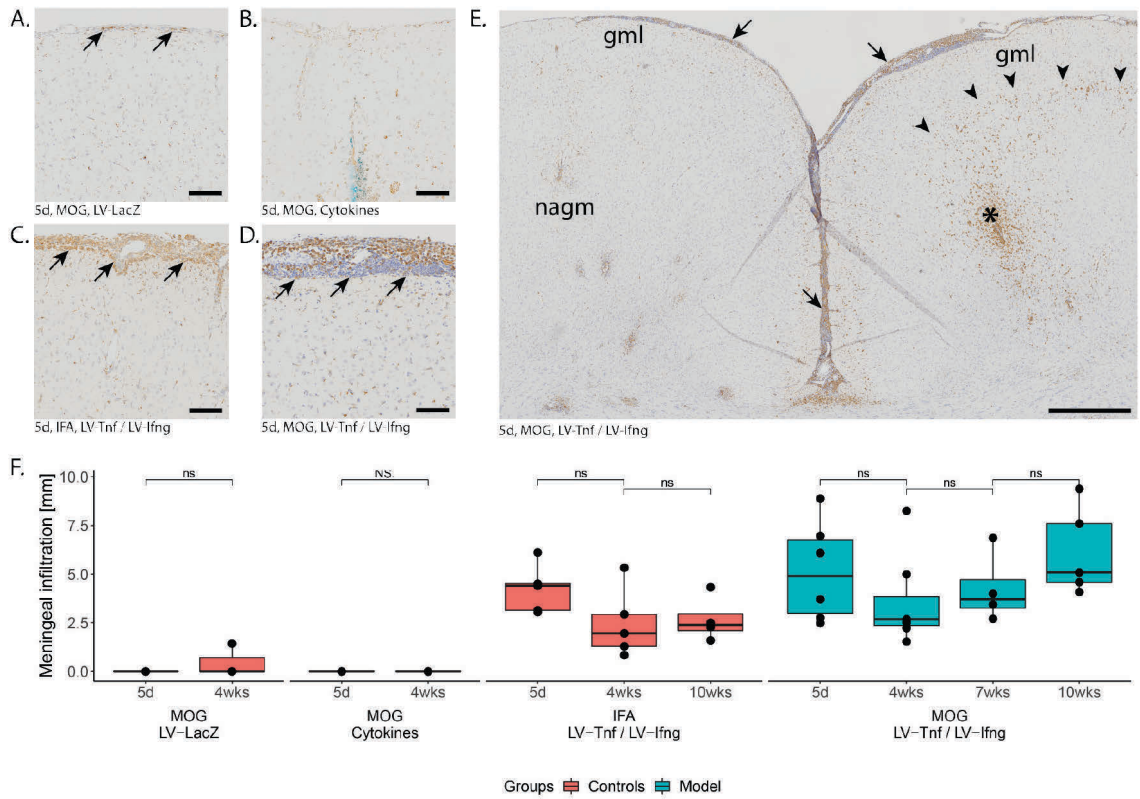

Figure 16. Meningeal and parenchymal infiltration.
Representative images of the anti-ED1 staining against macrophages and activated microglia 5 days after the intracerebral injection of (A) LV-LacZ, (B) recombinant protein Tnf and Ifng, (C) LV-Tnf and LV-Ifng in non-immunized animals and (D) LV-Tnf and LV-Ifng in MOG-immunized animals. (E) Overview of an anti-ED1 staining showing the meningeal infiltration (arrows), a dense infiltrate surrounding the injection site (asterisk) and a margin of ED1 staining at the edge of the demyelination (arrowheads). (F) Boxplots showing the length of the meningeal infiltrate as a measurement of meningeal inflammation. Abbreviations: gml: grey matter lesion; nagm: normal-appearing grey matter. A two-sided Welch t-test was performed to compare between the time points: ns: not significant; NS: not enough values.

The infiltrate comprised of macrophages, T-cells and B-cells (Figure 16, Figure 17, Figure 18), with a ratio of T-cells to B-cells of approximately 2:1. The meningeal infiltration declined over time, but was still present after 10 weeks (Figure 17, Figure 18).

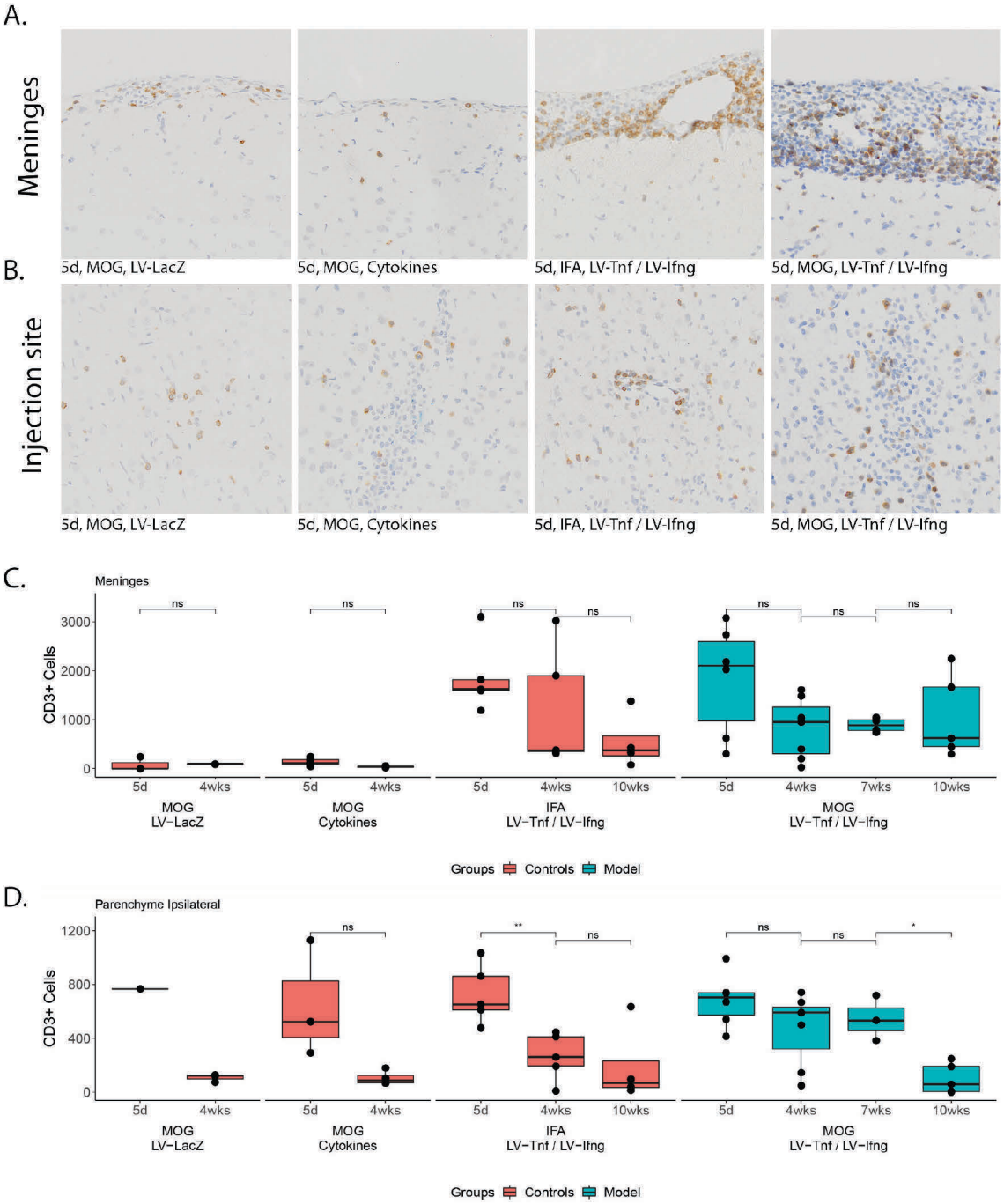

Figure 17. Meningeal and parenchymal infiltration with CD3 positive T-cells

Representative images of the (A) meningeal and (B) parenchymal infiltration with CD3 positive T-cells. (C) boxplot depicting the number of CD3 positive T-cells detected in the meninges and (D) in the parenchyma ipsilateral of the intracortical injection. A two-sided Welch t-test was performed to compare the time points: ns: not significant; *: p-value <0.05; **: p-value <0.01.

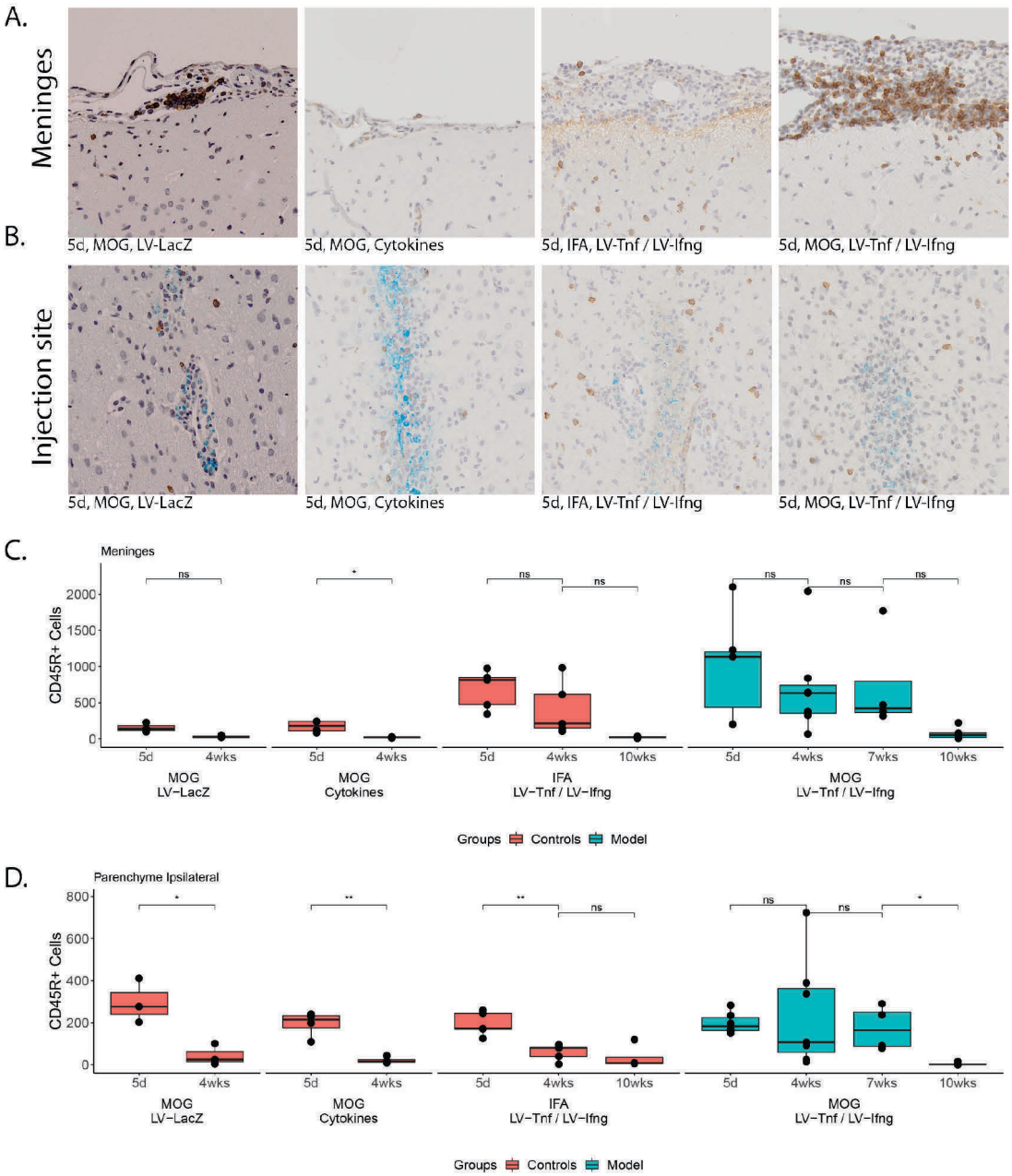

Figure 18. Meningeal and parenchymal infiltration with CD45R positive B-cells
Representative images of the (A) meningeal and (B) parenchymal infiltration with CD45R positive B-cells. (C) boxplot depicting the number of CD45R positive B-cells detected in the meninges and (D) in the parenchyma ipsilateral of the intracortical injection. A two-sided Welch t-test was performed to compare the time points: ns: not significant; *: p-value <0.05; **: p-value <0.01.

Demyelination correlates with the meningeal CD3+ cell count inflammation but not with the parenchymal inflammation in MOG-immunized animals

The observation that subpial demyelination correlates with meningeal inflammation in MS has led to the speculation of a mechanistic link between the two phenomena. To investigate this in our animal model we were intrigued to test for an association between demyelination and meningeal inflammation. Indeed, in the group immunized against MOG and injected with LV-

Tnf and LV-Ifng, we detected a strong correlation between the fraction of demyelinated cortex and the meningeal CD3 cell count (r=0.47, p=0.029, df=20, Figure 19A), whereas the correlation with the meningeal CD45R cell count did not reach statistical significance (r=0.4, p=0.065, df=20, Figure 19B). We further did not detect a statistically significant correlation between the fraction of demyelinated cortex and the parenchymal CD3 cell count (r=0.42, p=0.055, df=20, Figure 19C) and the parenchymal CD45R count (r=0.22, p=0.0.32, df=20, Figure 19D).

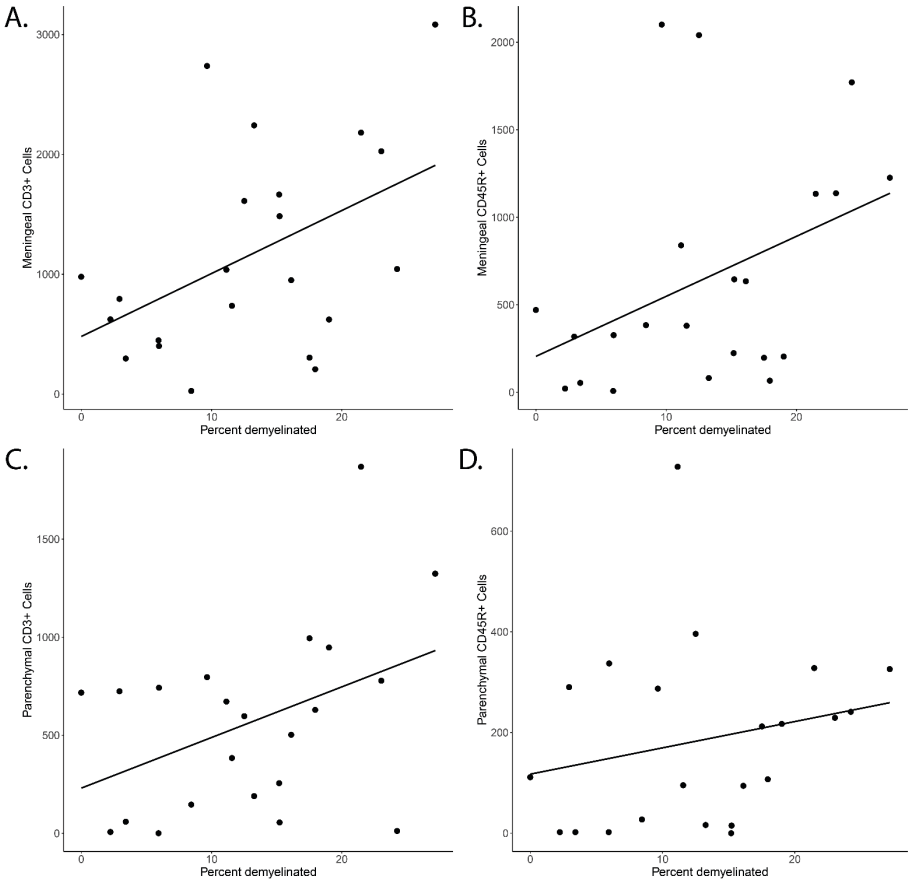

Figure 19. Correlation of inflammation and demyelination
(A) Statistically significant correlation of meningeal CD3-positive cell count and demyelination. (B) Correlation of meningeal CD45R-positive cell count and demyelination. (C) Correlation of parenchymal CD3-positive cell count and demyelination. (D) Correlation of parenchymal CD45R-positive cell count and demyelination.

8.3.5 Discussion

Our results demonstrate that a long term overexpression of Tnf and Ifng by lentiviral intracortical injection in MOG-immunized rats leads to chronic demyelination and meningeal inflammation, replicating key aspects of MS cortical pathology.

In a previously described animal model, MOG-immunized rats were injected with recombinant protein Tnf and Ifng, giving rise to subpial and intracortical demyelinated lesions with infiltrating immune cells, complement deposition, acute axonal damage and neuronal cell death, followed by a rapid resolution of the lesions (Merkler, Ernsting et al. 2006). A less traumatic version of this model was achieved by injecting the recombinant protein Tnf and Ifng into the subarachnoidal space. This approach gave rise to a highly similar pathology compared to the intracortical injections performed before (Gardner, Magliozzi et al. 2013). These models, using recombinant proteins, demonstrated that immunization against MOG and the injection of both cytokines Tnf and Ifng are required for demyelination to occur. In our model we demonstrated that the immunization against MOG is also necessary for demyelination to occur. Even a 10-week overexpression of Tnf and Ifng alone does not lead to demyelination. Demyelination thus cannot be a direct effect of cytokine expression and meningeal inflammation, but also requires a priming of the immune-system against a component of myelin.

The lesions we detected were largest in the animals injected with the combination of LV-Tnf and LV-Ifng. However, also the control virus LV-LacZ gave rise to subpial demyelination comparable to the injection of recombinant protein Tnf and Ifng. This could either be a consequence from the direct traumatic tissue damage caused by the intraparenchymal injection, leading to an opening of the blood-brain barrier, or could be a consequence of lentiviral particles being injected into parenchyma, provoking an immune-response. In contrast, Merkler et al. found only limited demyelination when injecting phosphate buffered saline into MOG-immunized animals instead of recombinant protein Tnf and Ifng (Merkler, Ernsting et al. 2006), suggesting that both proposed mechanisms might play a role in our model.

It has further been demonstrated that one cytokine alone is not sufficient to produce widespread acute cortical demyelination (Merkler, Ernsting et al. 2006, Gardner, Magliozzi et al. 2013). We have demonstrated that the simultaneous injection of both LV-Tnf and LV-Ifng leads to demyelination in MOG-immunized animals, but we did not individually test the lentiviruses. It is not per se evident that both cytokines are necessary in a long-term situation and one alone may suffice to initiate and uphold the demyelination and inflammation.

The previous acute models recovered within 2-4 weeks. In comparison with these models, our approach renders stable subpial demyelination for at least 10 weeks and possibly much longer. By installing a catheter at the border of the white and cortical grey matter of MOG-immunized animals for multiple injections of recombinant protein Tnf and Ifng produced lesions for at least 4 weeks (Ucal, Haindl et al. 2017). This approach however causes a direct trauma to the brain

parenchyma, potentially larger than the injection of the lentiviruses, and it depends on the permanent installation of foreign material, breaching the skin, skull and blood-brain barrier.
Further, we have shown that the meningeal inflammation depends only on the overexpression of Tnf and Ifng, as described before in the acute models (Gardner, Magliozzi et al. 2013). The parenchymal infiltration detected was primarily limited to the injection site and occurred irrespective of the type of lentivirus injected.
Both demyelination and meningeal inflammation were stable over 10 weeks, suggesting a chronic failure of the remyelination capacity. The previous models led to a rapid remyelination, even after repeated acute demyelination (Rodriguez, Wegner et al. 2014). In our model, remyelination might fail directly due to the chronic release of Tnf and Ifng or indirectly by effects caused by the meningeal inflammation.
In MS research, four patterns of cortical demyelination have been described: lesions bordering the white matter termed leukocortical or type I lesions, lesions bordering neither the white matter nor the meninges termed intracortical or type II lesions, lesions bordering the meninges but not the white matter termed subpial or type III lesions and lesions spreading from the meninges to the white matter termed pancortical or type IV lesions (Peterson, Bo et al. 2001, Bø, Vedeler et al. 2003). Type III has been shown to be the most common type of cortical MS lesions and it has been demonstrated to be unique for MS pathology (Moll, Rietsch et al. 2008, Junker, Wozniak et al. 2020). Interestingly, the acute models described previously and the model established here lead to a subpial demyelination pattern as seen in MS. While Merkler et al. discussed the drainage of the recombinant proteins along predetermined anatomical routes from the white matter to the meninges as a possible cause of this pattern (Merkler, Ernsting et al. 2006), Gardner et al. suggested that cytokines produced from the meningeal infiltrates may diffuse into the brain parenchyma and cause a subpial pattern of demyelination (Gardner, Magliozzi et al. 2013). In our model both mechanisms are possible: a direct effect from the lentiviral Tnf and Ifng, which both have been shown to lead to oligodendrocyte death and demyelination (Horwitz, Evans et al. 1997, Akassoglou, Bauer et al. 1998) or an indirect effect caused by cytokine production from the meningeal infiltrates. In MS an association between subpial demyelination and meningeal inflammation has repeatedly been demonstrated (Magliozzi, Howell et al. 2010, Howell, Reeves et al. 2011, Haider, Zrzavy et al. 2016). Analysis of our data revealed a statistically significant correlation between the demyelinated fraction of the cortex and the meningeal inflammation, whereas the parenchymal infiltration did not show such a correlation. We may however not conclude that meningeal inflammation is necessary for the development of subpial demyelination in our model.

The development of a chronic cortical demyelination model is important to study chronic changes such as failure of remyelination, chronically disturbed functionality of oligodendrocytes, neurons and astrocytes, brain atrophy and cognitive impairments.
We hope that in the future our model may lead to new insights on the different contributors to MS cortical pathology, chronic adaptations of the neuronal network and the supporting glia cells to a demyelinated environment and to the neighbouring inflamed meninges and into the determinants of cortical remyelination and recovery.

Currently we are evaluating the quantification of immunohistochemical stainings for neuronal loss, axonal injury, oligodendrocyte loss, oligodendrocyte precursor proliferation, and blood-brain barrier damage. This will give us further insights into how well this novel animal model also reflects neurodegenerative aspects of MS.

8.3.6 Acknowledgments

This study was supported by the Swiss Multiple Sclerosis Society, and by the French MS Society (ARSEP) all to N.S.W. and by the Swiss National Science Foundation MD-PhD grant 323530_171139, 2016-2019 to L.S.E.

9 Discussion

9.1 General discussion

Whereas the major hallmarks of chronic cortical pathology in MS, demyelination, meningeal and parenchymal inflammation and neurodegeneration, have been described to a large extent, the unique mechanisms contributing to disease progression and the necessary adaptations of the specific cells to a chronically disturbed environment remain unknown. In this thesis we demonstrated a link between the strongest genetic risk factor of MS, namely *HLA-DRB1*15:01*, its gene and protein expression and a major hallmark of cortical pathology, namely cortical grey matter demyelination. As we also demonstrated the elevated gene expression of HLA-DRB1 in all control cases carrying the *HLA-DRB1*15:01* allele, this is suggestive of a constitutive upregulation within the cortical grey matter irrespective of the disease status. This may hint towards brain intrinsic consequences of the *HLA-DRB1*15:01* allele, independent of the peripheral immune system.

We have further demonstrated the differential expression of olfactory receptors within cortical grey matter lesions and have demonstrated the presence of two such receptors on neurons and blood vessels. The distinct role of olfactory receptor expression within the human cortex remains elusive, so we may only speculate that they have a role in the physiological environment of the human cortex and are regulated upon chronic cortical grey matter damage. As olfactory receptors have previously been demonstrated to be differentially regulated within other neurodegenerative diseases, they might be part of more general mechanisms of neurodegeneration, not yet understood.

Last, we have demonstrated that chronic cortical demyelination and meningeal inflammation may be reproduced in an animal model by immunization against a myelin protein and subsequent overexpression of two cytokines within the cerebral cortex. To which extent this novel animal model also replicates neurodegenerative aspects remains to be understood.

9.2 Outlook

The chronic cortical pathology in MS is a piece in the larger puzzle of MS pathophysiology. Still, many basic questions, for example regarding the etiology and the relationship of inflammation, demyelination and degeneration, remain without a satisfactory answer. The perspectives are however changing, also due to insights gained from studies on the cortex, where inflammation plays a less apparent role compared to the white matter, opening the view

to broader disease processes. It remains to be investigated, which processes are antecedent, which are consequent and which are only subsequent. Further studies in the field of chronic cortical pathology will hopefully aid in disentangling the different processes taking place simultaneous and give us new insights into how especially the degenerative aspects may be influenced, halted or even prevented.

10 References

Adelmann, M., J. Wood, I. Benzel, P. Fiori, H. Lassmann, J. M. Matthieu, M. V. Gardinier, K. Dornmair and C. Linington (1995). "The N-terminal domain of the myelin oligodendrocyte glycoprotein (MOG) induces acute demyelinating experimental autoimmune encephalomyelitis in the Lewis rat." J Neuroimmunol **63**(1): 17-27.

Akaishi, T., I. Nakashima, D. K. Sato, T. Takahashi and K. Fujihara (2017). "Neuromyelitis Optica Spectrum Disorders." Neuroimaging Clin N Am **27**(2): 251-265.

Akassoglou, K., J. Bauer, G. Kassiotis, M. Pasparakis, H. Lassmann, G. Kollias and L. Probert (1998). "Oligodendrocyte apoptosis and primary demyelination induced by local TNF/p55TNF receptor signaling in the central nervous system of transgenic mice: models for multiple sclerosis with primary oligodendrogliopathy." Am J Pathol **153**(3): 801-813.

Albert, M., J. Antel, W. Bruck and C. Stadelmann (2007). "Extensive cortical remyelination in patients with chronic multiple sclerosis." Brain Pathol **17**(2): 129-138.

Alcina, A., M. Abad-Grau Mdel, M. Fedetz, G. Izquierdo, M. Lucas, O. Fernandez, D. Ndagire, A. Catala-Rabasa, A. Ruiz, J. Gayan, C. Delgado, C. Arnal and F. Matesanz (2012). "Multiple sclerosis risk variant HLA-DRB1*1501 associates with high expression of DRB1 gene in different human populations." PLoS One **7**(1): e29819.

Altschul, S. F., W. Gish, W. Miller, E. W. Myers and D. J. Lipman (1990). "Basic local alignment search tool." J Mol Biol **215**(3): 403-410.

Ansoleaga, B., P. Garcia-Esparcia, F. Llorens, J. Moreno, E. Aso and I. Ferrer (2013). "Dysregulation of brain olfactory and taste receptors in AD, PSP and CJD, and AD-related model." Neuroscience **248**: 369-382.

Ansoleaga, B., P. Garcia-Esparcia, R. Pinacho, J. M. Haro, B. Ramos and I. Ferrer (2015). "Decrease in olfactory and taste receptor expression in the dorsolateral prefrontal cortex in chronic schizophrenia." J Psychiatr Res **60**: 109-116.

Ascherio, A. and K. L. Munger (2007). "Environmental risk factors for multiple sclerosis. Part I: The role of infection." Annals of Neurology **61**(4): 288-299.

Ascherio, A. and K. L. Munger (2007). "Environmental risk factors for multiple sclerosis. Part II: Noninfectious factors." Annals of Neurology **61**(6): 504-513.

Babinski, J. (1885). "Recherches sur l´anatomie pathologique de la sclerose en plaque et etude comparative des diverses varietes de la scleroses de la moelle." Arch Physiol(5-6): 186-207.

Balo, J. (1928). "Encephalitis Periaxialis Concentrica." Archives of Neurology & Psychiatry **19**(2): 242-264.

Barnett, M. H. and J. W. Prineas (2004). "Relapsing and remitting multiple sclerosis: pathology of the newly forming lesion." Ann Neurol **55**(4): 458-468.

Bergsland, N., D. Horakova, M. G. Dwyer, O. Dolezal, Z. K. Seidl, M. Vaneckova, J. Krasensky, E. Havrdova and R. Zivadinov (2012). "Subcortical and cortical gray matter atrophy in a large sample of patients with clinically isolated syndrome and early relapsing-remitting multiple sclerosis." AJNR Am J Neuroradiol **33**(8): 1573-1578.

Blozik, E., R. Rapold, K. Eichler and O. Reich (2017). "Epidemiology and costs of multiple sclerosis in Switzerland: an analysis of health-care claims data, 2011-2015." Neuropsychiatric disease and treatment **13**: 2737-2745.

Bø, L., C. A. Vedeler, H. Nyland, B. D. Trapp and S. J. Mork (2003). "Intracortical multiple sclerosis lesions are not associated with increased lymphocyte infiltration." Mult Scler **9**(4): 323-331.

Bø, L., C. A. Vedeler, H. I. Nyland, B. D. Trapp and S. J. Mørk (2003). "Subpial Demyelination in the Cerebral Cortex of Multiple Sclerosis Patients." Journal of Neuropathology & Experimental Neurology **62**(7): 723-732.

Bottazzo, G. F., R. Pujol-Borrell, T. Hanafusa and M. Feldmann (1983). "Role of aberrant HLA-DR expression and antigen presentation in induction of endocrine autoimmunity." Lancet **2**(8359): 1115-1119.
Bourneville, D. M. and L. Guérard (1869). "De la sclérose en plaques disséminées: nouvelle étude sur quelques points de la sclérose en plaques disséminées par Bourneville." Adrien Delahaye.
Brass, S. D., R. H. Benedict, B. Weinstock-Guttman, F. Munschauer and R. Bakshi (2006). "Cognitive impairment is associated with subcortical magnetic resonance imaging grey matter T2 hypointensity in multiple sclerosis." Mult Scler **12**(4): 437-444.
Browne, P., D. Chandraratna, C. Angood, H. Tremlett, C. Baker, B. V. Taylor and A. J. Thompson (2014). "Atlas of Multiple Sclerosis 2013: A growing global problem with widespread inequity." Neurology **83**(11): 1022-1024.
Brownell, B. and J. T. Hughes (1962). "The distribution of plaques in the cerebrum in multiple sclerosis." J Neurol Neurosurg Psychiatry **25**: 315-320.
Calabrese, M., R. Magliozzi, O. Ciccarelli, J. J. Geurts, R. Reynolds and R. Martin (2015). "Exploring the origins of grey matter damage in multiple sclerosis." Nat Rev Neurosci **16**(3): 147-158.
Carswell, R. (1838). Pathological anatomy: illustrations of the elementary forms of disease, Longman, Orme, Brown, Green and Longman.
Charcot, M. (1868). "Histologie de la sclerose en plaque." Gaz. Hosp. **41**: 554-556.
Chiaravalloti, N. D. and J. DeLuca (2008). "Cognitive impairment in multiple sclerosis." Lancet Neurol **7**(12): 1139-1151.
Confavreux, C. and S. Vukusic (2006). "Natural history of multiple sclerosis: a unifying concept." Brain **129**(3): 606-616.
Confavreux, C., S. Vukusic, T. Moreau and P. Adeleine (2000). "Relapses and progression of disability in multiple sclerosis." N Engl J Med **343**(20): 1430-1438.
Corse, E., R. A. Gottschalk and J. P. Allison (2011). "Strength of TCR-peptide/MHC interactions and in vivo T cell responses." J Immunol **186**(9): 5039-5045.
Cruveilhier, J. (1829). "Anatomie pathologique du corps humain."
Dawson, J. W. (1916). "The Histology of Disseminated Sclerosis." Edinburgh Medical Journal **17**(4): 229-241.
Decarreau, J., M. Wagenbach, E. Lynch, A. R. Halpern, J. C. Vaughan, J. Kollman and L. Wordeman (2017). "The tetrameric kinesin Kif25 suppresses pre-mitotic centrosome separation to establish proper spindle orientation." Nat Cell Biol **19**(4): 384-390.
Devic, E. (1894). "Myélite subaiguë compliqueé de névrite optique." Le Bulletin Médicale **8**: 1033–1034.
Diebold, M. and T. Derfuss (2016). "Immunological treatment of multiple sclerosis." Semin Hematol **53 Suppl 1**: S54-57.
Dobson, R. and G. Giovannoni (2019). "Multiple sclerosis - a review." Eur J Neurol **26**(1): 27-40.
Dull, T., R. Zufferey, M. Kelly, R. J. Mandel, M. Nguyen, D. Trono and L. Naldini (1998). "A third-generation lentivirus vector with a conditional packaging system." J Virol **72**(11): 8463-8471.
Dustin, M. L. (2008). "T-cell activation through immunological synapses and kinapses." Immunol Rev **221**: 77-89.
Dutta, R., A. Chang, M. K. Doud, G. J. Kidd, M. V. Ribaudo, E. A. Young, R. J. Fox, S. M. Staugaitis and B. D. Trapp (2011). "Demyelination causes synaptic alterations in hippocampi from multiple sclerosis patients." Annals of Neurology **69**(3): 445-454.
Dutta, R., J. McDonough, A. Chang, L. Swamy, A. Siu, G. J. Kidd, R. Rudick, K. Mirnics and B. D. Trapp (2007). "Activation of the ciliary neurotrophic factor (CNTF) signalling pathway in cortical neurons of multiple sclerosis patients." Brain **130**(Pt 10): 2566-2576.

Dutta, R., J. McDonough, X. Yin, J. Peterson, A. Chang, T. Torres, T. Gudz, W. B. Macklin, D. A. Lewis, R. J. Fox, R. Rudick, K. Mirnics and B. D. Trapp (2006). "Mitochondrial dysfunction as a cause of axonal degeneration in multiple sclerosis patients." Ann Neurol **59**(3): 478-489.

Dyment, D. A., A. D. Sadnovich and G. C. Ebers (1997). "Genetics of Multiple Sclerosis." Human Molecular Genetics **6**(10): 1693-1698.

Edgar, R., M. Domrachev and A. E. Lash (2002). "Gene Expression Omnibus: NCBI gene expression and hybridization array data repository." Nucleic Acids Res **30**(1): 207-210.

Engelhardt, B., P. Vajkoczy and R. O. Weller (2017). "The movers and shapers in immune privilege of the CNS." Nat Immunol **18**(2): 123-131.

Fan, J. B., J. M. Yeakley, M. Bibikova, E. Chudin, E. Wickham, J. Chen, D. Doucet, P. Rigault, B. Zhang, R. Shen, C. McBride, H. R. Li, X. D. Fu, A. Oliphant, D. L. Barker and M. S. Chee (2004). "A versatile assay for high-throughput gene expression profiling on universal array matrices." Genome Res **14**(5): 878-885.

Feinstein, A., J. Freeman and A. C. Lo (2015). "Treatment of progressive multiple sclerosis: what works, what does not, and what is needed." Lancet Neurol **14**(2): 194-207.

Fert, I., N. Cagnard, S. Glatigny, F. Letourneur, S. Jacques, J. A. Smith, R. A. Colbert, J. D. Taurog, G. Chiocchia, L. M. Araujo and M. Breban (2014). "Reverse interferon signature is characteristic of antigen-presenting cells in human and rat spondyloarthritis." Arthritis Rheumatol **66**(4): 841-851.

Filippi, M., M. A. Rocca, O. Ciccarelli, N. De Stefano, N. Evangelou, L. Kappos, A. Rovira, J. Sastre-Garriga, M. Tintore, J. L. Frederiksen, C. Gasperini, J. Palace, D. S. Reich, B. Banwell, X. Montalban and F. Barkhof (2016). "MRI criteria for the diagnosis of multiple sclerosis: MAGNIMS consensus guidelines." Lancet Neurol **15**(3): 292-303.

Fischer, M. T., I. Wimmer, R. Hoftberger, S. Gerlach, L. Haider, T. Zrzavy, S. Hametner, D. Mahad, C. J. Binder, M. Krumbholz, J. Bauer, M. Bradl and H. Lassmann (2013). "Disease-specific molecular events in cortical multiple sclerosis lesions." Brain **136**(Pt 6): 1799-1815.

Fisniku, L. K., D. T. Chard, J. S. Jackson, V. M. Anderson, D. R. Altmann, K. A. Miszkiel, A. J. Thompson and D. H. Miller (2008). "Gray matter atrophy is related to long-term disability in multiple sclerosis." Ann Neurol **64**(3): 247-254.

Frischer, J. M., S. Bramow, A. Dal-Bianco, C. F. Lucchinetti, H. Rauschka, M. Schmidbauer, H. Laursen, P. S. Sorensen and H. Lassmann (2009). "The relation between inflammation and neurodegeneration in multiple sclerosis brains." Brain : a journal of neurology **132**(Pt 5): 1175-1189.

Frischer, J. M., S. D. Weigand, Y. Guo, N. Kale, J. E. Parisi, I. Pirko, J. Mandrekar, S. Bramow, I. Metz, W. Brück, H. Lassmann and C. F. Lucchinetti (2015). "Clinical and pathological insights into the dynamic nature of the white matter multiple sclerosis plaque." Annals of neurology **78**(5): 710-721.

Frohman, E. M., A. Shah, E. Eggenberger, L. Metz, R. Zivadinov and O. Stüve (2007). "Corticosteroids for multiple sclerosis: I. Application for treating exacerbations." Neurotherapeutics **4**(4): 618-626.

Frommann, C. (1878). "Untersuchungen über die Gewebsveränderungen bei der Multiplen Sklerose des Gehirns und des Rückenmarks." Gustav Fischer.

Garcia-Esparcia, P., A. Schluter, M. Carmona, J. Moreno, B. Ansoleaga, B. Torrejon-Escribano, S. Gustincich, A. Pujol and I. Ferrer (2013). "Functional genomics reveals dysregulation of cortical olfactory receptors in Parkinson disease: novel putative chemoreceptors in the human brain." J Neuropathol Exp Neurol **72**(6): 524-539.

Gardner, C., R. Magliozzi, P. F. Durrenberger, O. W. Howell, J. Rundle and R. Reynolds (2013). "Cortical grey matter demyelination can be induced by elevated pro-inflammatory cytokines in the subarachnoid space of MOG-immunized rats." Brain **136**(Pt 12): 3596-3608.

Gillett, A., M. Thessen Hedreul, M. Khademi, A. Espinosa, A. D. Beyeen, M. Jagodic, I. Kockum, R. A. Harris and T. Olsson (2010). "Interleukin 18 receptor 1 expression distinguishes patients with multiple sclerosis." Mult Scler **16**(9): 1056-1065.

Goodin, D. S. (2014). "Glucocorticoid treatment of multiple sclerosis." Handbook of clinical neurology **122**: 455-464.

Graumann, U., R. Reynolds, A. J. Steck and N. Schaeren-Wiemers (2003). "Molecular changes in normal appearing white matter in multiple sclerosis are characteristic of neuroprotective mechanisms against hypoxic insult." Brain Pathol **13**(4): 554-573.

Haider, L., C. Simeonidou, G. Steinberger, S. Hametner, N. Grigoriadis, G. Deretzi, G. G. Kovacs, A. Kutzelnigg, H. Lassmann and J. M. Frischer (2014). "Multiple sclerosis deep grey matter: the relation between demyelination, neurodegeneration, inflammation and iron." J Neurol Neurosurg Psychiatry **85**(12): 1386-1395.

Haider, L., T. Zrzavy, S. Hametner, R. Hoftberger, F. Bagnato, G. Grabner, S. Trattnig, S. Pfeifenbring, W. Bruck and H. Lassmann (2016). "The topograpy of demyelination and neurodegeneration in the multiple sclerosis brain." Brain **139**(Pt 3): 807-815.

Hametner, S., I. Wimmer, L. Haider, S. Pfeifenbring, W. Bruck and H. Lassmann (2013). "Iron and neurodegeneration in the multiple sclerosis brain." Ann Neurol **74**(6): 848-861.

Handel, A. E., A. J. Williamson, G. Disanto, L. Handunnetthi, G. Giovannoni and S. V. Ramagopalan (2010). "An updated meta-analysis of risk of multiple sclerosis following infectious mononucleosis." PLoS One **5**(9).

Hemmer, B., M. Kerschensteiner and T. Korn (2015). "Role of the innate and adaptive immune responses in the course of multiple sclerosis." The Lancet Neurology **14**(4): 406-419.

Hinson, S. R., S. J. Pittock, C. F. Lucchinetti, S. F. Roemer, J. P. Fryer, T. J. Kryzer and V. A. Lennon (2007). "Pathogenic potential of IgG binding to water channel extracellular domain in neuromyelitis optica." Neurology **69**(24): 2221-2231.

Hollenbach, J. A. and J. R. Oksenberg (2015). "The immunogenetics of multiple sclerosis: A comprehensive review." Journal of Autoimmunity **64**: 13-25.

Horwitz, M. S., C. F. Evans, D. B. McGavern, M. Rodriguez and M. B. A. Oldstone (1997). "Primary demyelination in transgenic mice expressing interferon-gamma." Nat Med **3**(9): 1037-1041.

Howard, J., S. Trevick and D. S. Younger (2016). "Epidemiology of Multiple Sclerosis." Neurologic Clinics **34**(4): 919-939.

Howell, O. W., C. A. Reeves, R. Nicholas, D. Carassiti, B. Radotra, S. M. Gentleman, B. Serafini, F. Aloisi, F. Roncaroli, R. Magliozzi and R. Reynolds (2011). "Meningeal inflammation is widespread and linked to cortical pathology in multiple sclerosis." Brain **134**(Pt 9): 2755-2771.

International Multiple Sclerosis Genetics Consortium, Wellcome Trust Case Control Consortium, S. Sawcer, G. Hellenthal, M. Pirinen, C. C. Spencer, N. A. Patsopoulos, L. Moutsianas, A. Dilthey, Z. Su, C. Freeman, S. E. Hunt, S. Edkins, E. Gray, D. R. Booth, S. C. Potter, A. Goris, G. Band, A. B. Oturai, A. Strange, J. Saarela, C. Bellenguez, B. Fontaine, M. Gillman, B. Hemmer, R. Gwilliam, F. Zipp, A. Jayakumar, R. Martin, S. Leslie, S. Hawkins, E. Giannoulatou, S. D'Alfonso, H. Blackburn, F. Martinelli Boneschi, J. Liddle, H. F. Harbo, M. L. Perez, A. Spurkland, M. J. Waller, M. P. Mycko, M. Ricketts, M. Comabella, N. Hammond, I. Kockum, O. T. McCann, M. Ban, P. Whittaker, A. Kemppinen, P. Weston, C. Hawkins, S. Widaa, J. Zajicek, S. Dronov, N. Robertson, S. J. Bumpstead, L. F. Barcellos, R. Ravindrarajah, R. Abraham, L. Alfredsson, K. Ardlie, C. Aubin, A. Baker, K. Baker, S. E. Baranzini, L. Bergamaschi, R. Bergamaschi, A. Bernstein, A. Berthele, M. Boggild, J. P. Bradfield, D. Brassat, S. A. Broadley, D. Buck, H. Butzkueven, R. Capra, W. M. Carroll, P. Cavalla, E. G. Celius, S. Cepok, R. Chiavacci, F. Clerget-Darpoux, K. Clysters, G. Comi, M. Cossburn, I. Cournu-Rebeix, M. B. Cox, W. Cozen, B. A. Cree, A. H. Cross, D. Cusi, M. J. Daly, E. Davis, P. I. de Bakker, M. Debouverie, B. D'Hooghe M,

K. Dixon, R. Dobosi, B. Dubois, D. Ellinghaus, I. Elovaara, F. Esposito, C. Fontenille, S. Foote, A. Franke, D. Galimberti, A. Ghezzi, J. Glessner, R. Gomez, O. Gout, C. Graham, S. F. Grant, F. R. Guerini, H. Hakonarson, P. Hall, A. Hamsten, H. P. Hartung, R. N. Heard, S. Heath, J. Hobart, M. Hoshi, C. Infante-Duarte, G. Ingram, W. Ingram, T. Islam, M. Jagodic, M. Kabesch, A. G. Kermode, T. J. Kilpatrick, C. Kim, N. Klopp, K. Koivisto, M. Larsson, M. Lathrop, J. S. Lechner-Scott, M. A. Leone, V. Leppa, U. Liljedahl, I. L. Bomfim, R. R. Lincoln, J. Link, J. Liu, A. R. Lorentzen, S. Lupoli, F. Macciardi, T. Mack, M. Marriott, V. Martinelli, D. Mason, J. L. McCauley, F. Mentch, I. L. Mero, T. Mihalova, X. Montalban, J. Mottershead, K. M. Myhr, P. Naldi, W. Ollier, A. Page, A. Palotie, J. Pelletier, L. Piccio, T. Pickersgill, F. Piehl, S. Pobywajlo, H. L. Quach, P. P. Ramsay, M. Reunanen, R. Reynolds, J. D. Rioux, M. Rodegher, S. Roesner, J. P. Rubio, I. M. Ruckert, M. Salvetti, E. Salvi, A. Santaniello, C. A. Schaefer, S. Schreiber, C. Schulze, R. J. Scott, F. Sellebjerg, K. W. Selmaj, D. Sexton, L. Shen, B. Simms-Acuna, S. Skidmore, P. M. Sleiman, C. Smestad, P. S. Sorensen, H. B. Sondergaard, J. Stankovich, R. C. Strange, A. M. Sulonen, E. Sundqvist, A. C. Syvanen, F. Taddeo, B. Taylor, J. M. Blackwell, P. Tienari, E. Bramon, A. Tourbah, M. A. Brown, E. Tronczynska, J. P. Casas, N. Tubridy, A. Corvin, J. Vickery, J. Jankowski, P. Villoslada, H. S. Markus, K. Wang, C. G. Mathew, J. Wason, C. N. Palmer, H. E. Wichmann, R. Plomin, E. Willoughby, A. Rautanen, J. Winkelmann, M. Wittig, R. C. Trembath, J. Yaouanq, A. C. Viswanathan, H. Zhang, N. W. Wood, R. Zuvich, P. Deloukas, C. Langford, A. Duncanson, J. R. Oksenberg, M. A. Pericak-Vance, J. L. Haines, T. Olsson, J. Hillert, A. J. Ivinson, P. L. De Jager, L. Peltonen, G. J. Stewart, D. A. Hafler, S. L. Hauser, G. McVean, P. Donnelly and A. Compston (2011). "Genetic risk and a primary role for cell-mediated immune mechanisms in multiple sclerosis." Nature **476**(7359): 214-219.

Jia, X., L. Madireddy, S. Caillier, A. Santaniello, F. Esposito, G. Comi, O. Stuve, Y. Zhou, B. Taylor, T. Kilpatrick, F. Martinelli-Boneschi, B. A. C. Cree, J. R. Oksenberg, S. L. Hauser and S. E. Baranzini (2018). "Genome sequencing uncovers phenocopies in primary progressive multiple sclerosis." Ann Neurol **84**(1): 51-63.

Jones, J. L. and A. J. Coles (2010). "New treatment strategies in multiple sclerosis." Exp Neurol **225**(1): 34-39.

Junker, A., J. Wozniak, D. Voigt, U. Scheidt, J. Antel, C. Wegner, W. Brück and C. Stadelmann (2020). "Extensive subpial cortical demyelination is specific to multiple sclerosis." Brain Pathology **n/a**(n/a).

Kawachi, I. and H. Lassmann (2017). "Neurodegeneration in multiple sclerosis and neuromyelitis optica." J Neurol Neurosurg Psychiatry **88**(2): 137-145.

Kennedy, A. E., U. Ozbek and M. T. Dorak (2017). "What has GWAS done for HLA and disease associations?" Int J Immunogenet **44**(5): 195-211.

Kerschensteiner, M., C. Stadelmann, B. S. Buddeberg, D. Merkler, F. M. Bareyre, D. C. Anthony, C. Linington, W. Bruck and M. E. Schwab (2004). "Targeting experimental autoimmune encephalomyelitis lesions to a predetermined axonal tract system allows for refined behavioral testing in an animal model of multiple sclerosis." Am J Pathol **164**(4): 1455-1469.

Kidd, D., F. Barkhof, R. McConnell, P. R. Algra, I. V. Allen and T. Revesz (1999). "Cortical lesions in multiple sclerosis." Brain **122 (Pt 1)**: 17-26.

Kilsdonk, I. D., L. E. Jonkman, R. Klaver, S. J. van Veluw, J. J. Zwanenburg, J. P. Kuijer, P. J. Pouwels, J. W. Twisk, M. P. Wattjes, P. R. Luijten, F. Barkhof and J. J. Geurts (2016). "Increased cortical grey matter lesion detection in multiple sclerosis with 7 T MRI: a post-mortem verification study." Brain **139**(Pt 5): 1472-1481.

Kingwell, E., J. J. Marriott, N. Jetté, T. Pringsheim, N. Makhani, S. A. Morrow, J. D. Fisk, C. Evans, S. G. Béland, S. Kulaga, J. Dykeman, C. Wolfson, M. W. Koch and R. A. Marrie (2013). "Incidence and prevalence of multiple sclerosis in Europe: a systematic review." BMC neurology **13**: 128-128.

Kondo, T., I. Cortese, S. Markovic-Plese, K. P. Wandinger, C. Carter, M. Brown, S. Leitman and R. Martin (2001). "Dendritic cells signal T cells in the absence of exogenous antigen." Nat Immunol **2**(10): 932-938.
Kurtzke, J. F. (1955). "A New Scale for Evaluating Disability in Multiple Sclerosis." Neurology **5**(8): 580-580.
Kurtzke, J. F. (2008). "Historical and Clinical Perspectives of the Expanded Disability Status Scale." Neuroepidemiology **31**(1): 1-9.
Kutzelnigg, A., J. C. Faber-Rod, J. Bauer, C. F. Lucchinetti, P. S. Sorensen, H. Laursen, C. Stadelmann, W. Bruck, H. Rauschka, M. Schmidbauer and H. Lassmann (2007). "Widespread demyelination in the cerebellar cortex in multiple sclerosis." Brain Pathol **17**(1): 38-44.
Kutzelnigg, A. and H. Lassmann (2014). Chapter 2 - Pathology of multiple sclerosis and related inflammatory demyelinating diseases. Handbook of Clinical Neurology. D. S. Goodin, Elsevier. **122:** 15-58.
Kutzelnigg, A. and H. Lassmann (2014). "Pathology of multiple sclerosis and related inflammatory demyelinating diseases." Handb Clin Neurol **122**: 15-58.
Kutzelnigg, A., C. F. Lucchinetti, C. Stadelmann, W. Bruck, H. Rauschka, M. Bergmann, M. Schmidbauer, J. E. Parisi and H. Lassmann (2005). "Cortical demyelination and diffuse white matter injury in multiple sclerosis." Brain **128**(Pt 11): 2705-2712.
Lang, H. L., H. Jacobsen, S. Ikemizu, C. Andersson, K. Harlos, L. Madsen, P. Hjorth, L. Sondergaard, A. Svejgaard, K. Wucherpfennig, D. I. Stuart, J. I. Bell, E. Y. Jones and L. Fugger (2002). "A functional and structural basis for TCR cross-reactivity in multiple sclerosis." Nat Immunol **3**(10): 940-943.
Lassmann, H. (2005). "Multiple sclerosis pathology: evolution of pathogenetic concepts." Brain Pathol **15**(3): 217-222.
Lassmann, H. (2018). "Multiple Sclerosis Pathology." Cold Spring Harb Perspect Med **8**(3).
Lassmann, H. (2019). "Pathogenic Mechanisms Associated With Different Clinical Courses of Multiple Sclerosis." Frontiers in immunology **9**: 3116-3116.
Lennon, V. A., D. M. Wingerchuk, T. J. Kryzer, S. J. Pittock, C. F. Lucchinetti, K. Fujihara, I. Nakashima and B. G. Weinshenker (2004). "A serum autoantibody marker of neuromyelitis optica: distinction from multiple sclerosis." Lancet **364**(9451): 2106-2112.
Lou, E., S. Fujisawa, A. Morozov, A. Barlas, Y. Romin, Y. Dogan, S. Gholami, A. L. Moreira, K. Manova-Todorova and M. A. Moore (2012). "Tunneling nanotubes provide a unique conduit for intercellular transfer of cellular contents in human malignant pleural mesothelioma." PLoS One **7**(3): e33093.
Lucchinetti, C. F., B. F. Popescu, R. F. Bunyan, N. M. Moll, S. F. Roemer, H. Lassmann, W. Bruck, J. E. Parisi, B. W. Scheithauer, C. Giannini, S. D. Weigand, J. Mandrekar and R. M. Ransohoff (2011). "Inflammatory cortical demyelination in early multiple sclerosis." N Engl J Med **365**(23): 2188-2197.
Luchetti, S., N. L. Fransen, C. G. van Eden, V. Ramaglia, M. Mason and I. Huitinga (2018). "Progressive multiple sclerosis patients show substantial lesion activity that correlates with clinical disease severity and sex: a retrospective autopsy cohort analysis." Acta neuropathologica **135**(4): 511-528.
Luo, Y., A. Nita-Lazar and R. S. Haltiwanger (2006). "Two distinct pathways for O-fucosylation of epidermal growth factor-like or thrombospondin type 1 repeats." J Biol Chem **281**(14): 9385-9392.
Macedo-Marquez, A., M. Vazquez-Acevedo, L. Ongay-Larios, H. Miranda-Astudillo, R. Hernandez-Munoz, D. Gonzalez-Halphen, S. Grolli and R. Ramoni (2014). "Overexpression of a monomeric form of the bovine odorant-binding protein protects Escherichia coli from chemical-induced oxidative stress." Free Radic Res **48**(7): 814-822.

Magliozzi, R., S. Hametner, F. Facchiano, D. Marastoni, S. Rossi, M. Castellaro, A. Poli, F. Lattanzi, A. Visconti, R. Nicholas, R. Reynolds, S. Monaco, H. Lassmann and M. Calabrese (2019). "Iron homeostasis, complement, and coagulation cascade as CSF signature of cortical lesions in early multiple sclerosis." Annals of Clinical and Translational Neurology **0**(0).

Magliozzi, R., O. W. Howell, C. Reeves, F. Roncaroli, R. Nicholas, B. Serafini, F. Aloisi and R. Reynolds (2010). "A Gradient of neuronal loss and meningeal inflammation in multiple sclerosis." Ann Neurol **68**(4): 477-493.

Mahad, D. H., B. D. Trapp and H. Lassmann (2015). "Pathological mechanisms in progressive multiple sclerosis." Lancet Neurol **14**(2): 183-193.

Maliekal, P., D. Vertommen, G. Delpierre and E. Van Schaftingen (2006). "Identification of the sequence encoding N-acetylneuraminate-9-phosphate phosphatase." Glycobiology **16**(2): 165-172.

Marburg, O. (1906). "Die sogenannte akute multiple Sklerose (Encephalomyelitis periaxialis scleroticans)." Jahrbücher für Psychiatrie und Neurologie **27**: 211-312.

Martinelli, V., M. Rodegher, L. Moiola and G. Comi (2004). "Late onset multiple sclerosis: clinical characteristics, prognostic factors and differential diagnosis." Neurol Sci **25 Suppl 4**: S350-355.

McDonald, W. I., A. Compston, G. Edan, D. Goodkin, H. P. Hartung, F. D. Lublin, H. F. McFarland, D. W. Paty, C. H. Polman, S. C. Reingold, M. Sandberg-Wollheim, W. Sibley, A. Thompson, S. van den Noort, B. Y. Weinshenker and J. S. Wolinsky (2001). "Recommended diagnostic criteria for multiple sclerosis: guidelines from the International Panel on the diagnosis of multiple sclerosis." Ann Neurol **50**(1): 121-127.

Merkler, D., T. Ernsting, M. Kerschensteiner, W. Bruck and C. Stadelmann (2006). "A new focal EAE model of cortical demyelination: multiple sclerosis-like lesions with rapid resolution of inflammation and extensive remyelination." Brain **129**(Pt 8): 1972-1983.

Mohme, M., C. Hotz, S. Stevanovic, T. Binder, J. H. Lee, M. Okoniewski, T. Eiermann, M. Sospedra, H. G. Rammensee and R. Martin (2013). "HLA-DR15-derived self-peptides are involved in increased autologous T cell proliferation in multiple sclerosis." Brain **136**(Pt 6): 1783-1798.

Mokry, L. E., S. Ross, O. S. Ahmad, V. Forgetta, G. D. Smith, A. Leong, C. M. T. Greenwood, G. Thanassoulis and J. B. Richards (2015). "Vitamin D and Risk of Multiple Sclerosis: A Mendelian Randomization Study." PLOS Medicine **12**(8): e1001866.

Moll, N. M., A. M. Rietsch, A. J. Ransohoff, M. B. Cossoy, D. Huang, F. S. Eichler, B. D. Trapp and R. M. Ransohoff (2008). "Cortical demyelination in PML and MS: Similarities and differences." Neurology **70**(5): 336-343.

Montalban, X., S. L. Hauser, L. Kappos, D. L. Arnold, A. Bar-Or, G. Comi, J. de Seze, G. Giovannoni, H. P. Hartung, B. Hemmer, F. Lublin, K. W. Rammohan, K. Selmaj, A. Traboulsee, A. Sauter, D. Masterman, P. Fontoura, S. Belachew, H. Garren, N. Mairon, P. Chin and J. S. Wolinsky (2017). "Ocrelizumab versus Placebo in Primary Progressive Multiple Sclerosis." N Engl J Med **376**(3): 209-220.

Montes Diaz, G., R. Hupperts, J. Fraussen and V. Somers (2018). "Dimethyl fumarate treatment in multiple sclerosis: Recent advances in clinical and immunological studies." Autoimmun Rev **17**(12): 1240-1250.

Morgulis, A., G. Coulouris, Y. Raytselis, T. L. Madden, R. Agarwala and A. A. Schaffer (2008). "Database indexing for production MegaBLAST searches." Bioinformatics **24**(16): 1757-1764.

Moutsianas, L., L. Jostins, A. H. Beecham, A. T. Dilthey, D. K. Xifara, M. Ban, T. S. Shah, N. A. Patsopoulos, L. Alfredsson, C. A. Anderson, K. E. Attfield, S. E. Baranzini, J. Barrett, T. M. C. Binder, D. Booth, D. Buck, E. G. Celius, C. Cotsapas, S. D'Alfonso, C. A. Dendrou, P. Donnelly, B. Dubois, B. Fontaine, L. Fugger, A. Goris, P. A. Gourraud, C. Graetz, B.

Hemmer, J. Hillert, I. Kockum, S. Leslie, C. M. Lill, F. Martinelli-Boneschi, J. R. Oksenberg, T. Olsson, A. Oturai, J. Saarela, H. B. Sondergaard, A. Spurkland, B. Taylor, J. Winkelmann, F. Zipp, J. L. Haines, M. A. Pericak-Vance, C. C. A. Spencer, G. Stewart, D. A. Hafler, A. J. Ivinson, H. F. Harbo, S. L. Hauser, P. L. De Jager, A. Compston, J. L. McCauley, S. Sawcer and G. McVean (2015). "Class II HLA interactions modulate genetic risk for multiple sclerosis." Nat Genet **47**(10): 1107-1113.

Nielsen, H. L., L. Ronnov-Jessen, R. Villadsen and O. W. Petersen (2002). "Identification of EPSTI1, a novel gene induced by epithelial-stromal interaction in human breast cancer." Genomics **79**(5): 703-710.

Noseworthy, J. H., C. Lucchinetti, M. Rodriguez and B. G. Weinshenker (2000). "Multiple sclerosis." N Engl J Med **343**(13): 938-952.

Oh, J., A. Vidal-Jordana and X. Montalban (2018). "Multiple sclerosis: clinical aspects." Curr Opin Neurol **31**(6): 752-759.

Olsson, T., L. F. Barcellos and L. Alfredsson (2017). "Interactions between genetic, lifestyle and environmental risk factors for multiple sclerosis." Nat Rev Neurol **13**(1): 25-36.

Pakpoor, J., G. Disanto, J. E. Gerber, R. Dobson, U. C. Meier, G. Giovannoni and S. V. Ramagopalan (2013). "The risk of developing multiple sclerosis in individuals seronegative for Epstein-Barr virus: a meta-analysis." Mult Scler **19**(2): 162-166.

Palacios, N., A. Alonso, H. Bronnum-Hansen and A. Ascherio (2011). "Smoking and increased risk of multiple sclerosis: parallel trends in the sex ratio reinforce the evidence." Ann Epidemiol **21**(7): 536-542.

Patrikios, P., C. Stadelmann, A. Kutzelnigg, H. Rauschka, M. Schmidbauer, H. Laursen, P. S. Sorensen, W. Bruck, C. Lucchinetti and H. Lassmann (2006). "Remyelination is extensive in a subset of multiple sclerosis patients." Brain **129**(Pt 12): 3165-3172.

Patsopoulos, N. A. (2018). "Genetics of Multiple Sclerosis: An Overview and New Directions." Cold Spring Harb Perspect Med **8**(7).

Patsopoulos, N. A., L. F. Barcellos, R. Q. Hintzen, C. Schaefer, C. M. van Duijn, J. A. Noble, T. Raj, P. A. Gourraud, B. E. Stranger, J. Oksenberg, T. Olsson, B. V. Taylor, S. Sawcer, D. A. Hafler, M. Carrington, P. L. De Jager and P. I. de Bakker (2013). "Fine-mapping the genetic association of the major histocompatibility complex in multiple sclerosis: HLA and non-HLA effects." PLoS Genet **9**(11): e1003926.

Peterson, J. W., L. Bo, S. Mork, A. Chang and B. D. Trapp (2001). "Transected neurites, apoptotic neurons, and reduced inflammation in cortical multiple sclerosis lesions." Ann Neurol **50**(3): 389-400.

Pfeifer, A., E. P. Brandon, N. Kootstra, F. H. Gage and I. M. Verma (2001). "Delivery of the Cre recombinase by a self-deleting lentiviral vector: efficient gene targeting in vivo." Proc Natl Acad Sci U S A **98**(20): 11450-11455.

Polman, C. H., S. C. Reingold, B. Banwell, M. Clanet, J. A. Cohen, M. Filippi, K. Fujihara, E. Havrdova, M. Hutchinson, L. Kappos, F. D. Lublin, X. Montalban, P. O'Connor, M. Sandberg-Wollheim, A. J. Thompson, E. Waubant, B. Weinshenker and J. S. Wolinsky (2011). "Diagnostic criteria for multiple sclerosis: 2010 revisions to the McDonald criteria." Ann Neurol **69**(2): 292-302.

Polman, C. H., S. C. Reingold, G. Edan, M. Filippi, H. P. Hartung, L. Kappos, F. D. Lublin, L. M. Metz, H. F. McFarland, P. W. O'Connor, M. Sandberg-Wollheim, A. J. Thompson, B. G. Weinshenker and J. S. Wolinsky (2005). "Diagnostic criteria for multiple sclerosis: 2005 revisions to the "McDonald Criteria"." Ann Neurol **58**(6): 840-846.

Poser, C. M., D. W. Paty, L. Scheinberg, W. I. McDonald, F. A. Davis, G. C. Ebers, K. P. Johnson, W. A. Sibley, D. H. Silberberg and W. W. Tourtellotte (1983). "New diagnostic criteria for multiple sclerosis: guidelines for research protocols." Ann Neurol **13**(3): 227-231.

Prat, E., U. Tomaru, L. Sabater, D. M. Park, R. Granger, N. Kruse, J. M. Ohayon, M. P. Bettinotti and R. Martin (2005). "HLA-DRB5*0101 and -DRB1*1501 expression in the multiple sclerosis-associated HLA-DR15 haplotype." J Neuroimmunol **167**(1-2): 108-119.

Prineas, J. W., R. O. Barnard, E. E. Kwon, L. R. Sharer and E. S. Cho (1993). "Multiple sclerosis: remyelination of nascent lesions." Ann Neurol **33**(2): 137-151.

Pugliatti, M., G. Rosati, H. Carton, T. Riise, J. Drulovic, L. Vécsei and I. Milanov (2006). "The epidemiology of multiple sclerosis in Europe." European Journal of Neurology **13**(7): 700-722.

Quandt, J. A., J. Huh, M. Baig, K. Yao, N. Ito, M. Bryant, K. Kawamura, C. Pinilla, H. F. McFarland, R. Martin and K. Ito (2012). "Myelin basic protein-specific TCR/HLA-DRB5*01:01 transgenic mice support the etiologic role of DRB5*01:01 in multiple sclerosis." J Immunol **189**(6): 2897-2908.

R Development Core Team (2010). "R: A language and environment for statistical computing."

Reith, W., S. LeibundGut-Landmann and J. M. Waldburger (2005). "Regulation of MHC class II gene expression by the class II transactivator." Nat Rev Immunol **5**(10): 793-806.

Reynolds, R., F. Roncaroli, R. Nicholas, B. Radotra, D. Gveric and O. Howell (2011). "The neuropathological basis of clinical progression in multiple sclerosis." Acta Neuropathol **122**(2): 155-170.

Ribbons, K. A., P. McElduff, C. Boz, M. Trojano, G. Izquierdo, P. Duquette, M. Girard, F. Grand'Maison, R. Hupperts, P. Grammond, C. Oreja-Guevara, T. Petersen, R. Bergamaschi, G. Giuliani, M. Barnett, V. van Pesch, M.-P. Amato, G. Iuliano, M. Fiol, M. Slee, F. Verheul, E. Cristiano, R. Fernandez-Bolanos, M.-L. Saladino, M. E. Rio, J. Cabrera-Gomez, H. Butzkueven, E. van Munster, L. Den Braber-Moerland, D. La Spitaleri, A. Lugaresi, V. Shaygannejad, O. Gray, N. Deri, R. Alroughani and J. Lechner-Scott (2015). "Male Sex Is Independently Associated with Faster Disability Accumulation in Relapse-Onset MS but Not in Primary Progressive MS." PloS one **10**(6): e0122686-e0122686.

Rindfleisch, E. (1863). "Histologisches Detail zu der grauen Degeneration von Gehirn und Rückenmark.(Zugleich ein Beitrag zu der Lehre von der Entstehung und Verwandlung der Zelle.)." Virchows Archiv **26**(5): 474-483.

Robinson, J., J. A. Halliwell, J. D. Hayhurst, P. Flicek, P. Parham and S. G. Marsh (2015). "The IPD and IMGT/HLA database: allele variant databases." Nucleic Acids Res **43**(Database issue): D423-431.

Robinson, J., A. Malik, P. Parham, J. G. Bodmer and S. G. Marsh (2000). "IMGT/HLA database--a sequence database for the human major histocompatibility complex." Tissue Antigens **55**(3): 280-287.

Rodriguez, E. G., C. Wegner, M. Kreutzfeldt, K. Neid, D. R. Thal, T. Jurgens, W. Bruck, C. Stadelmann and D. Merkler (2014). "Oligodendroglia in cortical multiple sclerosis lesions decrease with disease progression, but regenerate after repeated experimental demyelination." Acta Neuropathol **128**(2): 231-246.

Roosendaal, S. D., K. Bendfeldt, H. Vrenken, C. H. Polman, S. Borgwardt, E. W. Radue, L. Kappos, D. Pelletier, S. L. Hauser, P. M. Matthews, F. Barkhof and J. J. Geurts (2011). "Grey matter volume in a large cohort of MS patients: relation to MRI parameters and disability." Mult Scler **17**(9): 1098-1106.

Rudick, R. A., J. C. Lee, K. Nakamura and E. Fisher (2009). "Gray matter atrophy correlates with MS disability progression measured with MSFC but not EDSS." J Neurol Sci **282**(1-2): 106-111.

Rueden, C. T., J. Schindelin, M. C. Hiner, B. E. DeZonia, A. E. Walter, E. T. Arena and K. W. Eliceiri (2017). "ImageJ2: ImageJ for the next generation of scientific image data." BMC Bioinformatics **18**(1): 529.

Sawcer, S., R. J. M. Franklin and M. Ban (2014). "Multiple sclerosis genetics." The Lancet Neurology **13**(7): 700-709.

Schilder, P. (1912). "Zur Kenntnis der sogenannten diffusen Sklerose. (Über Encephalitis periaxialis diffusa.)." Zeitschrift für die gesamte Neurologie und Psychiatrie **10**(1): 1.
Schindelin, J., I. Arganda-Carreras, E. Frise, V. Kaynig, M. Longair, T. Pietzsch, S. Preibisch, C. Rueden, S. Saalfeld, B. Schmid, J. Y. Tinevez, D. J. White, V. Hartenstein, K. Eliceiri, P. Tomancak and A. Cardona (2012). "Fiji: an open-source platform for biological-image analysis." Nat Methods **9**(7): 676-682.
Schoggins, J. W., S. J. Wilson, M. Panis, M. Y. Murphy, C. T. Jones, P. Bieniasz and C. M. Rice (2011). "A diverse range of gene products are effectors of the type I interferon antiviral response." Nature **472**(7344): 481-485.
Schumacher, G. A., G. Beebe, R. F. Kibler, L. T. Kurland, J. F. Kurtzke, F. McDowell, B. Nagler, W. A. Sibley, W. W. Tourtellotte and T. L. Willmon (1965). "Problems Of Experimental Trials Of Therapy In Multiple Sclerosis: Report By The Panel On The Evaluation Of Experimental Trials Of Therapy In Multiple Sclerosis." Ann N Y Acad Sci **122**: 552-568.
Shamseldin, H. E., I. Masuho, A. Alenizi, S. Alyamani, D. N. Patil, N. Ibrahim, K. A. Martemyanov and F. S. Alkuraya (2016). "GNB5 mutation causes a novel neuropsychiatric disorder featuring attention deficit hyperactivity disorder, severely impaired language development and normal cognition." Genome Biol **17**(1): 195.
Simpson, S., L. Blizzard, P. Otahal, I. Van der Mei and B. Taylor (2011). "Latitude is significantly associated with the prevalence of multiple sclerosis: a meta-analysis." Journal of Neurology, Neurosurgery & Psychiatry **82**(10): 1132.
Sospedra, M., P. A. Muraro, I. Stefanova, Y. Zhao, K. Chung, Y. Li, M. Giulianotti, R. Simon, R. Mariuzza, C. Pinilla and R. Martin (2006). "Redundancy in antigen-presenting function of the HLA-DR and -DQ molecules in the multiple sclerosis-associated HLA-DR2 haplotype." J Immunol **176**(3): 1951-1961.
Stadelmann, C., M. Albert, C. Wegner and W. Bruck (2008). "Cortical pathology in multiple sclerosis." Curr Opin Neurol **21**(3): 229-234.
Stangel, M., I. K. Penner, B. A. Kallmann, C. Lukas and B. C. Kieseier (2014). "Towards the implementation of 'no evidence of disease activity' in multiple sclerosis treatment: the multiple sclerosis decision model." Therapeutic Advances in Neurological Disorders **8**(1): 3-13.
Stopkova, R., B. Dudkova, P. Hajkova and P. Stopka (2014). "Complementary roles of mouse lipocalins in chemical communication and immunity." Biochem Soc Trans **42**(4): 893-898.
Stys, P. K., G. W. Zamponi, J. van Minnen and J. J. Geurts (2012). "Will the real multiple sclerosis please stand up?" Nat Rev Neurosci **13**(7): 507-514.
Takahashi, T., K. Fujihara, I. Nakashima, T. Misu, I. Miyazawa, M. Nakamura, S. Watanabe, Y. Shiga, C. Kanaoka, J. Fujimori, S. Sato and Y. Itoyama (2007). "Anti-aquaporin-4 antibody is involved in the pathogenesis of NMO: a study on antibody titre." Brain **130**(Pt 5): 1235-1243.
Thompson, A. J., S. E. Baranzini, J. Geurts, B. Hemmer and O. Ciccarelli (2018). "Multiple sclerosis." The Lancet **391**(10130): 1622-1636.
Torkildsen, O., C. Stansberg, S. M. Angelskar, E. J. Kooi, J. J. Geurts, P. van der Valk, K. M. Myhr, V. M. Steen and L. Bo (2010). "Upregulation of immunoglobulin-related genes in cortical sections from multiple sclerosis patients." Brain Pathol **20**(4): 720-729.
Traugott, U., E. L. Reinherz and C. S. Raine (1983). "Multiple sclerosis: distribution of T cell subsets within active chronic lesions." Science **219**(4582): 308-310.
Trimmer, C., L. L. Snyder and J. D. Mainland (2014). "High-throughput analysis of mammalian olfactory receptors: measurement of receptor activation via luciferase activity." Journal of visualized experiments : JoVE(88): 51640.
Ucal, M., M. T. Haindl, M. Z. Adzemovic, J. Strasser, L. Theisl, M. Zeitelhofer, K. Kraitsy, S. Ropele, U. Schafer, F. Fazekas and S. Hochmeister (2017). "Widespread cortical

demyelination of both hemispheres can be induced by injection of pro-inflammatory cytokines via an implanted catheter in the cortex of MOG-immunized rats." Exp Neurol **294**: 32-44.

van Munster, C. E., L. E. Jonkman, H. C. Weinstein, B. M. Uitdehaag and J. J. Geurts (2015). "Gray matter damage in multiple sclerosis: Impact on clinical symptoms." Neuroscience **303**: 446-461.

Wattjes, M. P., A. Rovira, D. Miller, T. A. Yousry, M. P. Sormani, M. P. de Stefano, M. Tintore, C. Auger, C. Tur, M. Filippi, M. A. Rocca, F. Fazekas, L. Kappos, C. Polman, B. Frederik and M. Xavier (2015). "Evidence-based guidelines: MAGNIMS consensus guidelines on the use of MRI in multiple sclerosis--establishing disease prognosis and monitoring patients." Nat Rev Neurol **11**(10): 597-606.

Wegner, C., M. M. Esiri, S. A. Chance, J. Palace and P. M. Matthews (2006). "Neocortical neuronal, synaptic, and glial loss in multiple sclerosis." Neurology **67**(6): 960-967.

Wegner, C. and C. Stadelmann (2009). "Gray matter pathology and multiple sclerosis." Curr Neurol Neurosci Rep **9**(5): 399-404.

Wu, G. C., H. F. Pan, R. X. Leng, D. G. Wang, X. P. Li, X. M. Li and D. Q. Ye (2015). "Emerging role of long noncoding RNAs in autoimmune diseases." Autoimmun Rev **14**(9): 798-805.

Yaldizli, O., V. Sethi, M. Pardini, C. Tur, K. Y. Mok, N. Muhlert, Z. Liu, R. S. Samson, C. A. Wheeler-Kingshott, T. A. Yousry, H. Houlden, J. Hardy, D. H. Miller and D. T. Chard (2016). "HLA-DRB*1501 associations with magnetic resonance imaging measures of grey matter pathology in multiple sclerosis." Mult Scler Relat Disord **7**: 47-52.

Yaouanq, J., G. Semana, S. Eichenbaum, E. Quelvennec, M. P. Roth, M. Clanet, G. Edan and F. Clerget-Darpoux (1997). "Evidence for linkage disequilibrium between HLA-DRB1 gene and multiple sclerosis. The French Research Group on Genetic Susceptibility to MS." Science **276**(5313): 664-665.

Yates, R. L., M. M. Esiri, J. Palace, A. Mittal and G. C. DeLuca (2015). "The influence of HLA-DRB1*15 on motor cortical pathology in multiple sclerosis." Neuropathol Appl Neurobiol **41**(3): 371-384.

Zeis, T., I. Allaman, M. Gentner, K. Schroder, J. Tschopp, P. J. Magistretti and N. Schaeren-Wiemers (2015). "Metabolic gene expression changes in astrocytes in Multiple Sclerosis cerebral cortex are indicative of immune-mediated signaling." Brain Behav Immun **48**: 313-325.

Zeis, T., L. Enz and N. Schaeren-Wiemers (2016). "The immunomodulatory oligodendrocyte." Brain Res **1641**(Pt A): 139-148.

Zeis, T., U. Graumann, R. Reynolds and N. Schaeren-Wiemers (2008). "Normal-appearing white matter in multiple sclerosis is in a subtle balance between inflammation and neuroprotection." Brain **131**(Pt 1): 288-303.

Zeis, T., O. W. Howell, R. Reynolds and N. Schaeren-Wiemers (2018). "Molecular pathology of Multiple Sclerosis lesions reveals a heterogeneous expression pattern of genes involved in oligodendrogliogenesis." Exp Neurol **305**: 76-88.

Zhang, X., O. De la Cruz, J. M. Pinto, D. Nicolae, S. Firestein and Y. Gilad (2007). "Characterizing the expression of the human olfactory receptor gene family using a novel DNA microarray." Genome Biol **8**(5): R86.

Zhang, Y., A. Salter, E. Wallström, G. Cutter and O. Stüve (2019). "Evolution of clinical trials in multiple sclerosis." Ther Adv Neurol Disord **12**: 1756286419826547.

Zhang, Z., S. Schwartz, L. Wagner and W. Miller (2000). "A greedy algorithm for aligning DNA sequences." J Comput Biol **7**(1-2): 203-214.

11 Curriculum vitae

Personal Data

Contact	lukas.enz@unibas.ch
Date of birth	25. Feb. 1991
Nationality	Swiss

Current employment

Oct. 2016–March 2020 **MD-PhD student**, Swiss National Science Foundation MD-PhD Stipendium, Prof. Nicole Schaeren-Wiemers, Neurobiology, Department of Biomedicine, University and University Hospital Basel, Switzerland

Education

Aug. 2013–Sep. 2016 **Master of Medicine** and **Federal Authorization**
University of Basel
Master thesis: *Establishment and comprehensive quantitative analysis of a histological database of brain tissues from clinically well-defined Multiple Sclerosis and control cases*, Prof. Nicole Schaeren-Wiemers, Neurobiology, Department of Biomedicine, University and University Hospital Basel, Switzerland

Aug. 2010–Aug. 2013 **Bachelor of Medicine**
University of Basel

Publications

Enz, L. S., Zeis, T., Schmid, D., Geier, F., van der Meer, F., Steiner, G., Certa, U., Binder, T. M. C., Stadelmann, C., Martin, R., Schaeren-Wiemers, N. (2020). Increased HLA-DR expression and cortical demyelination in MS links with HLA-DR15. *Neurol Neuroimmunol Neuroinflamm*, 7 (2) e656. doi: 10.1212/NXI.0000000000000656

Enz, L. S., Zeis, T., Hauck, A., Linington, C., Schaeren-Wiemers, N. (2019). Combinatory Multifactor Treatment Effects on Primary Nanofiber Oligodendrocyte Cultures. *Cells*, 12, 8 (11). doi:10.3390/cells8111422

Perriard, G., Mathias, A., **Enz, L.**, Canales, M., Schluep, M., Gentner, M., ... Du Pasquier, R. A. (2015). Interleukin-22 is increased in multiple sclerosis patients and targets astrocytes. *J Neuroinflammation*, 12, 119. doi:10.1186/s12974-015-0335-3

Weil, M. T., Mobius, W., Winkler, A., . . . **Enz, L.**, . . . Simons, M. (2016). Loss of Myelin Basic Protein Function Triggers Myelin Breakdown in Models of Demyelinating Diseases. *Cell Rep*, 16(2), 314-322. doi:10.1016/j.celrep.2016.06.008

Zeis, T., **Enz, L.**, & Schaeren-Wiemers, N. (2016). The immunomodulatory oligodendrocyte. *Brain Res,* 1641(Pt A), 139-148. doi:10.1016/j.brainres.2015.09.021

Attended Meetings

Date	Meeting	Contribution	Title
2.-4.3.2017	Current topics in myelin research. Myelin-Netzwerk e.V. **Kassel, Germany**	Poster	Quantitative histological analysis of Multiple sclerosis and control brain tissues.
18.-20.5.2017	DBM PhD Retreat. **Quarten, Switzerland.**	Poster	A novel animal model to study chronic grey matter changes in the brain.
9.6.2017	MS Meeting Paris, Swiss & French MS Meeting - Paris 2017. ARSEP and SMSG. **Paris, France.**	Poster	Development of a large scale comprehensive human brain tissue expression database for Multiple Sclerosis.
12.-13.6.2017	Heterogeneity of autoimmune diseases. **Zürich, Switzerland**	Poster	Development of a large scale comprehensive human brain tissue expression database for Multiple Sclerosis.
16.-17.6.2017	Young Investigator Meeting in Multiple Sclerosis Research. **Bern, Switzerland.**	**Talk**	Development of a large scale comprehensive human brain tissue expression database for Multiple Sclerosis.
26.1.2018	Researcher Meeting, Swiss MS Society. **Lucerne, Switzerland.**	Poster	Development of a large scale comprehensive human brain tissue expression database for Multiple Sclerosis.
26.1.2019	21st State of the Art Symposium. **Lucerne, Switzerland.**	Poster	Functional impact of genes potentially involved in de- and remyelination in cultured oligodendrocytes on nanofibers.
7.- 9.6.2018	DBM PhD Retreat. **Einsiedeln, Switzerland.**	**Talk**	HLA-DRB1*15:01 specific increase of HLA-DRB1 expression is associated with grey matter lesion size in Multiple Sclerosis.
13.-15.6.2019	DBM PhD Retreat. **Schwarzenburg, Switzerland.**	Poster	Increased HLA-DR expression and cortical demyelination in multiple sclerosis patients are linked with the HLA-DR15 haplotype.
11.-13.9.2019	European Committee for Treatment and Research in Multiple Sclerosis, ECTRIMS. **Stockholm, Sweden.**	2 Posters	Combinatory multifactor treatment effects on nanofiber oligodendrocyte cultures to assess proliferation and differentiation And Increased HLA-DR expression and cortical demyelination in multiple sclerosis patients are linked with the HLA-DR15 haplotype.

Organized Meetings

Date	Meeting
18.-20.5.2017	Department of Biomedicine PhD Retreat 2017, Quarten, Switzerland.
7.-9.6.2018	Department of Biomedicine PhD Retreat 2018, Einsiedeln, Switzerland.
13.-15.6.2019	Department of Biomedicine PhD Retreat 2019, Schwarzenburg, Switzerland.